

DIABLO CANYON SITE

UNIT NO. 2

REPORT OF CONTAINMENT STRUCTURE

STRUCTURAL INTEGRITY TEST

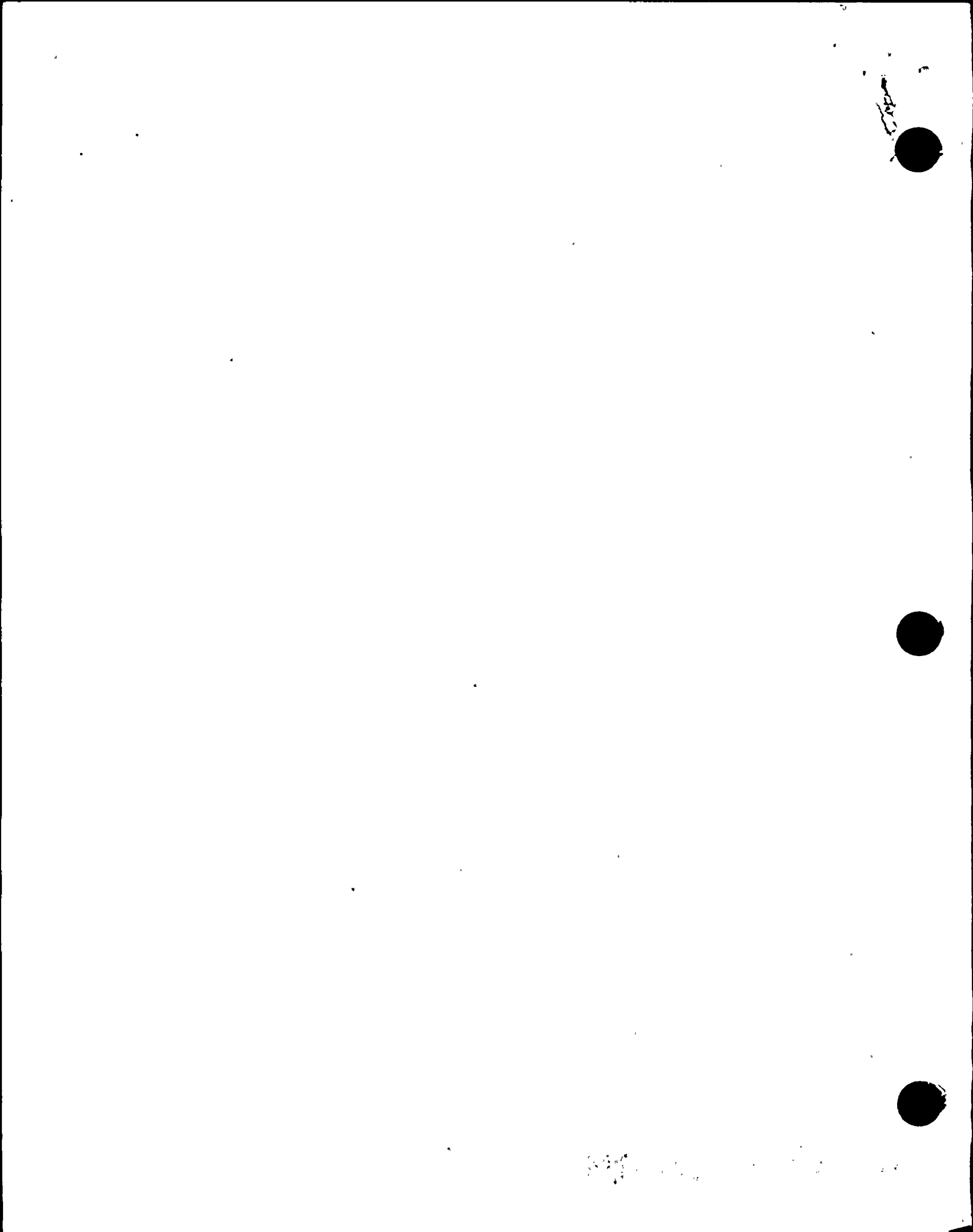
PACIFIC GAS & ELECTRIC CO.

77 BEALE STREET

SAN FRANCISCO, CALIFORNIA 94106

March, 1981

8107300015 810722
PDR ADOCK 05000275
A PDR



CONTENTS

	<u>Page</u>
General Summary	1
Description of the Containment Structure	1 - 3
Predicted Response	4 - 5
Test Procedure and Instrumentation	6 - 10
Test Results and Observations	11 - 16
Evaluation of Structure's Performance and Safety Margin	17 - 18
References	19

List of Tables

Table I	Crack Summary
Table II	Radial Deformation Measurements

List of Figures

Figure 1	General Outline - Containment and Adjoining Structures
Figure 2	Reinforcing Steel Arrangement
Figure 3	Cylinder - Base Slab Juncture
Figure 4	Hexagonal Collars
Figure 5	Predicted Response of Containment Structure to 54 PSIG Test Pressure
Figure 6	Time History - Pressure vs. Time
Figure 7	Whitewash Areas for Crack Inspection
Figures 8.1, 8.2	Location of Observation Points
Figures 9 - 11	Location of Strain Gages
Figures 12.1 - 12.10	Crack Pattern at 54 PSIG
Figures 13.1 - 13.24	Radial Deformations vs. Pressure Diagrams



4

GENERAL SUMMARY

This report presents the results of the Structural Integrity Test of the Unit No. 2 containment structure at the Diablo Canyon Site conducted between October 26 and November 4, 1977, in accordance with the Regulatory Guide 1.18.

During the test the structure was subjected to a maximum internal pressure of 54 PSIG (115 percent of the design pressure of 47 PSIG). The performance of the structure during the test indicates that its structural capacity under the test conditions meets or exceeds the acceptance criteria.

This conclusion is supported by following observations:

1. Most of the Structural Integrity Test instrumentation performed well, and the recorded data appear valid.
2. Measured displacements were close to the calculated values and within the limits set in the acceptance criteria.
3. The crack patterns and spacing were in good agreement with those predicted. Very few cracks exceeded the minimum measurable width of 0.01".
4. Stresses derived from strain gage readings corroborate the conclusions of analysis, displacement measurements, and crack observations.
5. The test results were essentially identical to those of the prototype Unit 1 containment structure.

DESCRIPTION OF THE CONTAINMENT STRUCTURE

The Containment Structure is a cylindrical/hemispherical reinforced concrete shell, supported on a circular base.

The shell consists of a 142' high, 140' ID, 3'-8" thick cylindrical portion, topped with a 2'-8" thick hemispherical dome.



The base slab is 153' dia., and 14'-6" thick founded on sandstone. Figure 1 shows general outline of containment and adjoining structures. The test pressure generates primarily membrane tension in the containment shell designed to be resisted by the main reinforcing alone. The reinforcing consists of: 2 layers of #18S hoop bars spaced at 8½" cc in the cylindrical portion and diagonal bars forming continuous loops starting at the base slab as "right hand" helical bars (#18S @ 8½" cc) wrapping around the dome and going back into the base slab as "left hand" helical bars.

The resulting reinforcing pattern forms equilateral triangles in the cylinder and a geodesic pattern affording the most uniform bar density in the dome. This reinforcing was placed as the exterior layer of reinforcing of the shell.

Additional diagonal bars were also placed as the interior layer of reinforcing in the lower part of the cylindrical wall which is subjected to the largest seismic forces. Figure 2 shows the reinforcing pattern in the Containment.

The interior surface of the shell is lined with 3/8" steel plate providing a leaktight pressure boundary. Although not considered in the stress calculations, the liner plate is expected to act as part of the composite system and is considered in the calculated test pressure response.

The cylindrical wall diagonal reinforcing and liner are anchored into the base slab, which restrains radial movements of the wall at the juncture.

In order to minimize and limit the extent of shears and moments generated by this restraint, a special 3-layer construction was introduced in the wall base slab juncture area (see Figure 3). It includes a layer of 20' long structural steel beams designed to provide the required minimum shear and moment capacity where concrete shear strength was not considered effective because of the biaxial tension.

100



Base slab reinforcing is placed at the bottom of the slab with a maximum of seven layers of #18S bars @ 24" cc. Near the periphery of the base slab, the bars are bent up at 45°, continuing as top bars, as they pass through the curtain of wall diagonals. Thus, the uplift force from the wall is transmitted directly into the bent bars insuring direct stress transfer to the base slab.

The two major openings in the containment shell are the 18'-6" dia. Equipment Hatch and the 9'-7" dia. Personnel Hatch. At these locations hexagonal steel collars are provided to transfer load in re-bars interrupted by the opening. At all other openings the reinforcing is bent to bypass the opening without interruption.

Hexagonal plate details are shown on Figure 4. Materials used in the containment structure are as follows:

Concrete - 3000 PSI 28-day strength (Exterior Shell)

5000 PSI 28-day strength (Base Mat)

Reinforcing - deformed billet steel ASTM A615 Grade 60

Liner, Hexagonal Collars - ASTM A516 Grade 70



PREDICTED RESPONSE

The predicted response is based on theoretical calculations modified to account for those factors which could not be quantified, such as, modeling assumptions, "as built" conditions, and the like. It also takes into account Unit 1 test experience.

CALCULATED RESPONSE

The predominant effect of the internal pressure is radial expansion of the containment shell. The maximum calculated value of radial expansion is 0.95" corresponding to a maximum strain of 0.00108. Vertical strains are much smaller varying from 0.00004 at the base to approximately 0.00076 in the dome resulting in total elongation from base to spring line of 0.41" and from base to the apex of 1.07". (Based on prototype Unit 1 testing experience, no additional vertical displacements due to base slab flexure are expected). Figure 5 shows diagrams of calculated response the test pressure including stresses in the liner plate and reinforcing.

DISPLACEMENTS

Twenty percent margin of error was allowed for the calculated displacements to account for errors in measurements and modeling assumptions. Allowance was also made for shape adjustments due to out-of-roundness of the structure. Under internal pressure the shell is expected to seek a circular shape. Based on Unit 1 experience, up to 0.25" outward shell movement was allowed at locations where the "as built" position of the shell was inward from the theoretical.



The actual radial growth was approximated by calculating average displacement at each level. Variations from the average is considered a result of shape adjustments.

CRACKING

The basic parameters determining the size of cracks are strains and spacing of cracks. The usual spacing of cracks in concrete tends to be about twice the thickness of the reinforcing cover or about 6" in the case of the containment wall (Ref.: ACI Journal Nov. 1965). Corresponding typical crack widths would then be as follows:

Cylinder, vertical cracks	- 0.007" (strain 0.00108)
Cylinder, horizontal cracks	- 0.001" (strain 0.00015)
Dome	- 0.005" (strain 0.00080)

Based on Unit 1 test experience, actual cracks were expected to follow a random pattern with substantial variations from these typical values. An acceptance limit of 0.06" was allowed for isolated, occasional cracks.

STRAINS, STRESSES

Calculated stresses shown on Figure 5 were used for evaluation of the strain gage readings.



TEST PROCEDURE AND INSTRUMENTATION

The test was conducted in accordance with the PG&E Co. Test Procedure No. 39.4. Following is the summary of essential parameters of the test as actually performed.

PRESSURE

The containment was pressurized in steps with a constant pressure maintained at plateaus 15, 25, 35, 47, and 54 PSIG for a minimum period of one hour while measurements and observations were recorded.

Similar procedure was followed during depressurization.

The time history of pressure is shown on Figure 6.

GENERAL OBSERVATIONS

Both the interior and exterior accessible surfaces were visually examined for structural defects before and after the test.

During the test the following accessible exterior surfaces were inspected for structural deterioration:

Concrete shell accessible from floors at elevation 85', 100', 115', and 140'
Areas around equipment hatch and personnel airlock
Emergency personnel airlock
Main steam and feedwater penetration lines
Mechanical and electrical penetrations
Dome apex



CRACK PROPAGATION INSPECTION

Crack propagation inspection was performed in specially designated whitewash areas:

A 40' x 40' area around the equipment hatch and nine 40 ft. 2 areas located on three azimuths at three elevations. Layout of these areas is shown on Figure 7.

Each whitewash area was subdivided into a 1 ft. square grid numbered for identification. Observations were made at each designated pressure plateau. Each area was photographed and cracks exceeding 0.01" were mapped at 0, 35, 54, and 0 PSIG levels. Crack width was determined using crack comparators.

DEFORMATION MEASUREMENTS

Figures 8.1 and 8.2 show a developed view of the containment exterior showing the location of measurement points.

Radial deformations

Radial deformations were measured at these locations:

1. Point located 13 feet from the apex at azimuth 205° (note: radius is almost vertical).
2. Six points at elevation 231' (springline) at azimuths 14° , 70° , 112° , 190° , 250° , and 310° .
3. Six points at elevation 160' (same azimuths).
4. Six points on vertical ϕ of equipment hatch at elevation 178', 172', 165', 137', 130', and 124'.

(Above measurements were made by sighting back lighted targets with theodolites or jig transits.)



5. Six points on horizontal ℓ of Equipment Hatch.
6. Twelve points located at azimuths 14°, 73°, 114°, 205°, 259°, and 310° near the base slab juncture (at elevations 92' and 93'). These measurements were made by attaching linear motion transducers to the containment liner and interior concrete.

Vertical deformations

Vertical deformations were measured at these locations:

1. Six points at elevation 231' at azimuths 20°, 70°, 130°, 190°, 250°, and 310°.
2. At six points located on vertical ℓ of equipment hatch at elevations 178', 172', 165', 137', 130', and 124'.

The measurements were taken by sighting tapes with automatic levels.

Tangential movements

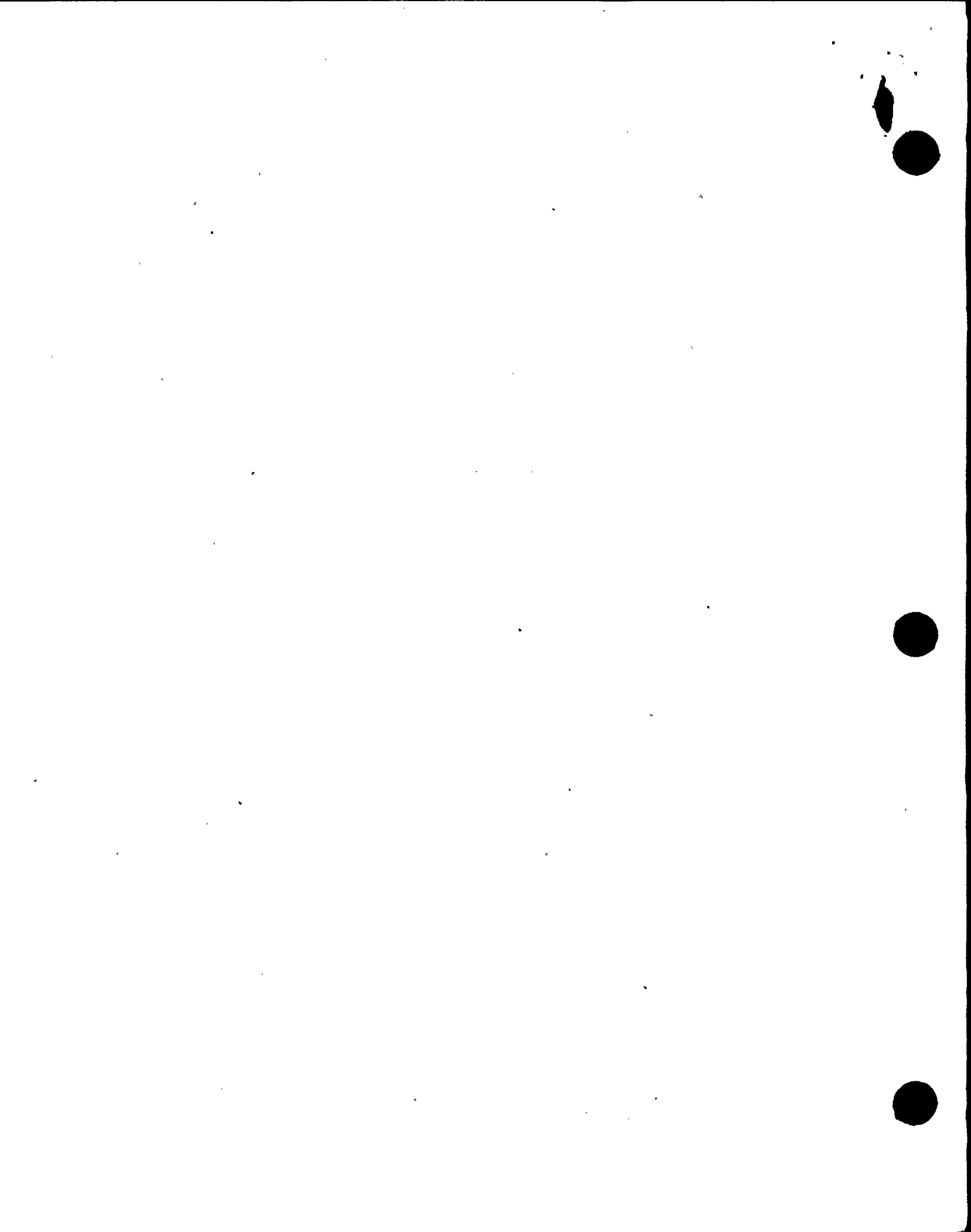
Tangential movements were measured by theodolites at six locations along the horizontal ℓ of equipment hatch.

STRAIN MEASUREMENTS

Strain gages were placed as shown on Figures 9-11. Following is a summary of the strain gage instrumentation:

Main reinforcing

1. One complete hoop re-bar at elevation 208'-7" was instrumented with four equally spaced gages (Code HH).
2. One diagonal bar was instrumented with seven gages, spaced 40' apart (Code 1CCW).



Hexagonal ring plate

Personnel hatch plate was instrumented with three axial strain rosettes placed at ten points (Code PC, Figure 11).

Containment liner

1. Ten points spaced at 30' along the meridian at azimuth 110° were instrumented with two axial strain rosettes (Code 1LM). In addition, four rosettes were also placed at the base slab juncture (Code 1LB).
2. The liner was also instrumented near major openings where three axial strain rosettes were used as follows:
 - 6 rosettes at equipment hatch (Code EH)
 - 10 rosettes at emergency hatch (Code EL)

(See Figure 10)



TEST RESULTS AND OBSERVATIONS

CRACKING

Cracking monitored at the designated whitewash areas (Figure 7) was reasonably close to the predicted response.

Table I gives a summary of cracks mapped which exceeded 10 mils during the test. Three whitewash areas - 1A, 1B, 1C - located at elevation 95' show no cracks in excess of 10 mils. The other six areas at elevations 163' and 231' showed a maximum of 11 cracks in excess of 10 mils in any one area, the largest being 40 mils.

Areas 1D, 2D, 3D, and 4D around the equipment hatch, each about 320 ft.², showed a maximum of 17 cracks over 10 mils with the largest being 40 mils.

Figures 12.1 through 12.10 show the cracks plotted in the whitewash areas.

RADIAL DEFORMATION

Radial deformation measurements are shown in Table II. They indicate excellent agreement with the calculated response and with Unit 1 test results.

At elevation 231' the average displacement is .64" or 80 percent of the calculated value at that elevation. At elevation 160' the average displacement is 0.78" or 83 percent of the calculated value.

At the equipment hatch the measured average displacements were:

.92" or 98 percent of the calculated value at the vertical ϵ
.80" or 109 percent of the calculated value at the horizontal ϵ

Figures 13.1 through 13.24 show plots of radial deformation measurements vs. pressure and the most probable load/deformation diagram developed from these plots.



At elevations 92' and 93' near the cylinder/base slab juncture, the average displacements were .121" and .156" respectively. These values are within 3 percent of the corresponding Unit 1 test measurements and considered to be acceptable.

VERTICAL DEFORMATION

Springline - elevation 231', the measured displacements ranged from 5/16" to 3/8" - averaging 0.34" compared to a calculated value of 0.41".

Equipment hatch 4 - elevations 124' - 178', the measured displacements ranged from 0 to 3/32" with the maximum calculated displacement of 0.12".

Dome apex - elevation 303', the maximum measured displacement was 7/16" - the theoretically estimated displacement was 0.590".

TANGENTIAL MOVEMENTS

Tangential measurements showed negligible movement, which is consistent with the analysis.

STRAIN GAGE READINGS

Containment liner: two axial strain rosettes (Identification 1LM) placed on the containment liner in the protected environment provided (as in Unit 1 containment) the most reliable data.

Shown below for comparison are the average strain gage readings in Units 1 and 2 and the calculated stresses:

<u>Location</u>		<u>Unit 2</u>	<u>Unit 1</u>	<u>Calculated Stress</u>
Dome	σ_x	19.89 ksi	20.19 ksi	25.3 ksi
	σ_y	16.89	17.42	24.2
Springline	σ_x	23.53	22.75	30.0
	σ_y	14.81	15.61	23.5
Cylinder	σ_x	33.96	32.12	36.0
	σ_y	13.16	13.30	17.5

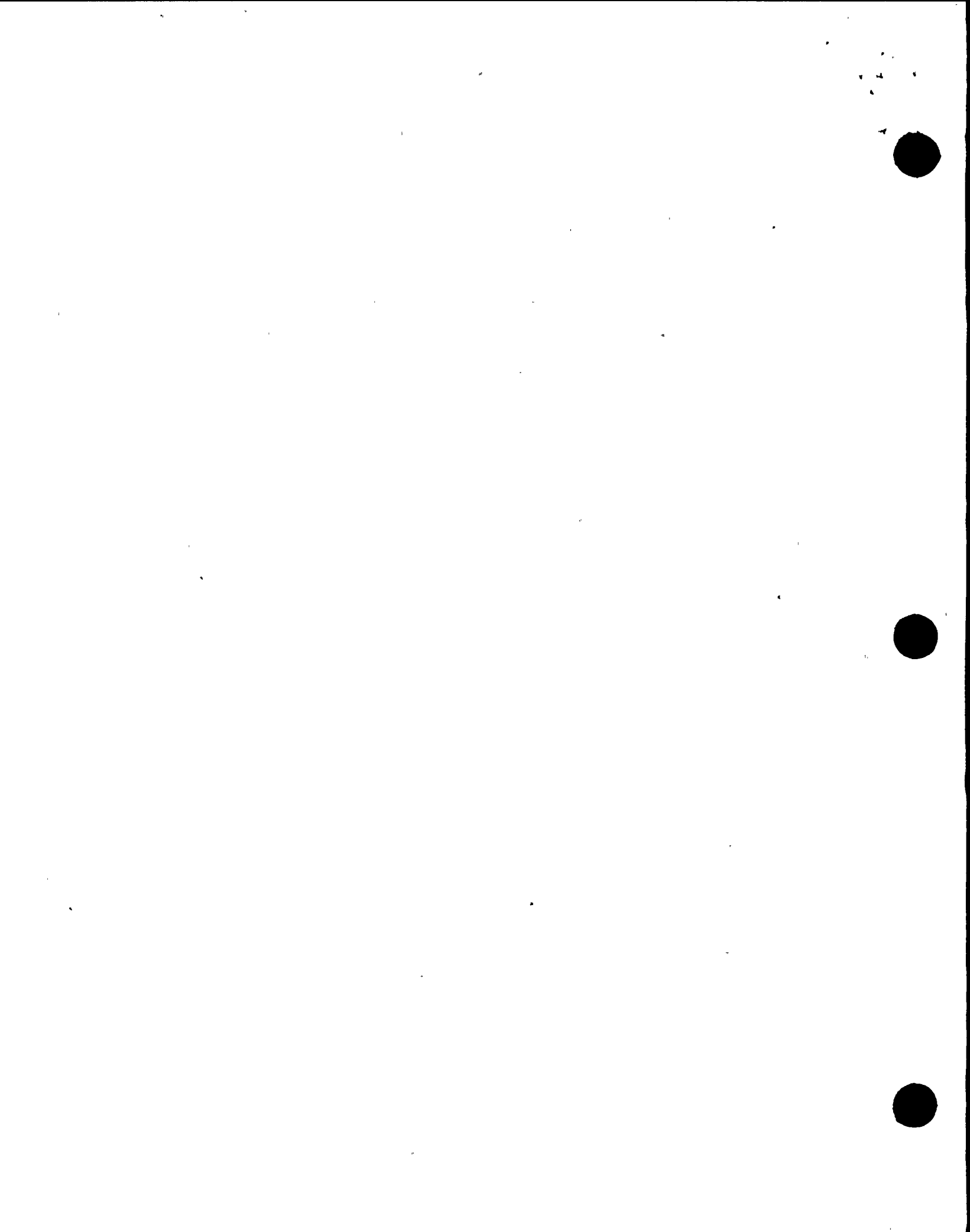


Additional liner strain gages placed in the vicinity of the equipment hatch and emergency personnel openings (Identification EH, EL) to monitor potential stress concentrations show similar stress levels and no stress concentrations. The maximum reading recorded was 32.11 ksi.

Hoop Reinforcing (Identification HH): Three strain gages showed stresses of 22.4 ksi, 32.8 ksi, 27.5 ksi, which are in good agreement with the calculated stress of 29.0 ksi. The fourth hoop bar gage failed.

Diagonal Reinforcing (Identification ICCW): six strain gage readings show stresses ranging from 6.7 ksi to 18.3 ksi while the calculated stresses range between 8.7 ksi and 18.0 ksi. The seventh gage shows a compressive stress of 1.3 ksi which must be interpreted as due to faulty gage.

Personnel hatch hexagonal collar plate (Identification PC): Ten triaxial strain rosettes show relatively low stress levels. The maximum tensile stress is 9.8 ksi. Such low readings were not expected and are interpreted as due to gage deterioration rather than actual strains.



EVALUATION OF STRUCTURE'S PERFORMANCE AND SAFETY MARGIN

The structure performed extremely well and responded to the test load essentially the same as the prototype Unit 1 containment. In all areas where an analytical model could be well defined, the actual response was generally 10-20 percent lower than the calculated as summarized below.

<u>RESPONSE</u>	<u>ACTUAL</u>	<u>CALCULATED</u>	<u>ACTUAL CALCULATED</u>
Radial displacement at el. 231'	0.64"	0.80"	.80
Radial displacement at el. 160'	0.78"	0.93"	.83
Vertical displacement at el. 231'	0.34"	0.41"	.83
Liner hoop stress (cylinder)	33.96 KSI	36.0 KSI	.94
Liner vertical stress (cylinder)	13.16 KSI	17.5 KSI	.75
Liner hoop stress (dome)	19.89 KSI	25.3 KSI	.79
Liner meridional stress (dome)	16.89 KSI	24.2 KSI	.70

The cracking observed during the test was similar to that of Unit 1 test. At some whitewash areas no cracks over 0.01" were observed, and virtually no horizontal cracks were observed elsewhere. Cracking was in very good agreement with the predicted pattern. No areas of more extensive or concentrated cracking were observed anywhere in the structure.

The safety margins demonstrated by the test are basically the same as the Unit 1 margins:

2 or more with respect to yield strength

3 or more with respect to ultimate strength



REFERENCES

1. Regulatory Guide 1.18
2. PG&E Co. Test Procedure No. 39.4 "Containment Standard Integrity and Integrated Leak Rate Test"
3. PG&E Co. "Diablo Canyon Site, Unit No. 1, Report of Containment Structure Structural Integrity Test", December 5, 1975



TABLE I

CRACK SUMMARY

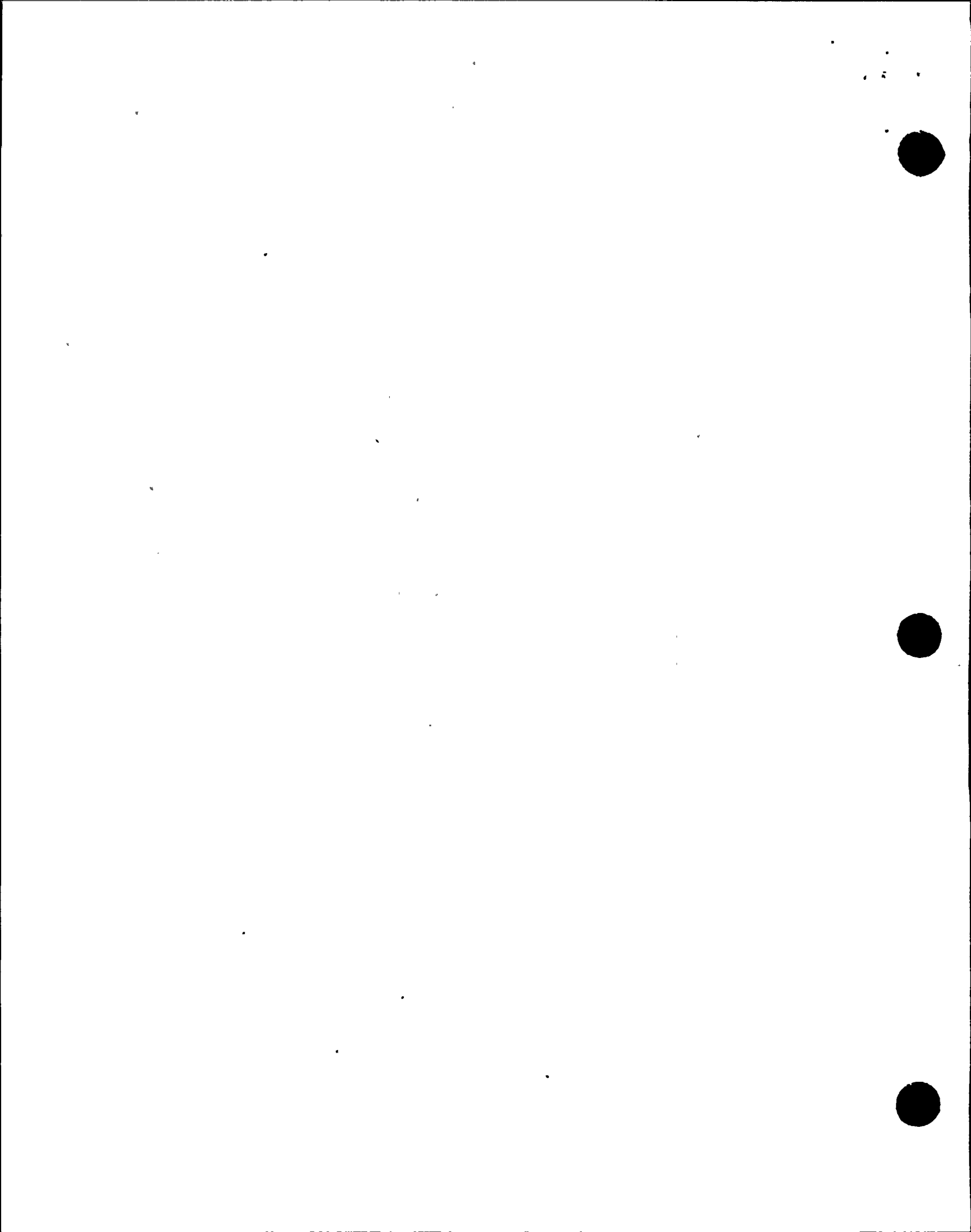
AREA	CRACK SIZE (Mils)	TEST PRESSURE (PSIG)			
		0	35	54	0
		NUMBER OF CRACKS			
1A	10	-	-	-	-
1B	"	-	-	-	-
1C	"	-	-	-	-
2A	10-15	-	2	5	-
	16-20	-	-	2	-
2B	10-15	-	1	-	-
	16-20	-	1	1	-
	21-25	-	-	1	-
2C	10-15	-	-	5	-
3A	10-15	-	7	5	-
	16-20	-	1	5	-
	21-25	-	-	-	-
	26-30	-	-	1	-
3B	10-15	-	2	4	-
	16-20	-	-	5	-
	21-25	-	-	1	-
3C	10-15	-	3	1	2
	16-21	-	-	1	-
	21-25	-	1	1	-
	26-40	-	-	1	-
1D	10-15	-	8	7	1
	16-20	-	2	6	-
	21-25	-	-	1	-
	26-30	-	1	2	-
	31-40	-	-	1	-
2D	10-15	-	4	6	-
	16-20	-	2	2	-
	21-25	-	-	3	-
	26-30	-	1	3	-
3D	10-15	-	4	8	5
	16-20	-	-	1	-
	21-25	-	1	1	-
	26-30	-	1	2	-
4D	10-15	-	-	7	-
	16-20	-	1	-	-
	21-25	-	-	1	-



TABLE II

RADIAL DEFORMATION MEASUREMENTS

LOCATION	POINT NO.	AZIMUTH OR ELEVATION	CALCULATED DISPLACEMENT	ACCEPTANCE LIMIT	MEASURED DISPLACEMENT	% OF ACCEPTANCE LIMIT	
SPRING LINE EL. 231'	1	14°	.80 in	1.21 in	.75 in	62	$\frac{\text{AVE. DISPL.}}{\text{CALCULATED DISPL.}} = 80\%$
	3	70°	"	.96	.63	65	
	5	112°	"	.96	.56	59	
	7	190°	"	1.06	.66	62	
	9	250°	"	1.16	.59	51	
	11	310°	"	.96	.63	65	
	AVERAGE			"		.64	
EL. 160'	2	14°	.93 in	1.37 in	.84 in	62	$\frac{\text{AVE. DISPL.}}{\text{CALCULATED DISPL.}} = 83\%$
	4	70°	"	1.12	.81	73	
	6	112°	"	"	.63	55	
	8	190°	"	"	.69	61	
	10	250°	"	"	.84	75	
	12	310°	"	"	.84	75	
	AVERAGE			"		.78	
VERTICAL OF EQUIP. HATCH AZIMUTH 153°	13	El. 124'	.94 in	1.13 in	.75 in	66	$\frac{\text{AVE. DISPL.}}{\text{AVE. CALCULATED DISPL.}} = 98\%$
	14	El. 130'	.93	1.12	.81	73	
	15	El. 137'	"	1.12	.88	78	
	16	El. 165'	"	1.37	.94	68	
	17	El. 172'	.92	1.36	1.00	74	
	18	El. 178'	"	1.36	1.09	80	
	AVERAGE				.91	73	
VERTICAL OF EQUIP. HATCH EL. 151'	31		.78	.94	.59	63	$\frac{\text{AVE. DISPL.}}{\text{AVE. CALCULATED DISPL.}} = 109\%$
	32		.74	1.14	.81	71	
	33		.68	1.07	.81	76	
	34		.68	1.07	.88	82	
	35		.74	.89	.88	98	
	36		.78	.94	.84	89	
	AVERAGE			.73		.80	



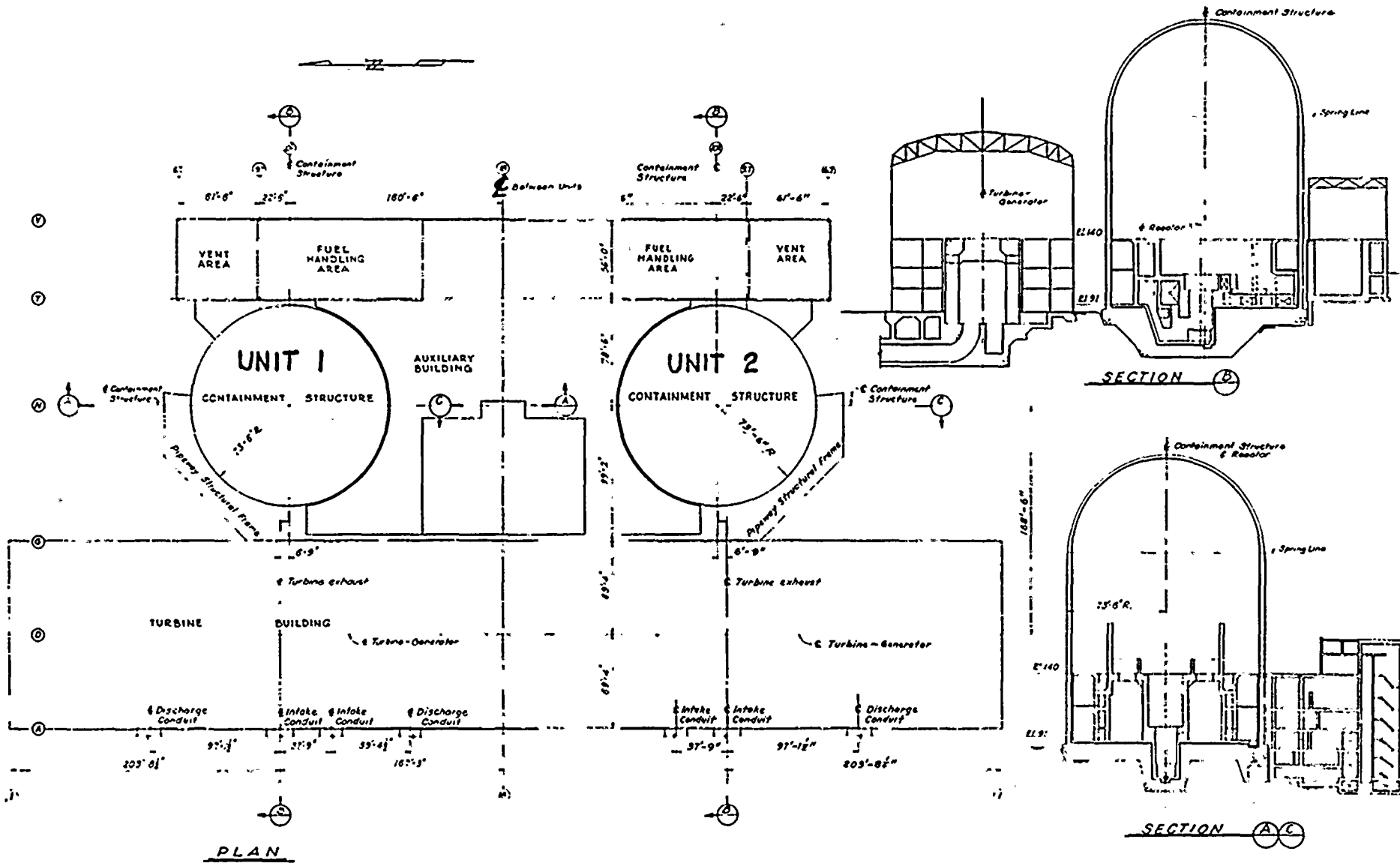
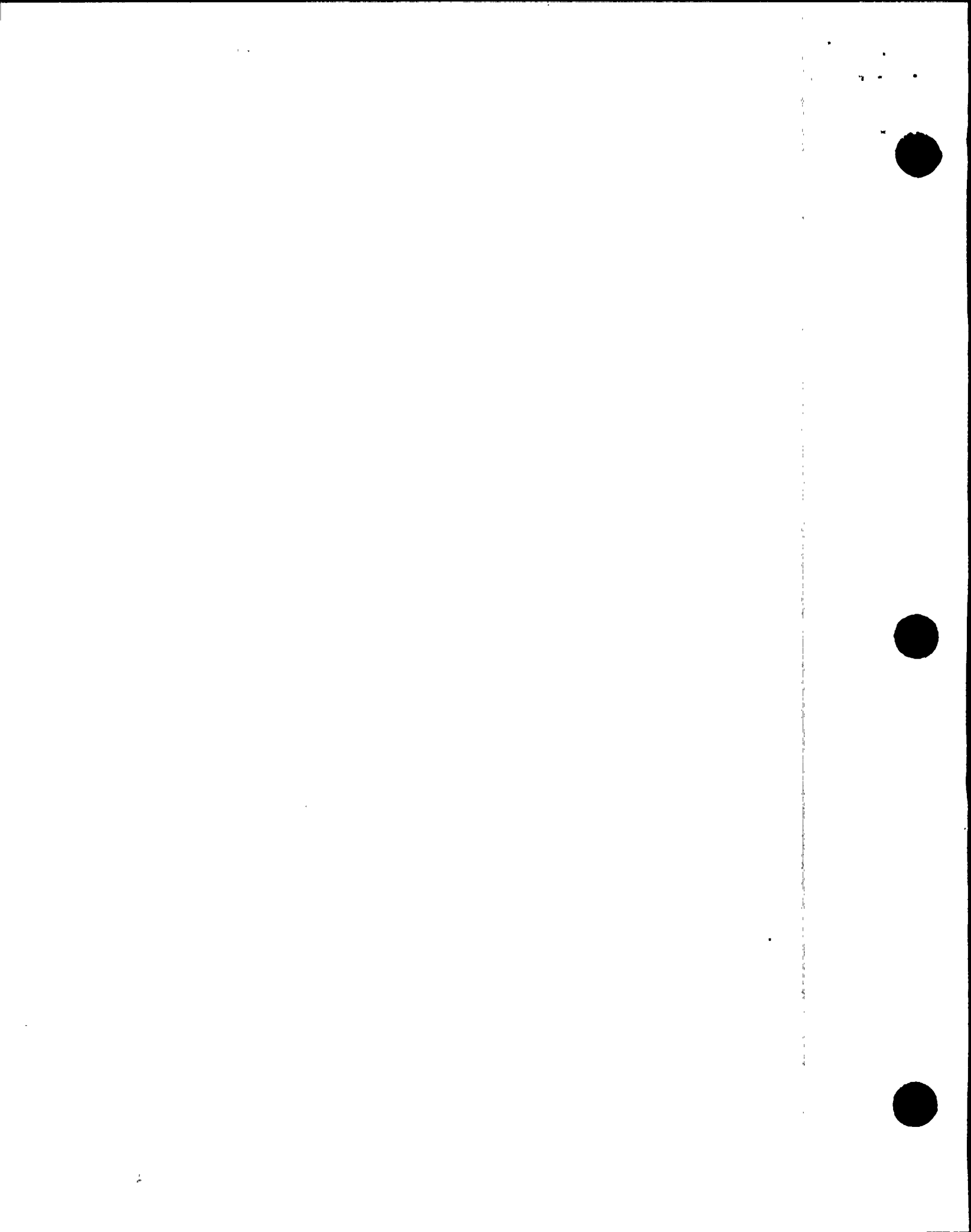
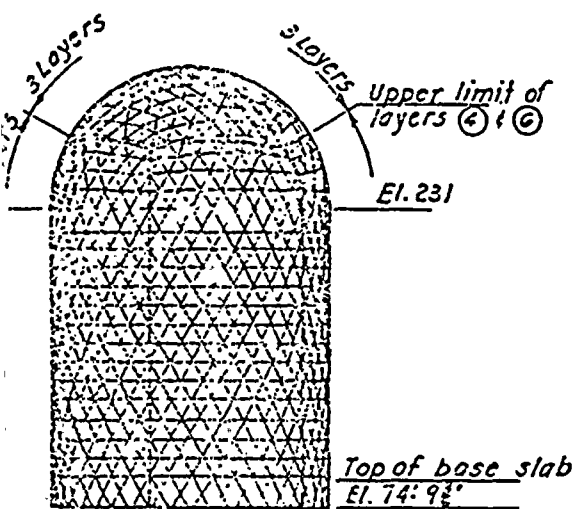
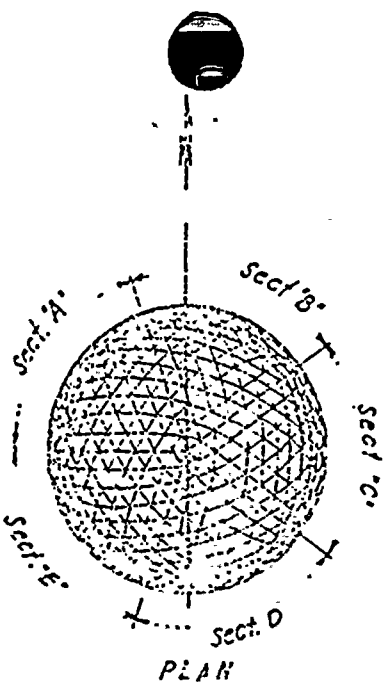
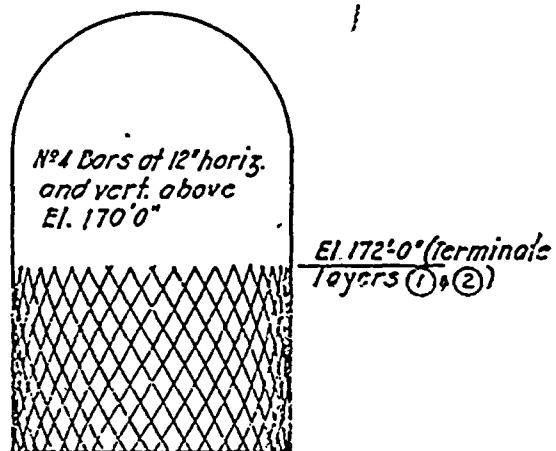


FIGURE 1
GENERAL OUTLINE
CONTAINMENT AND ADJOINING
STRUCTURES





LAYERS 3, 4, 5 & 6



LAYERS 1 & 2

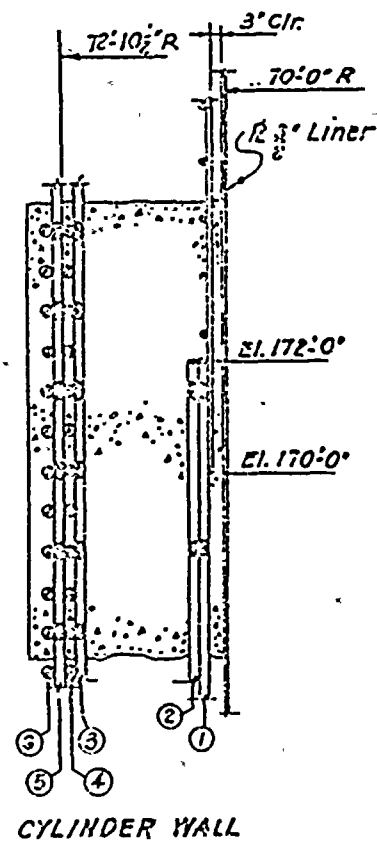
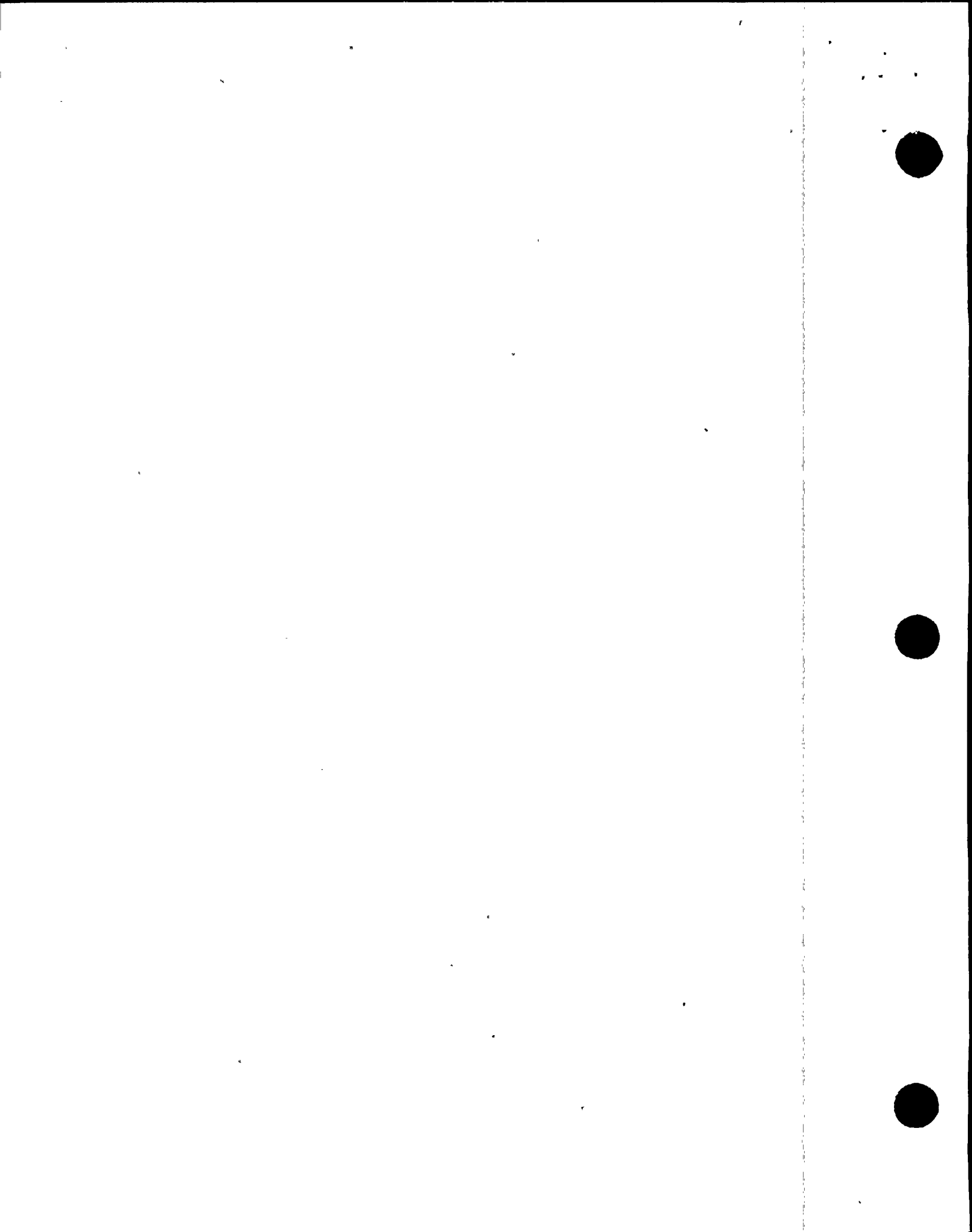
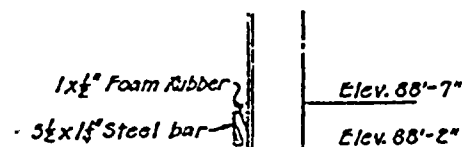
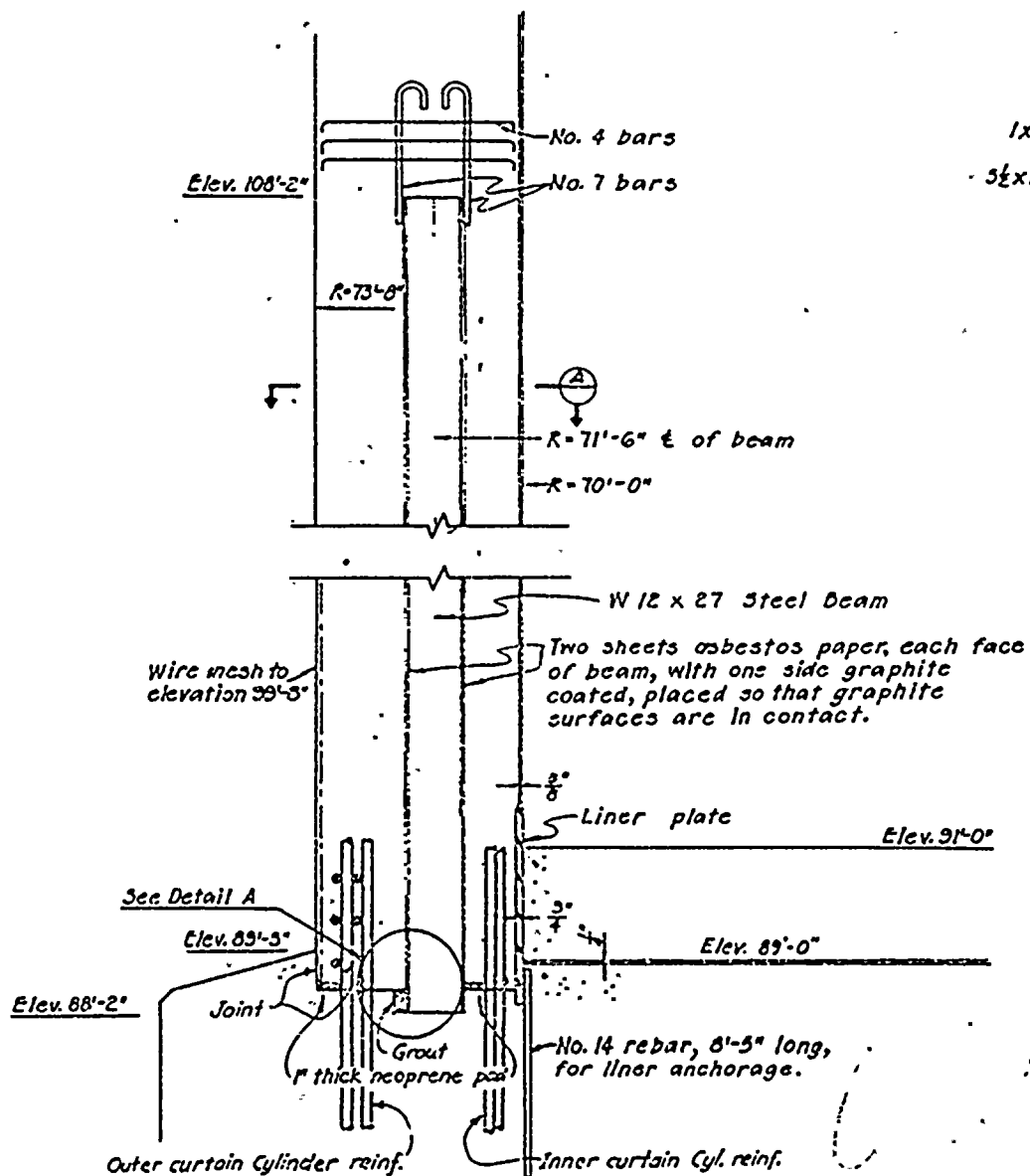


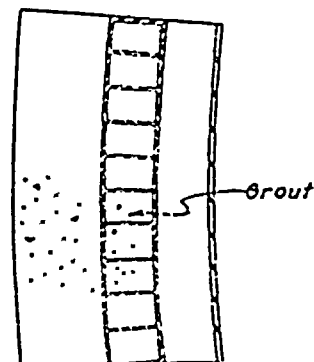
FIGURE 2

CONTAINMENT STRUCTURE
REINFORCING STEEL ARRANGEMENT





DETAIL A

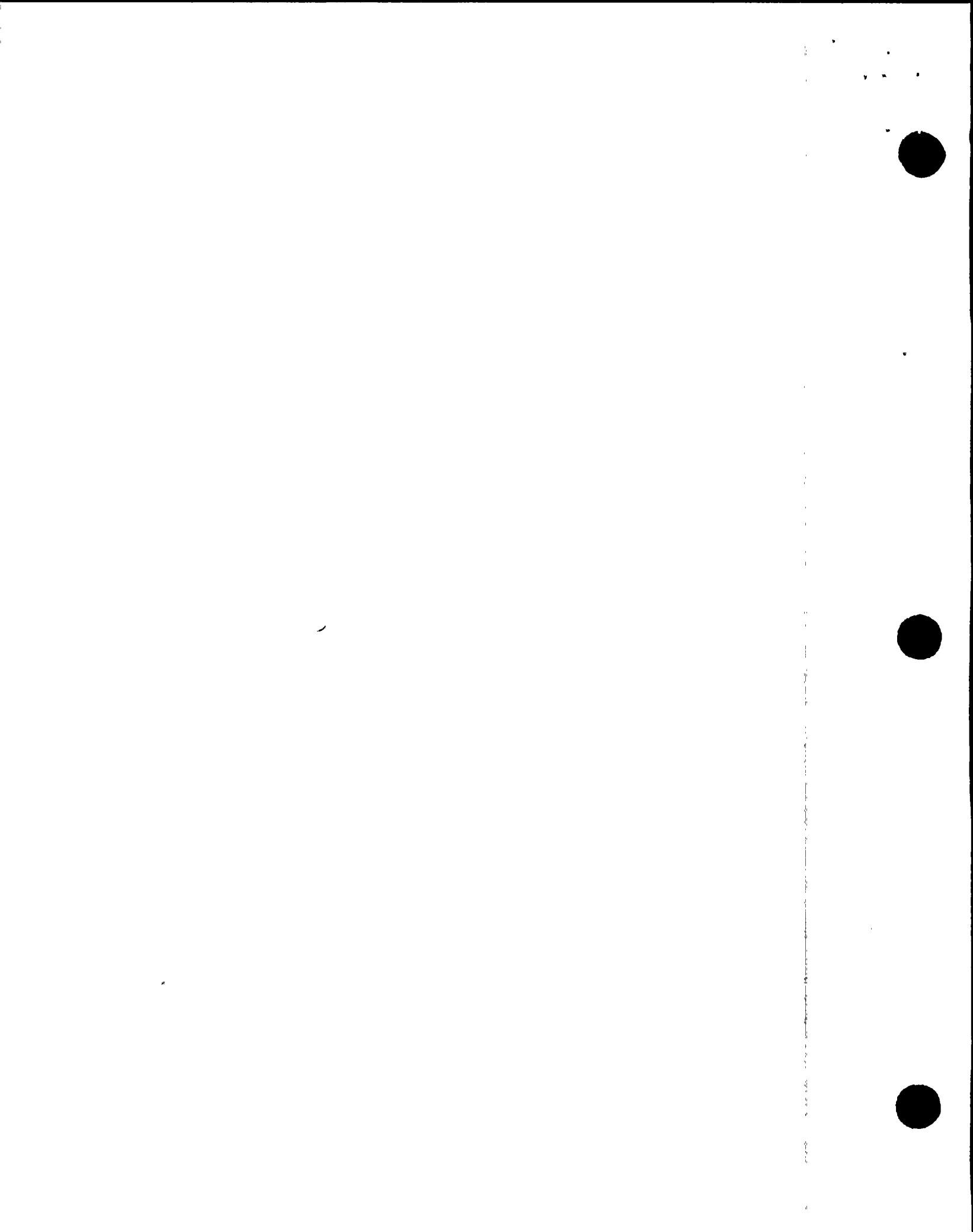


SECTION A

NOTES:

SEE FIGURE 3.8-15 FOR REINFORCING STEEL IN THIS REGION.

FIGURE 3
 CONTAINMENT STRUCTURE
 EMBEDDED BEAMS
 CYLINDER-BASE SLAB JUNCTURE



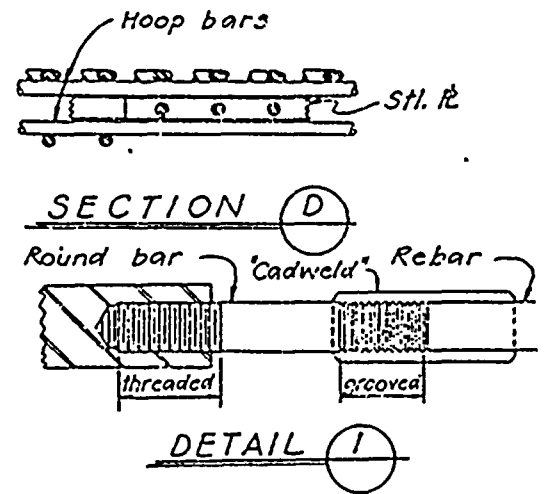
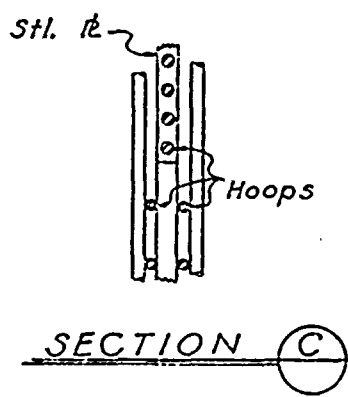
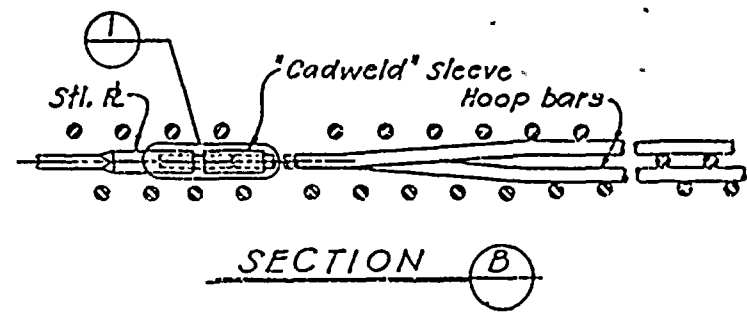
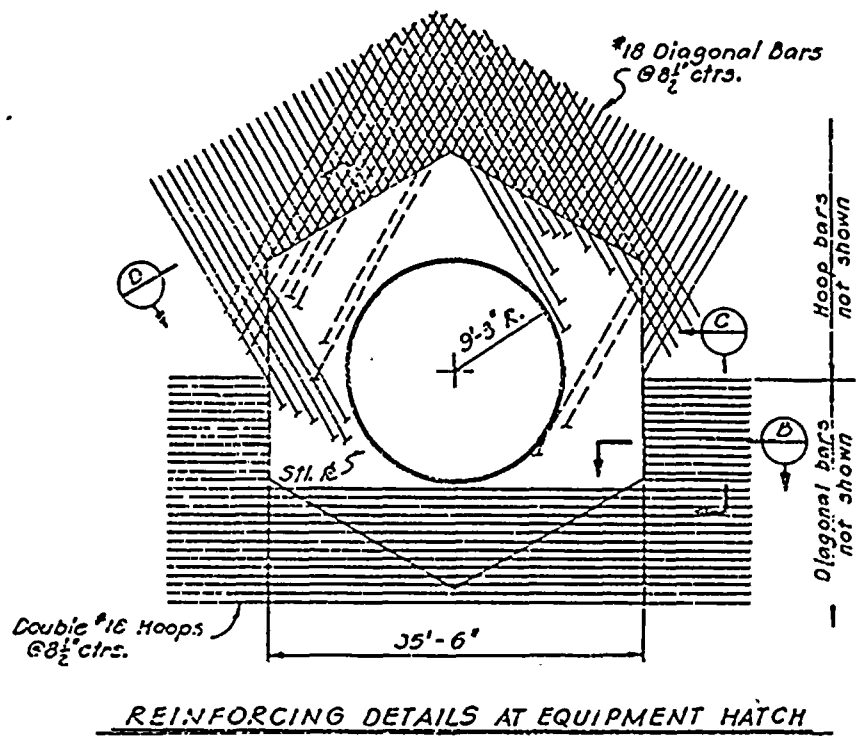


FIGURE 4
CONTAINMENT STRUCTURE
HEXAGONAL COLLARS



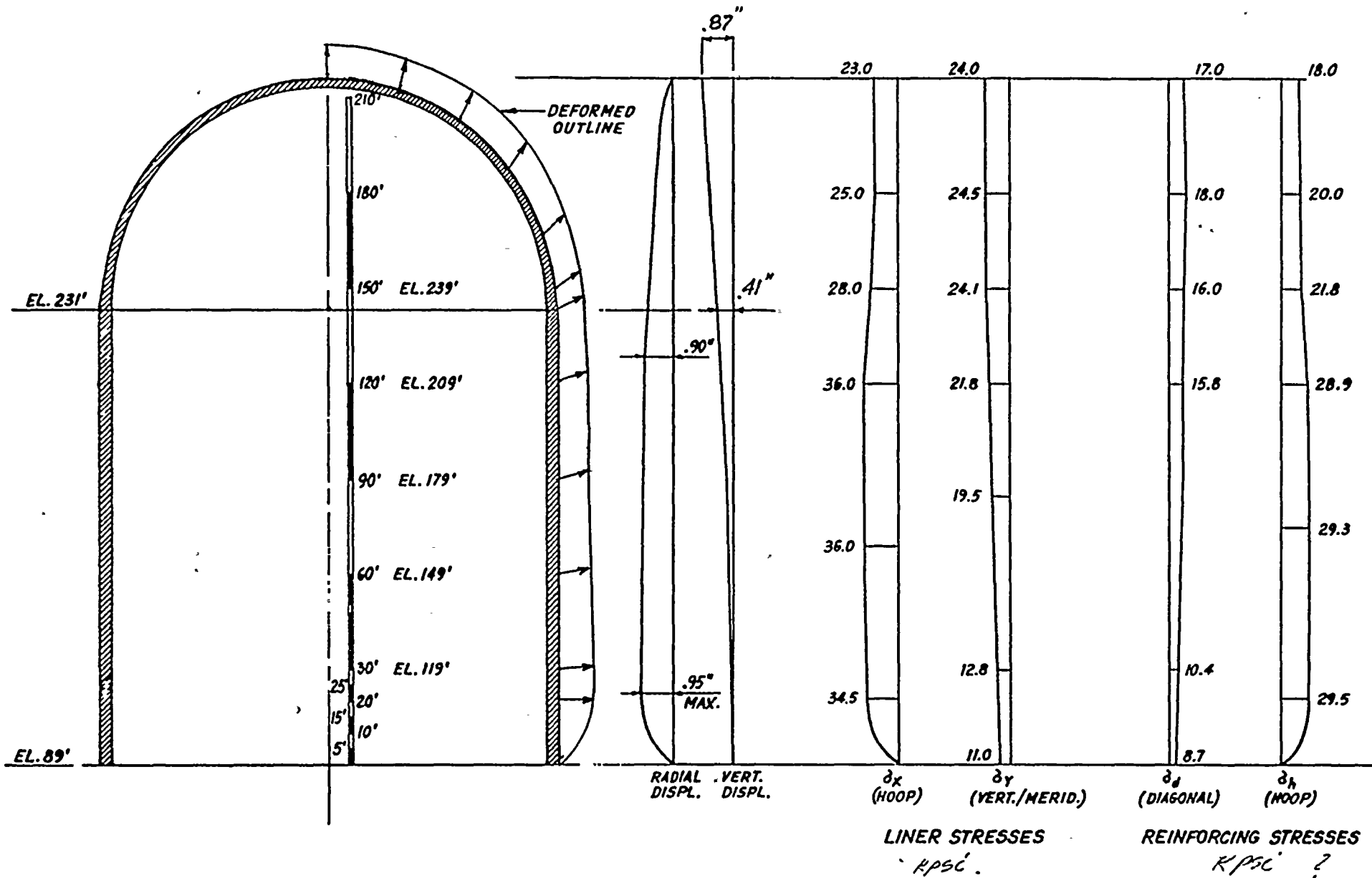
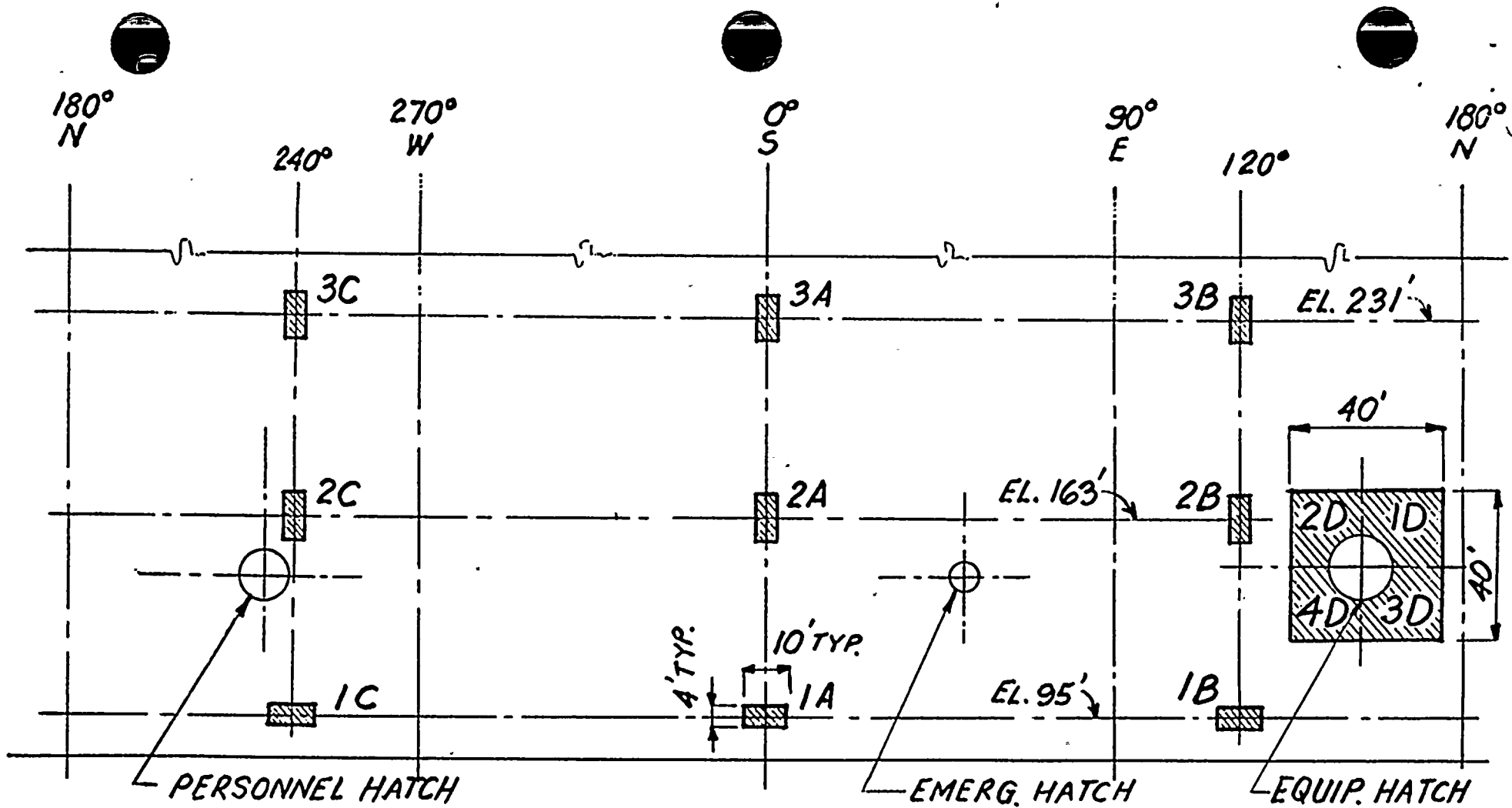


FIGURE 5
 PREDICTED RESPONSE OF CONTAINMENT TO
 54 PSIG TEST PRESSURE

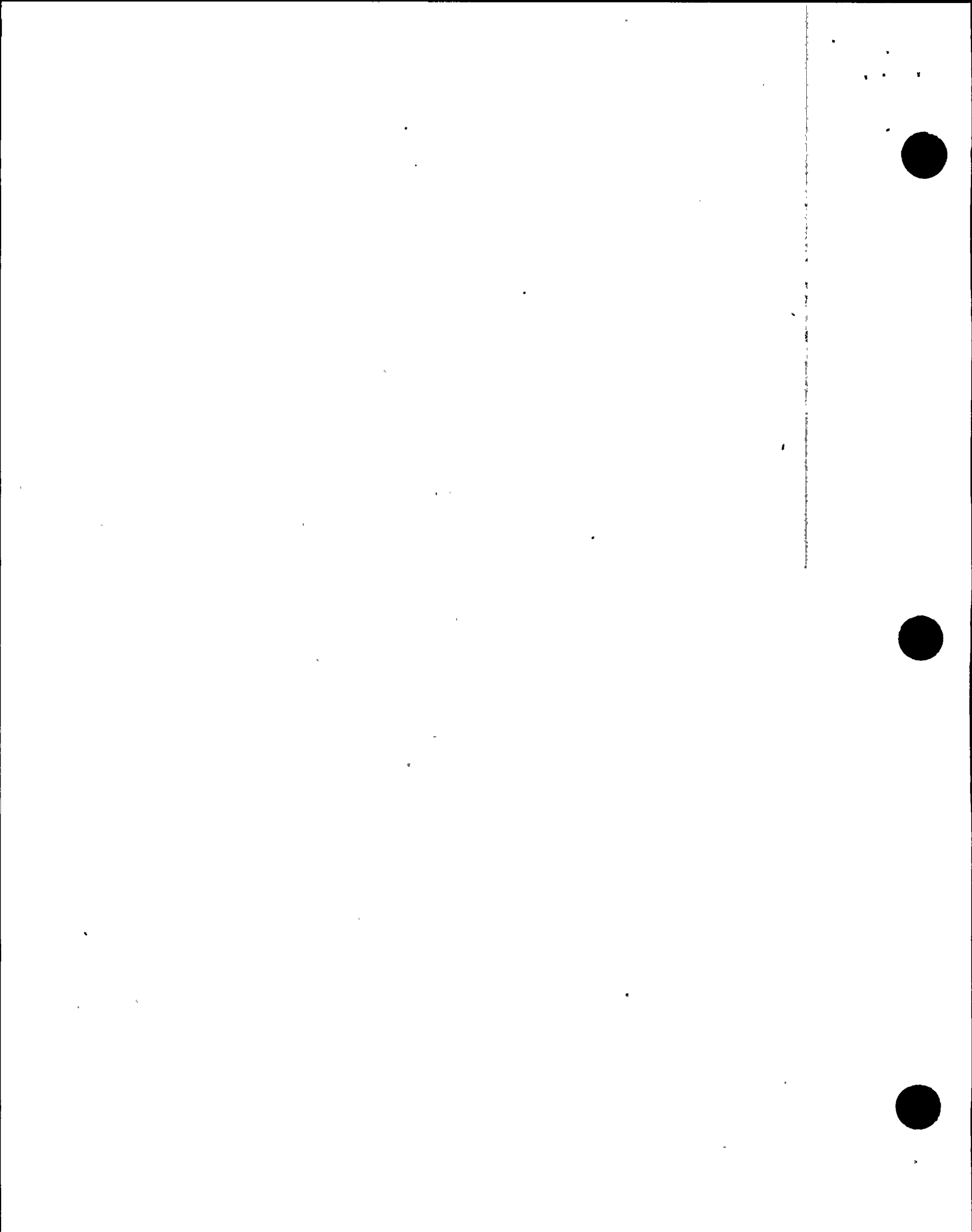
19/12





WHITEWASH AREAS FOR CRACK INSPECTION

FIGURE 7



DIABLO CANYON POWER PLANT

UNIT No. II

CONTAINMENT STRUCTURAL INTEGRITY-INTEGRATED LEAK RATE TEST

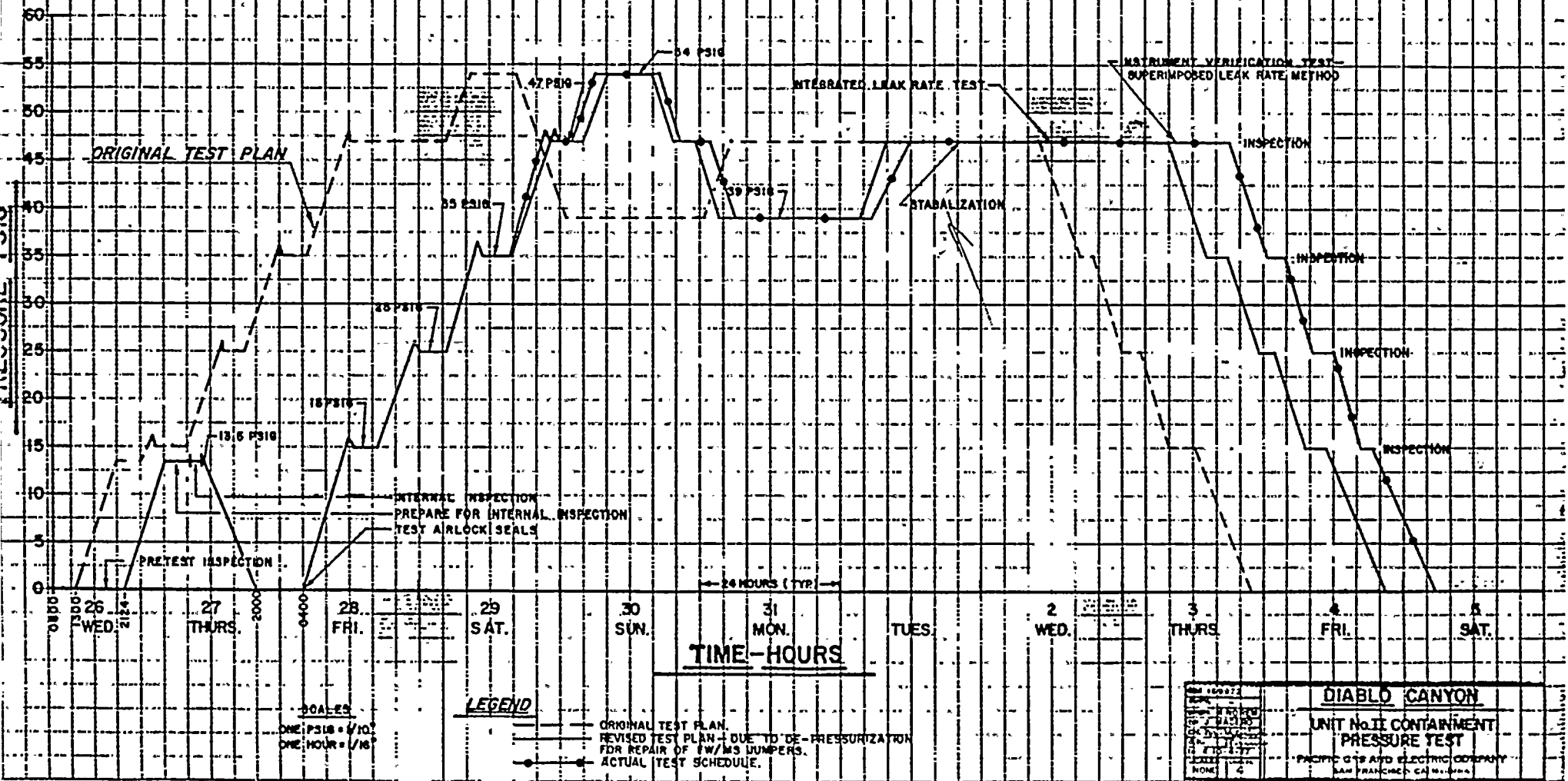
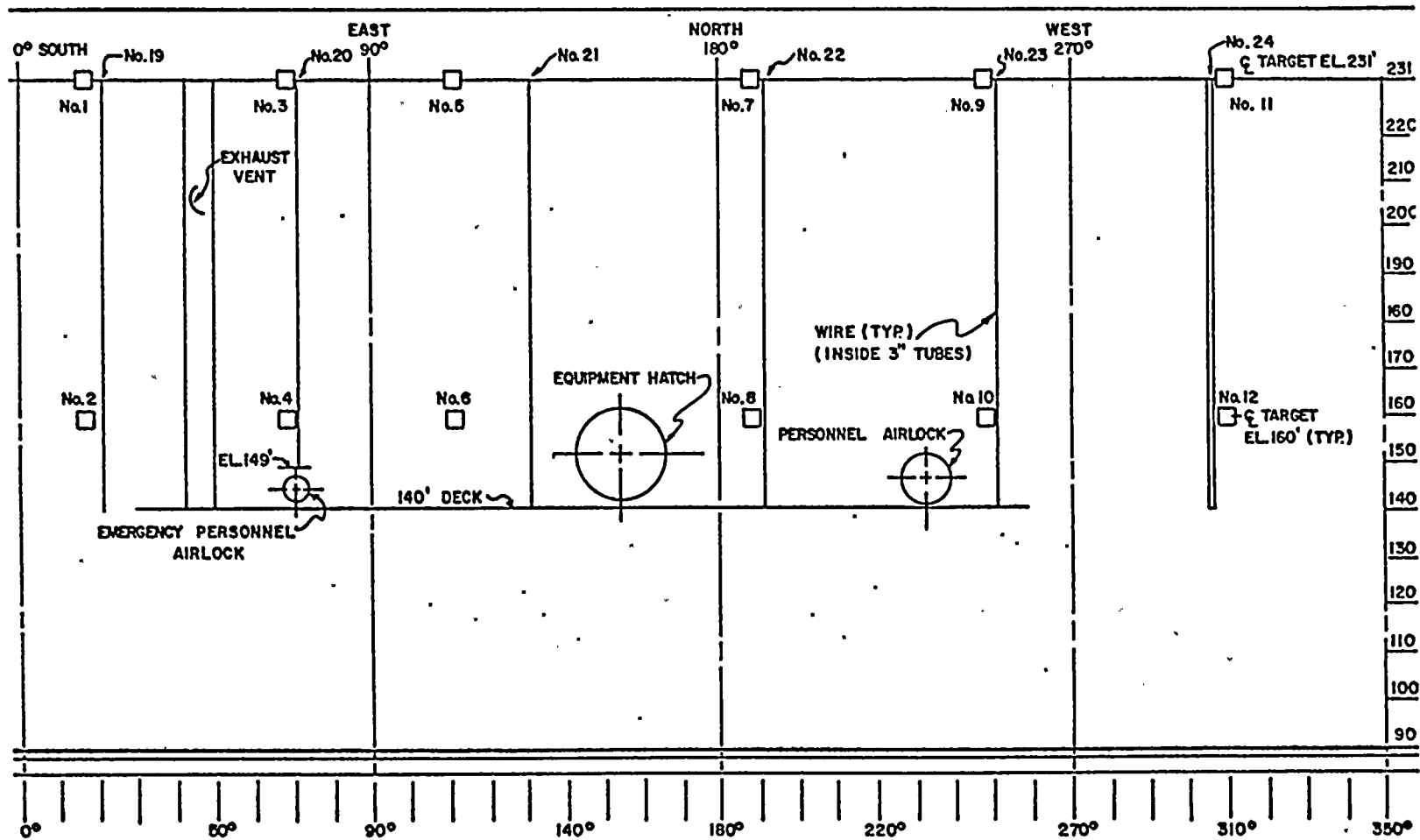


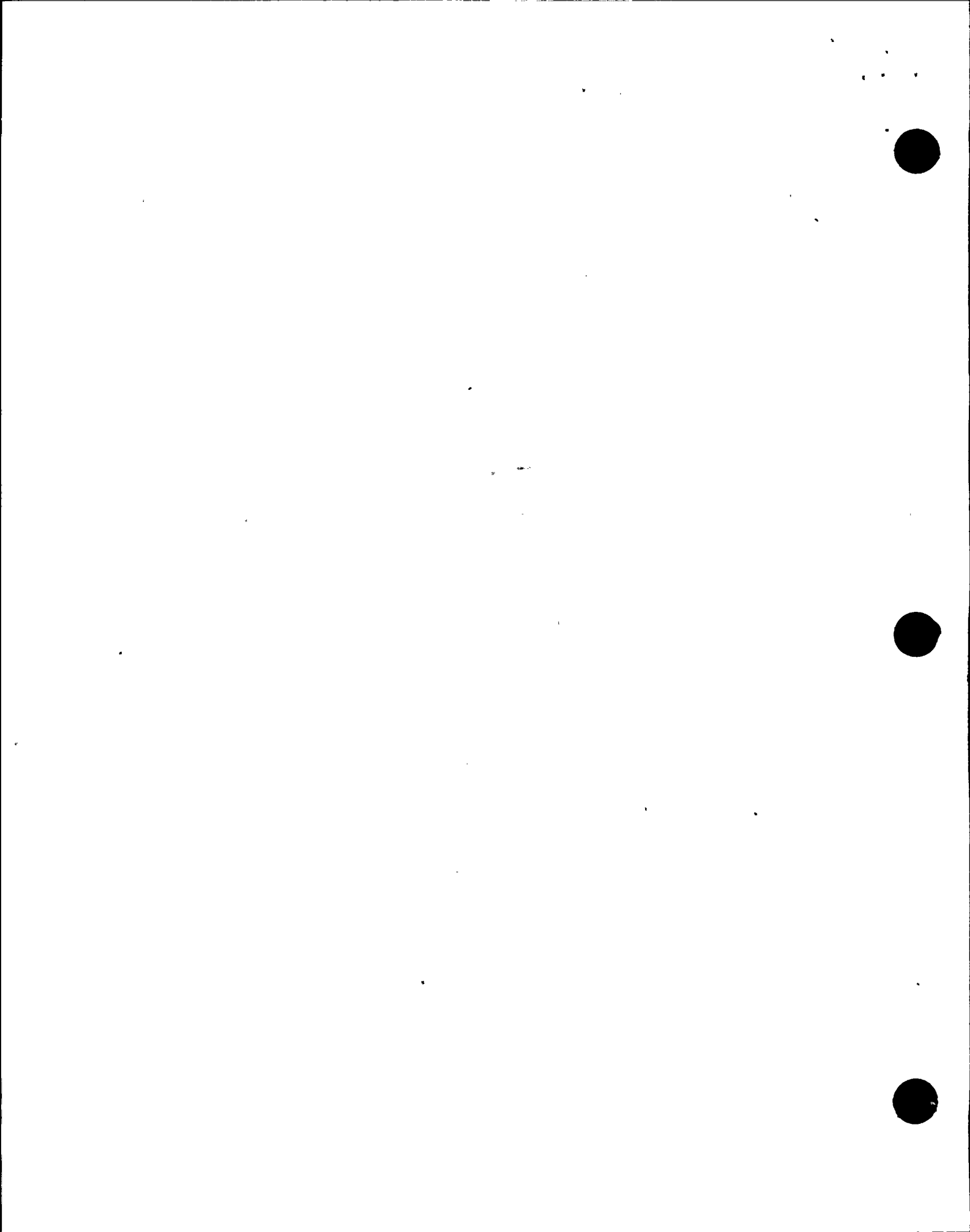
FIGURE 6

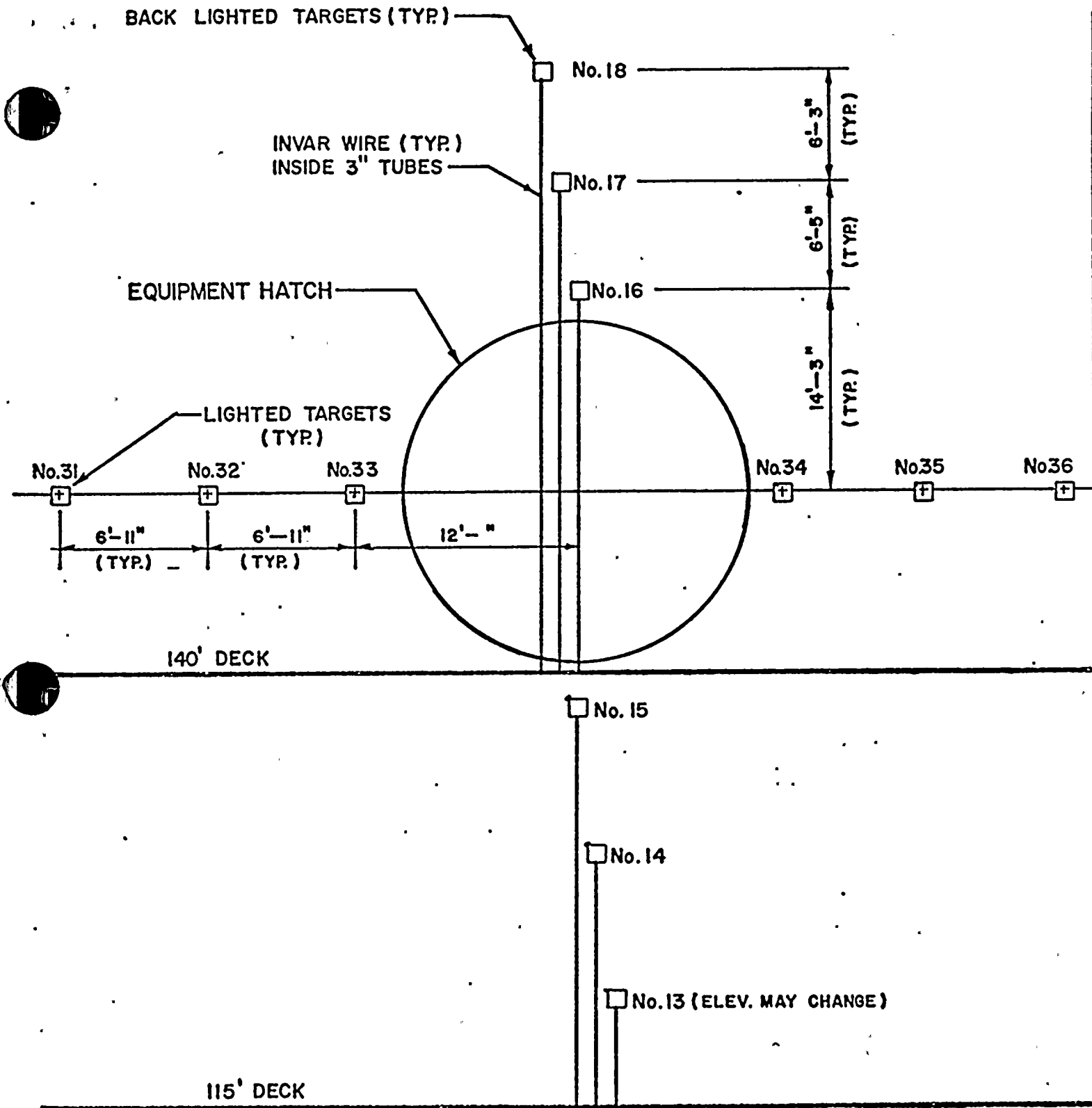




DEVELOPED VIEW CONTAINMENT EXTERIOR
 LOCATION OF TAPES AND BACK LIGHTED TARGETS

FIGURE 8.1





CONTAINMENT UNIT-2
(LOOKING SOUTH)

LOCATION OF OBSERVATION POINTS AROUND THE EQUIPMENT HATCH

FIGURE 8.2



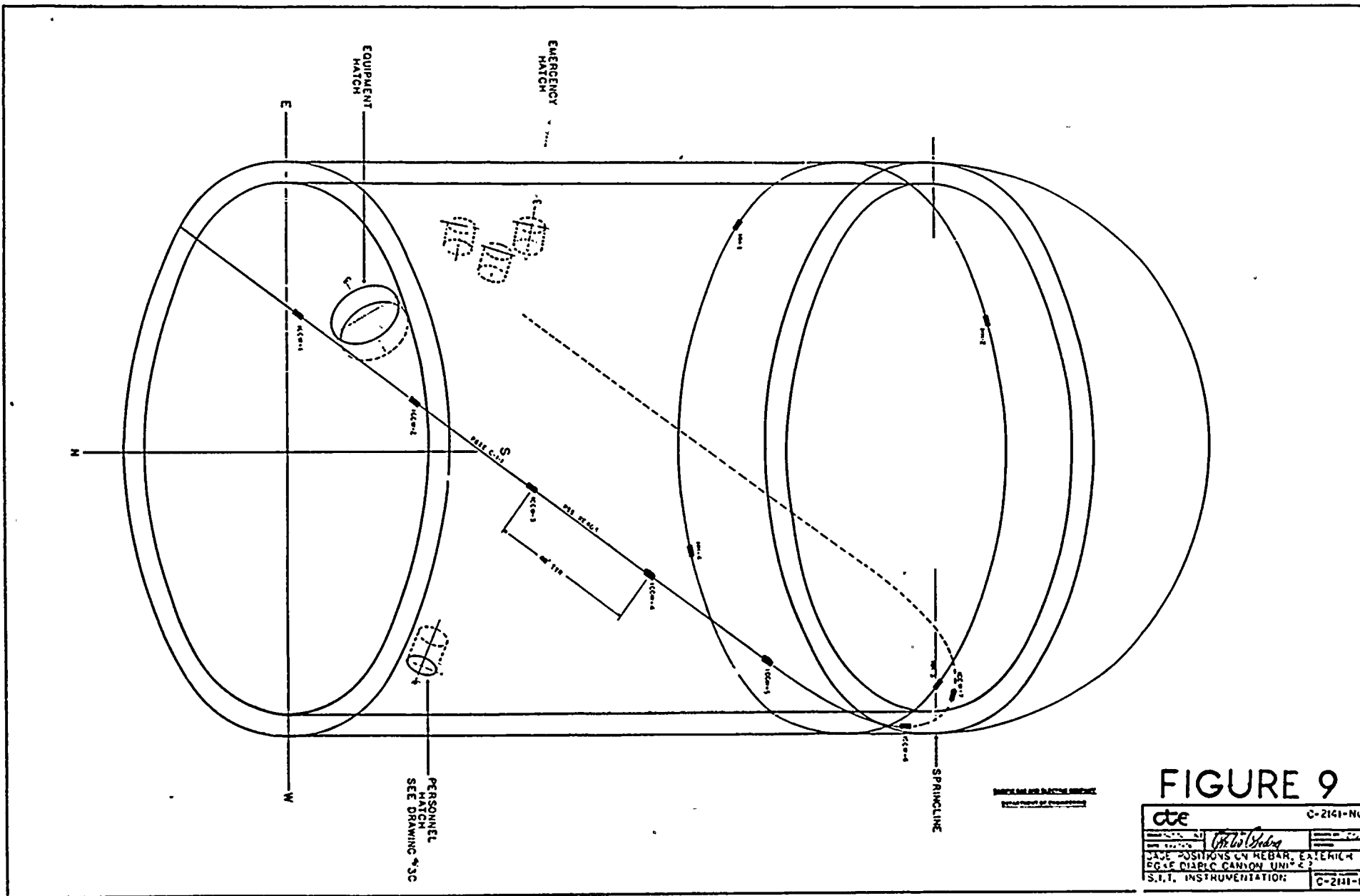


FIGURE 9

cte		C-2141-NL1
DATE	BY <i>W. J. ...</i>	NO.
LAGE POSITIONS ON REBAR, EXTERIOR		
DO OF DIAPHRAGM CANYON UNIT		
S.I.T. INSTRUMENTATION:		C-2141-1



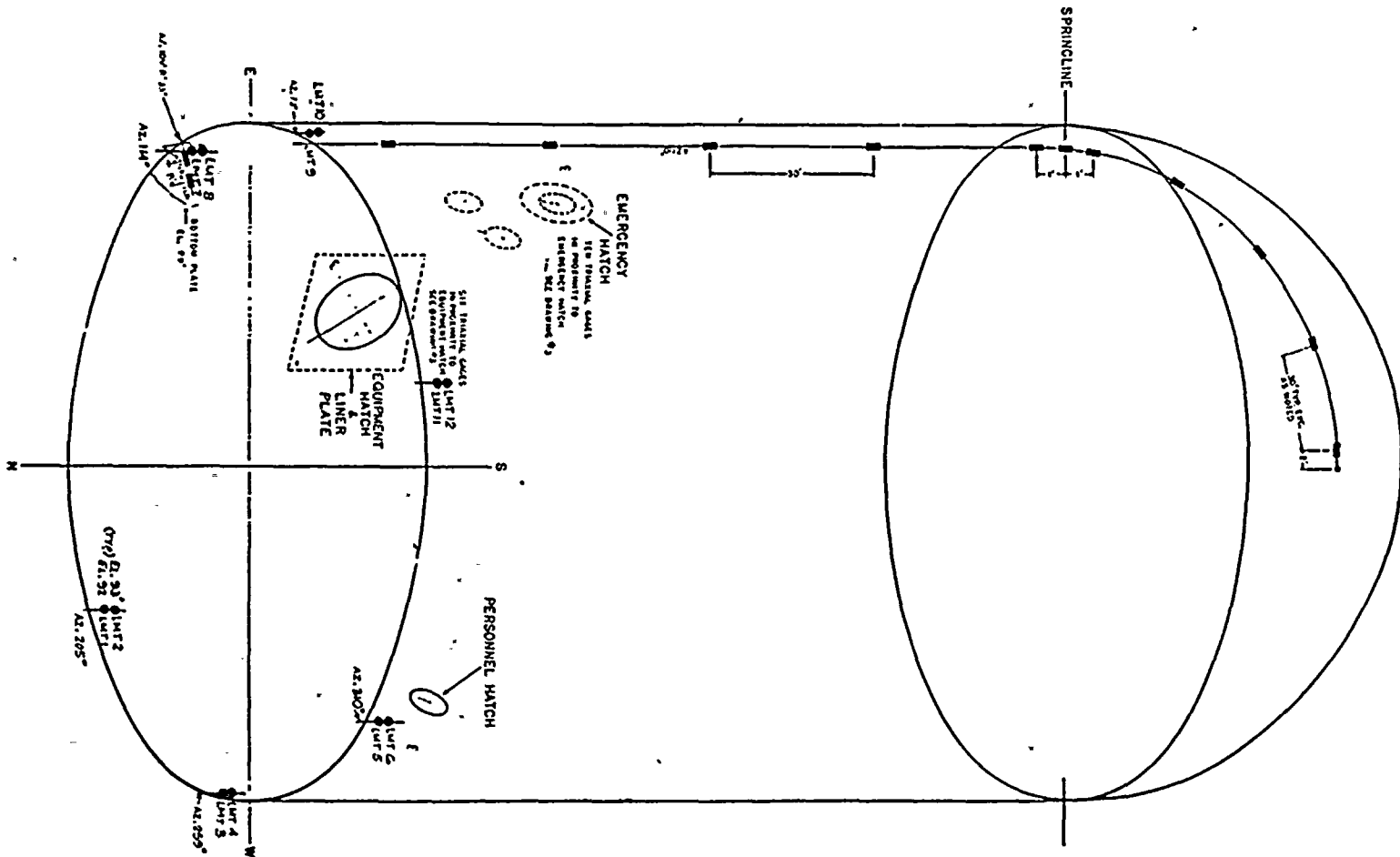
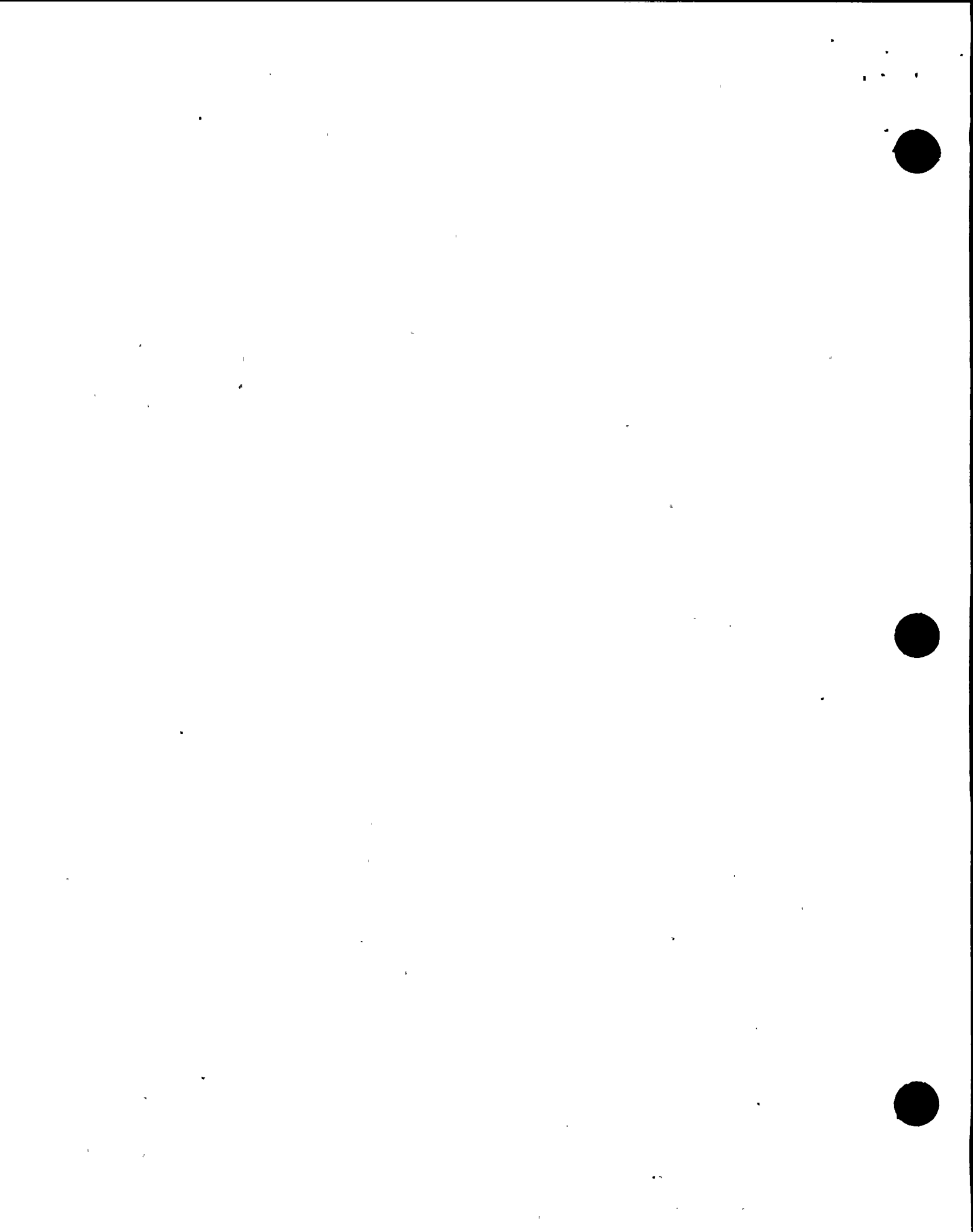


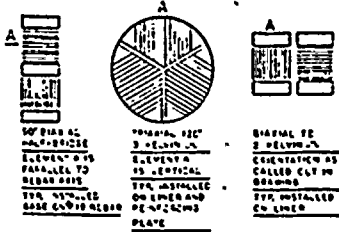
FIGURE 10

SPACECRAFT INSTRUMENTATION
 SYMBOLS & DIMENSIONS

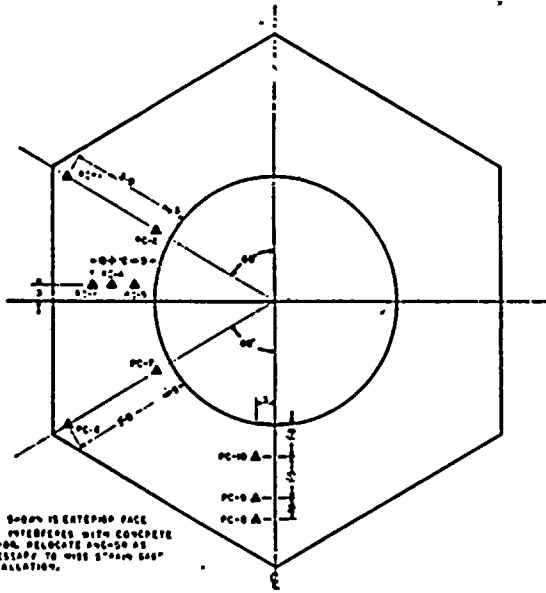
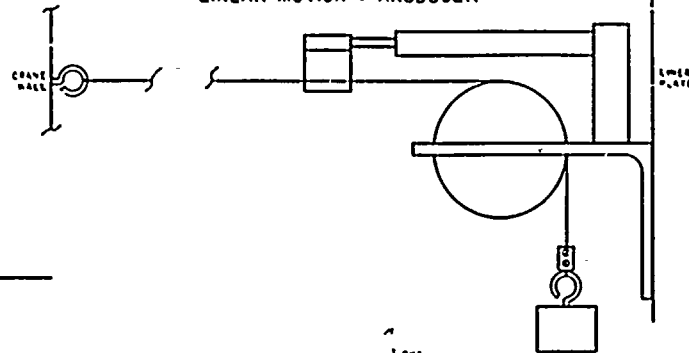
cte	C-2141-N01
<i>V. J. J. J. J.</i>	
SPACE POSITIONING CELL: ER, POSE	
ST. T. INSTRUMENTATION	5-21-12



GAGE ELEMENT ORIENTATION

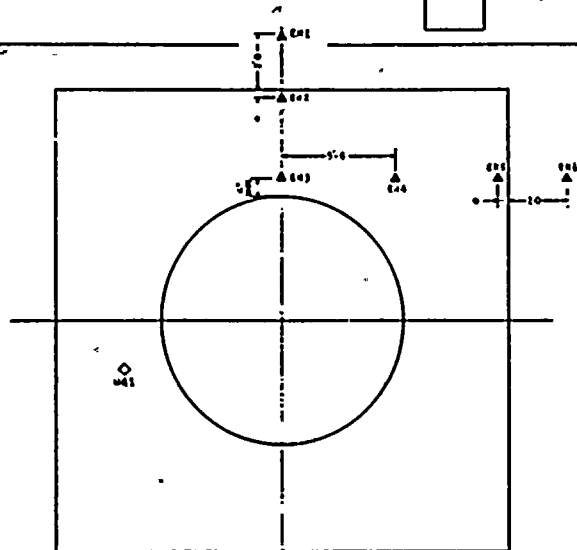


LINEAR MOTION TRANSDUCER



1. VIEW 3-0000 REINTERPRET FACE
2. PC-6 INTERFERES WITH COMPLETE
ANALYSIS. RELOCATE PC-6-50 AS
NECESSARY TO CLEAR 3-0000 GAGE
INSTALLATION.

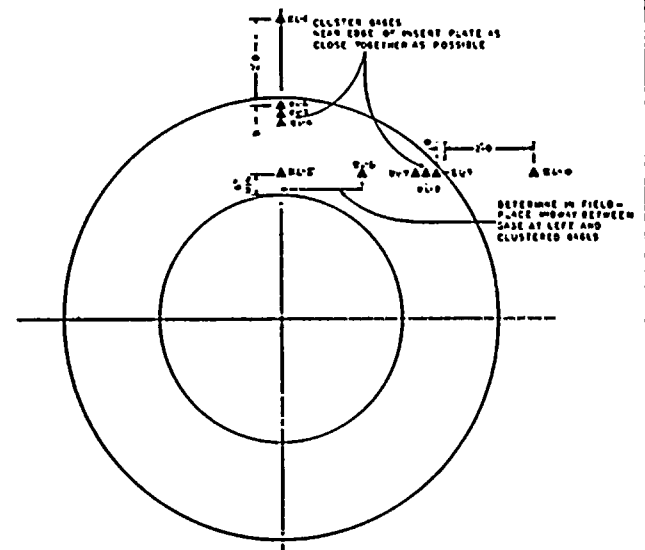
PERSONNEL HATCH



HATCH VIEWED FROM
INSIDE CONTAINMENT

NOTES:
1. PLACE GAGE AS CLOSE TO BEAM
AS POSSIBLE
2. GAGES MAY BE RELOCATED 90° TO
AVOID FIELD CONFLICTS ALONG
CENTERLINE - ADVISE PAGE

EQUIPMENT HATCH



HATCH VIEWED FROM
INSIDE CONTAINMENT

NOTES:
1. PLACE GAGE AS CLOSE TO BEAM AS POSSIBLE.
2. GAGES MAY BE RELOCATED 90° TO AVOID FIELD
CONFLICTS ALONG CENTERLINE - ADVISE PAGE

EMERGENCY HATCH **FIGURE 11**

cto	C-2141-NO1
<p>DATE: 1/10/70 BY: J. L. ... SIT INSTRUMENTATION - SUMMARY OF ENLARGED VIEWS</p>	
	21-1-3



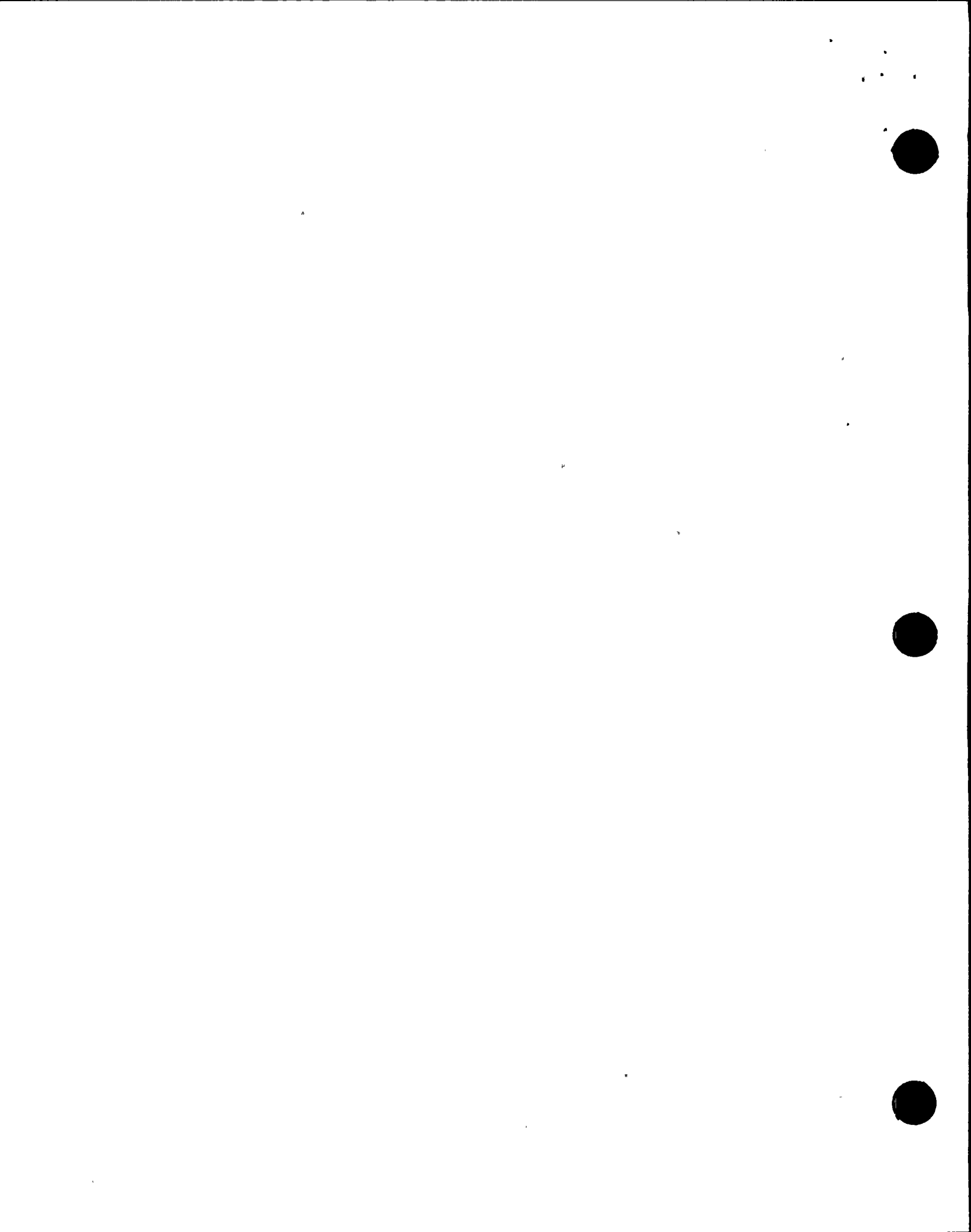
Hexagonal ring plate

Personnel hatch plate was instrumented with three axial strain rosettes placed at ten points (Code PC, Figure 11).

Containment liner

1. Ten points spaced at 30' along the meridian at azimuth 110° were instrumented with two axial strain rosettes (Code 1LM). In addition, four rosettes were also placed at the base slab juncture (Code 1LB).
2. The liner was also instrumented near major openings where three axial strain rosettes were used as follows:
 - 6 rosettes at equipment hatch (Code EH)
 - 10 rosettes at emergency hatch (Code EL)

(See Figure 10)



CRACK OBSERVATION AREA NO. 2A

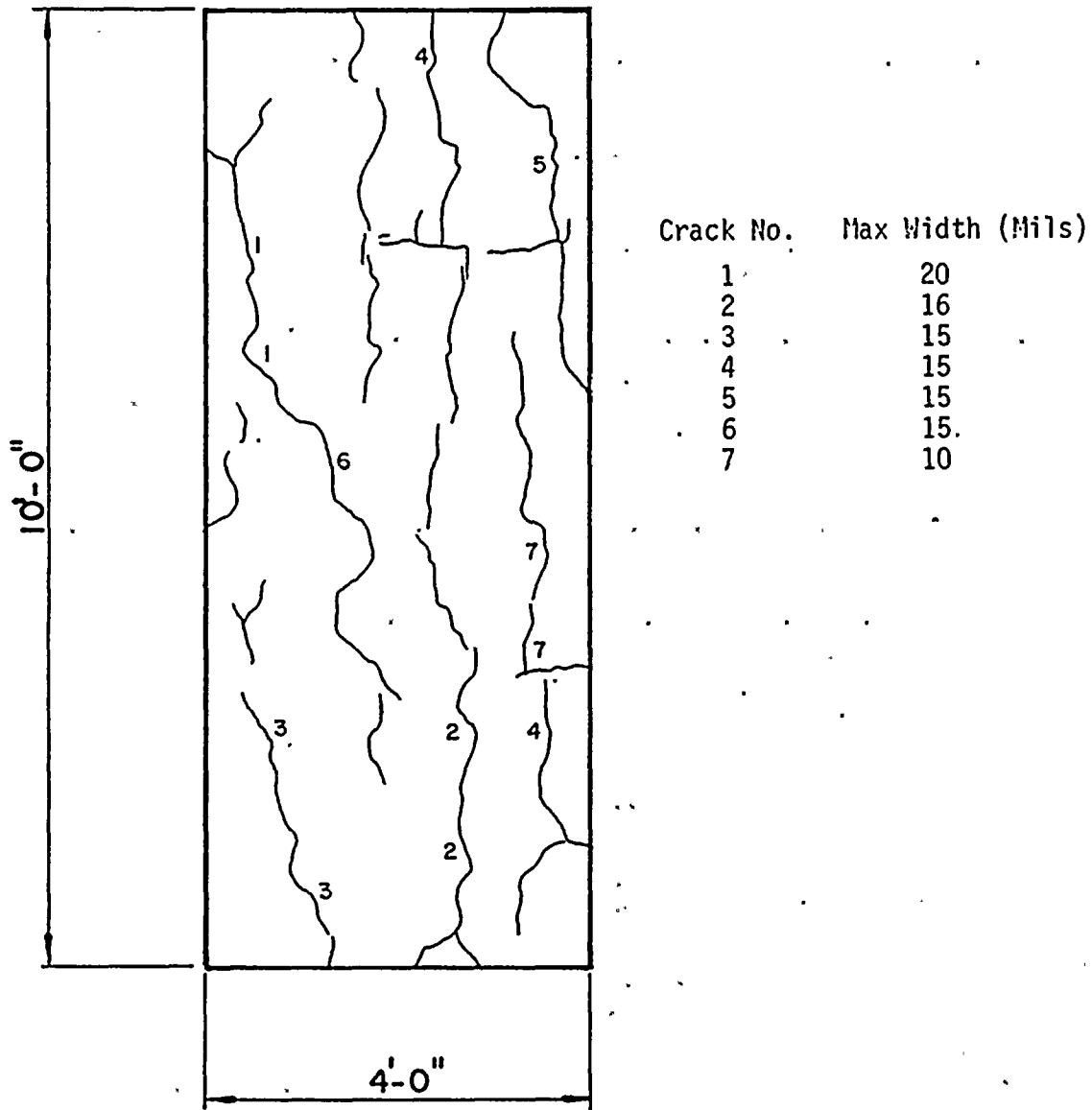
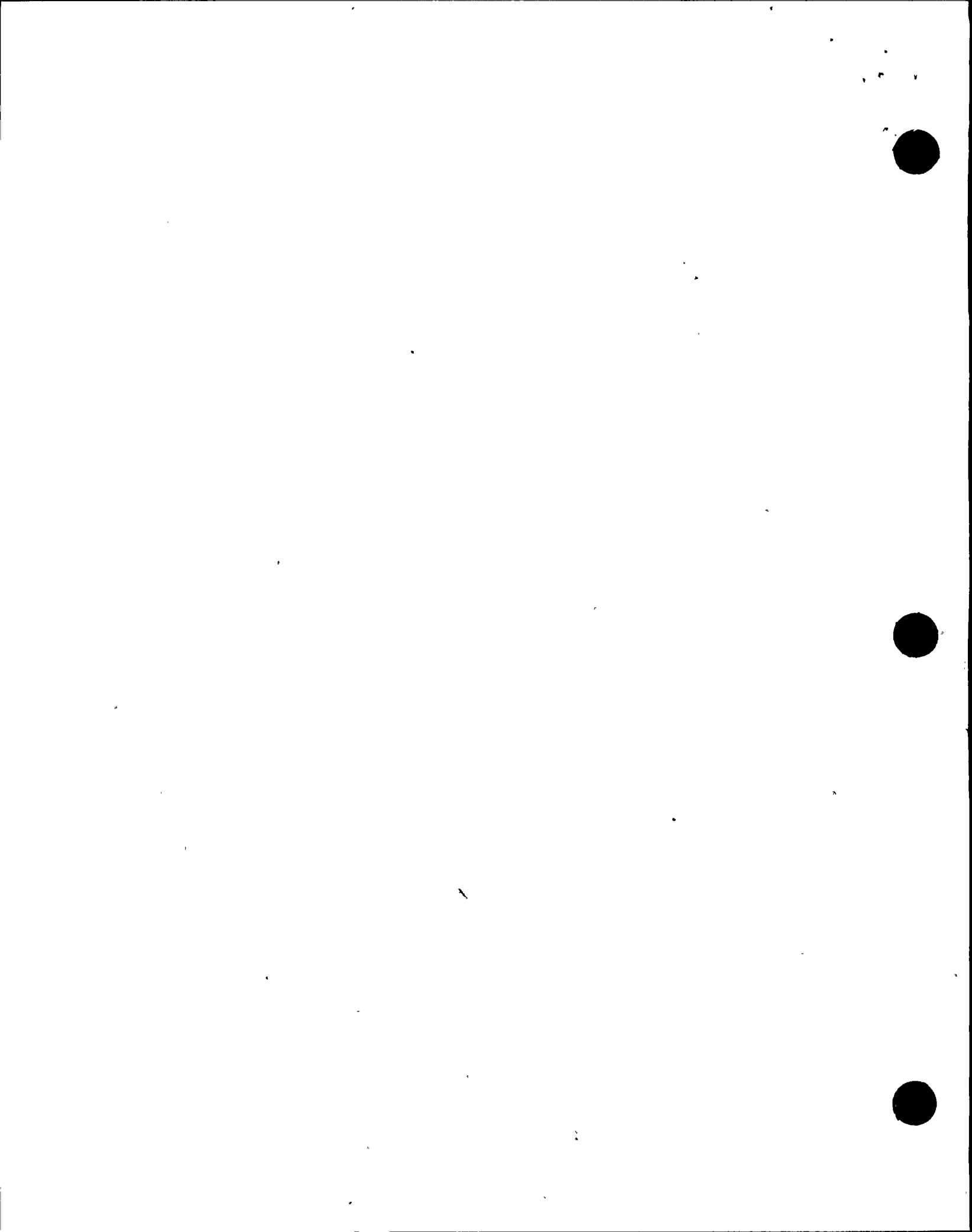
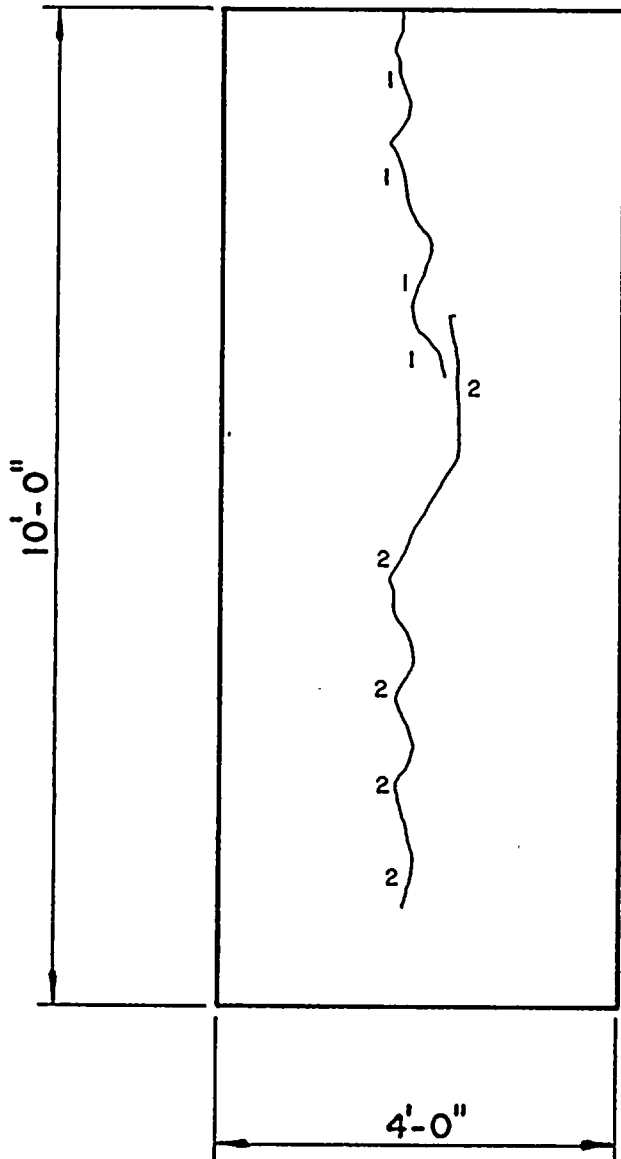


FIGURE 12.1 - Crack Pattern at 54 PSIG

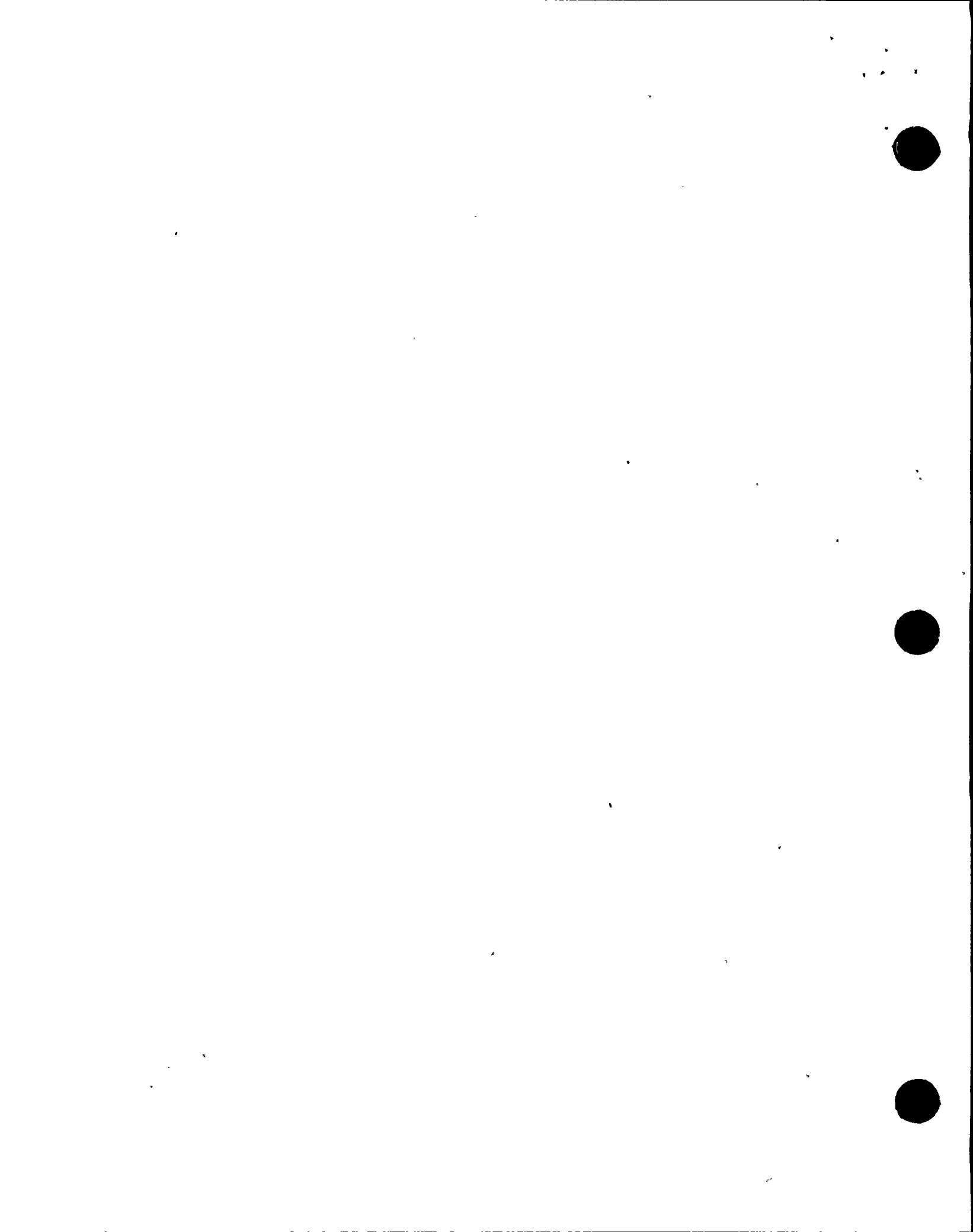


CRACK OBSERVATION AREA NO. 2B

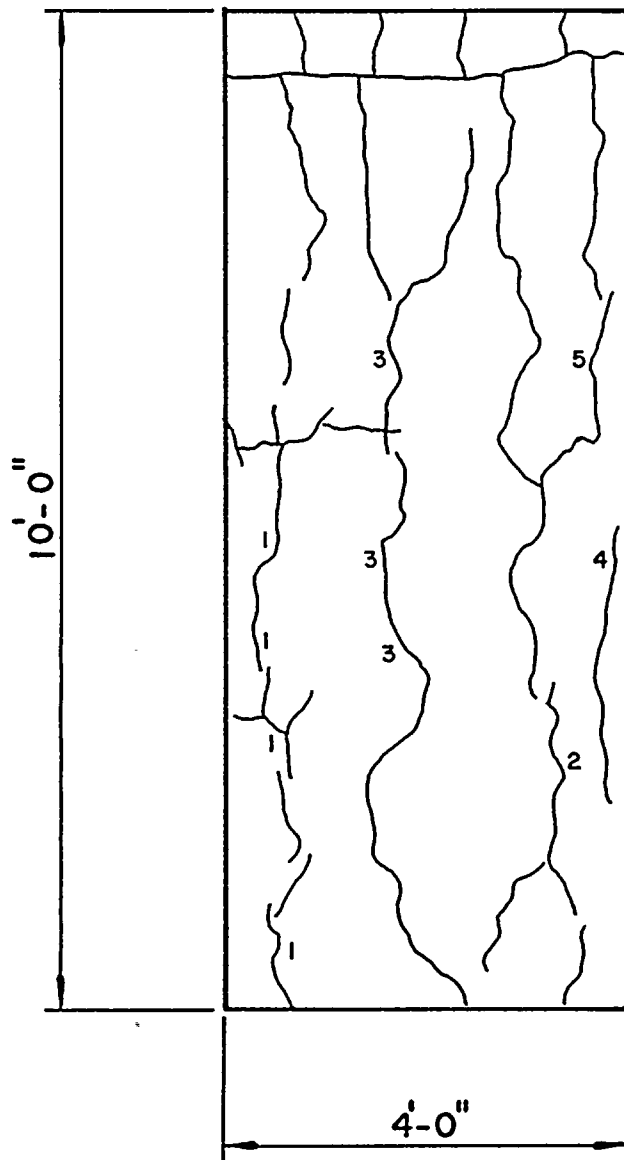


Crack No.	Max Width (Mils)
1	18
2	25

FIGURE 12.2 - Crack Pattern at 54 PSIG



CRACK OBSERVATION AREA NO. 2C

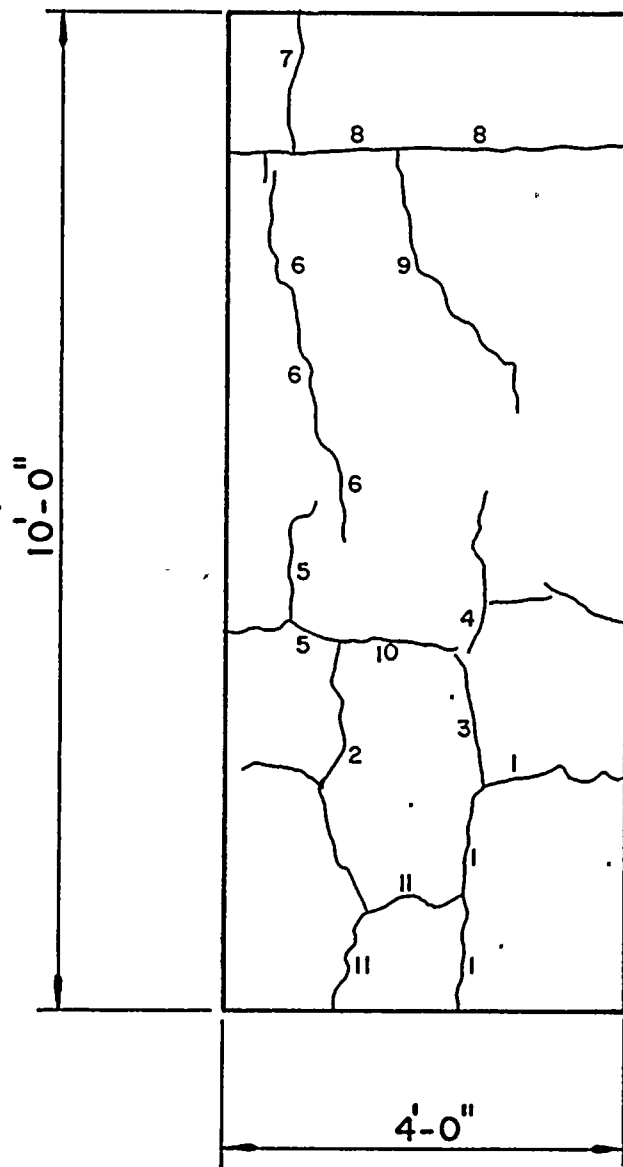


Crack No.	Max Width (Mils)
1	10
2	10
3	15
4	10
5	10

FIGURE 12.3 - Crack Pattern at 54 PSIG



CRACK OBSERVATION AREA NO. 3A

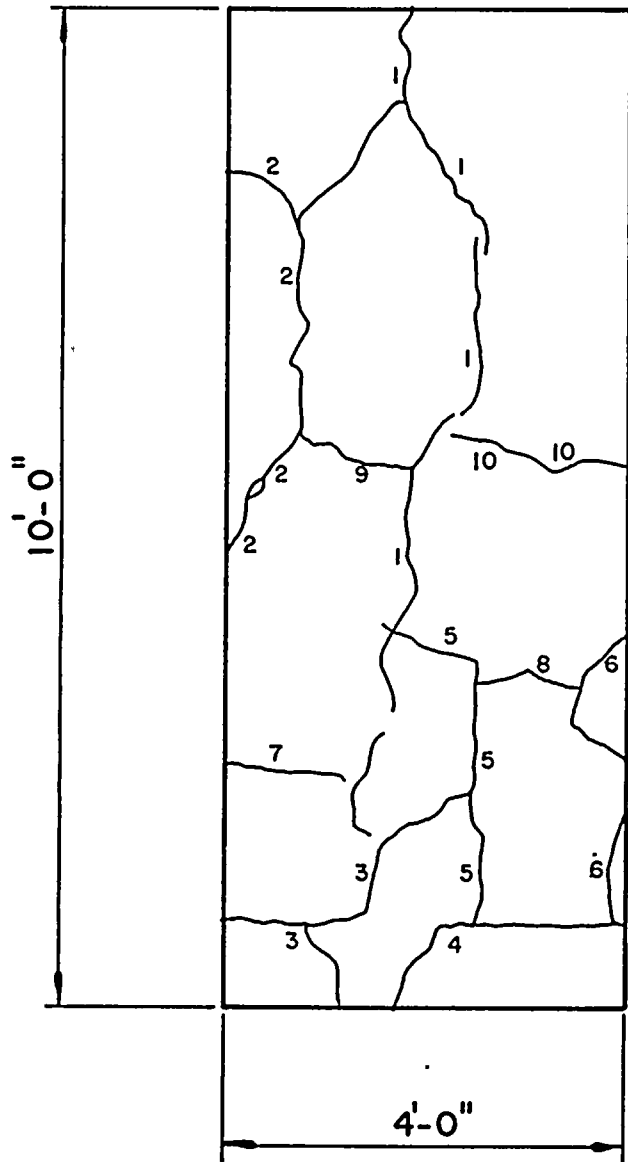


Crack No.	Max Width (Mils)
1	20
2	15
3	20
4	15
5	20
6	20
7	20
8	30
9	15
10	13
11	15

FIGURE 12.4 - Crack Pattern at 54 PSIG



CRACK OBSERVATION AREA NO. 3B



Crack No.	Max Width (Mils)
1	25
2	19
3	13
4	15
5	15
6	16
7	15
8	16
9	18
10	20

FIGURE 12.5 - Crack Pattern at 54 PSIG



CRACK OBSERVATION AREA NO. 3C

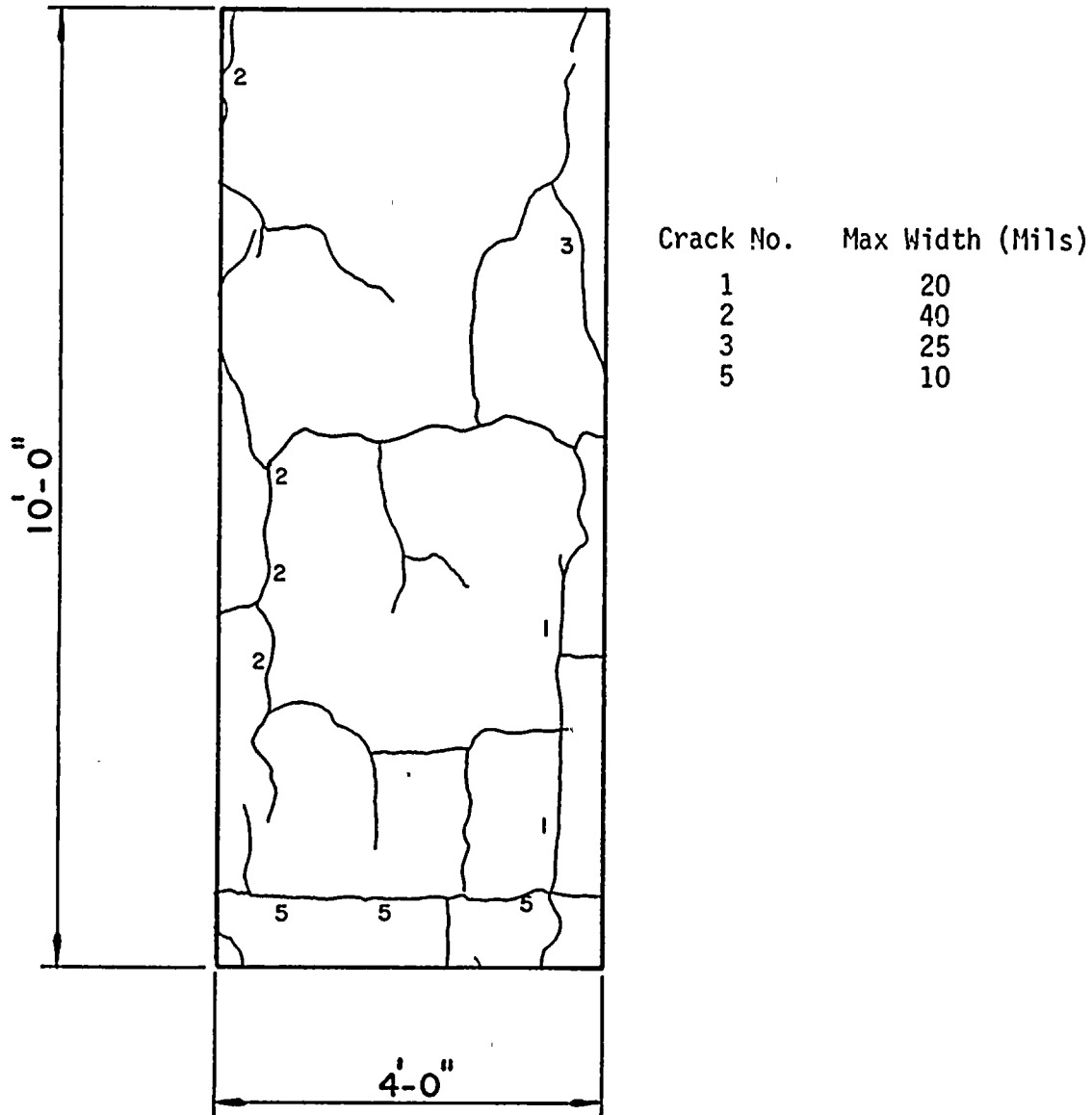
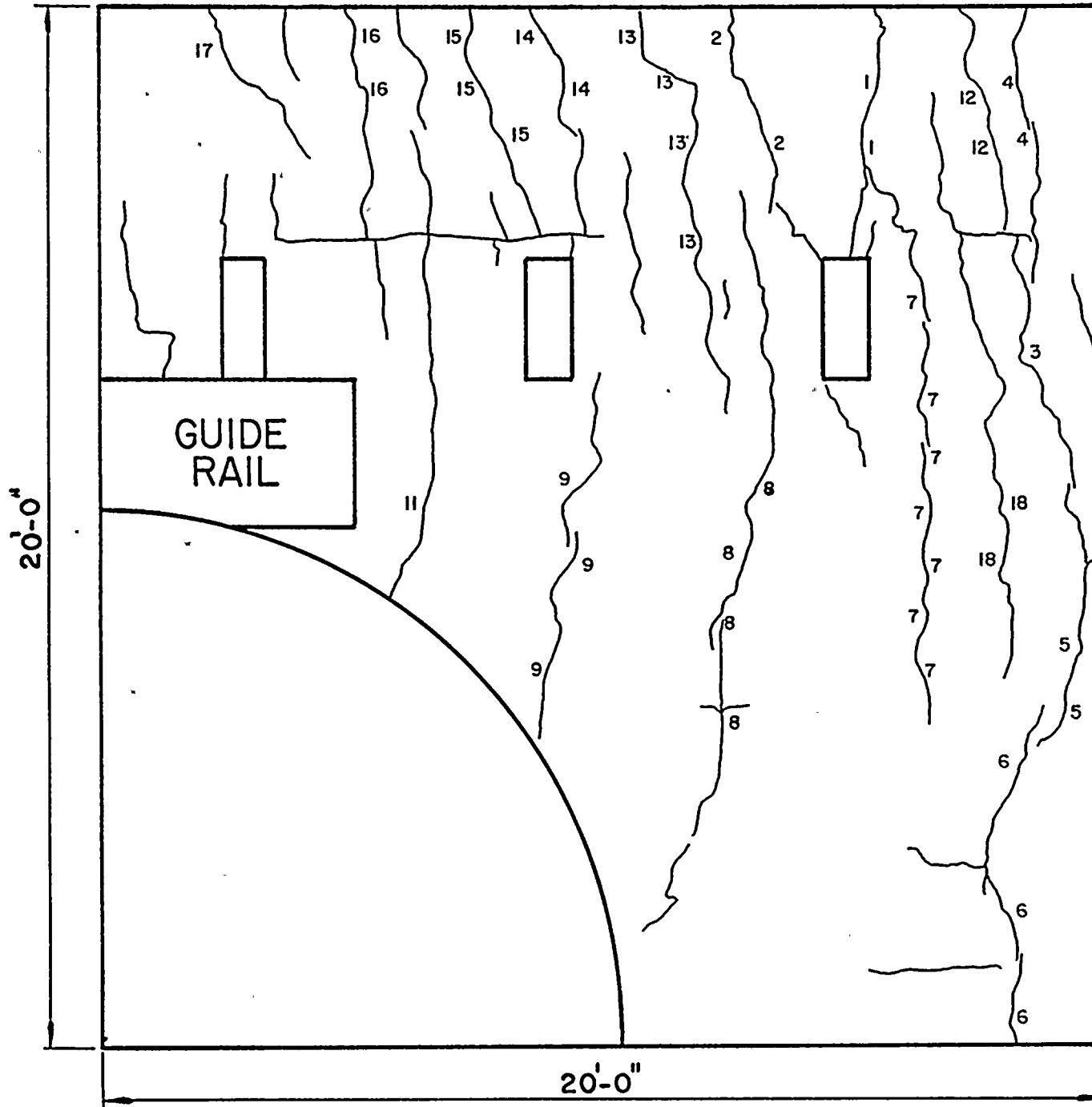


FIGURE 12.6 - Crack Pattern at 54 PSIG



CRACK OBSERVATION AREA NO. I-D

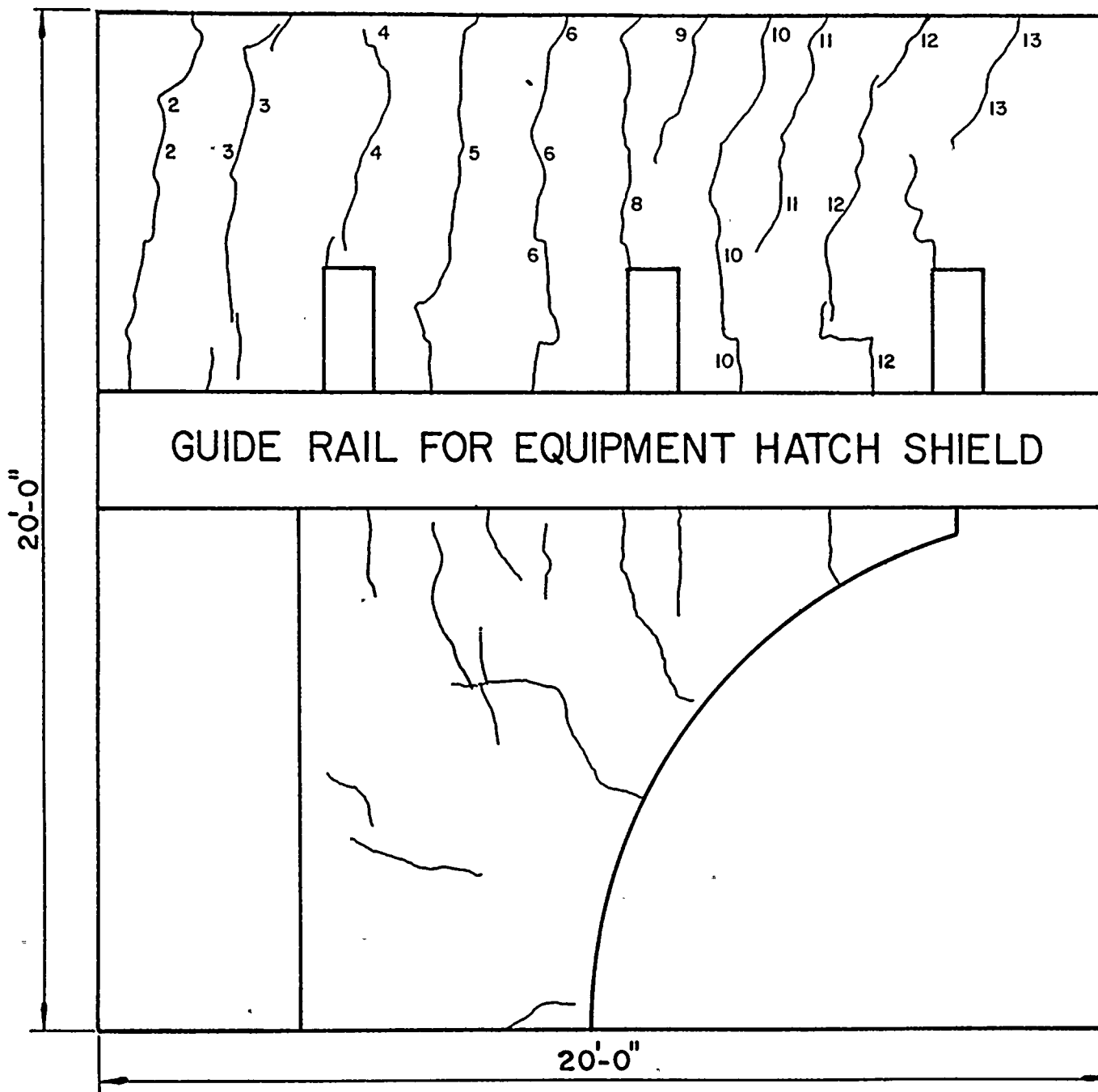


Crack No.	Max Width
1	30
2	25
3	20
4	15
5	40
6	30
7	20
8	20
9	20
11	20
12	20
13	15
14	15
16	13
17	13
18	15

FIGURE 12.7 - Crack Pattern at 54 PSIG



CRACK OBSERVATION AREA NO. 2-D

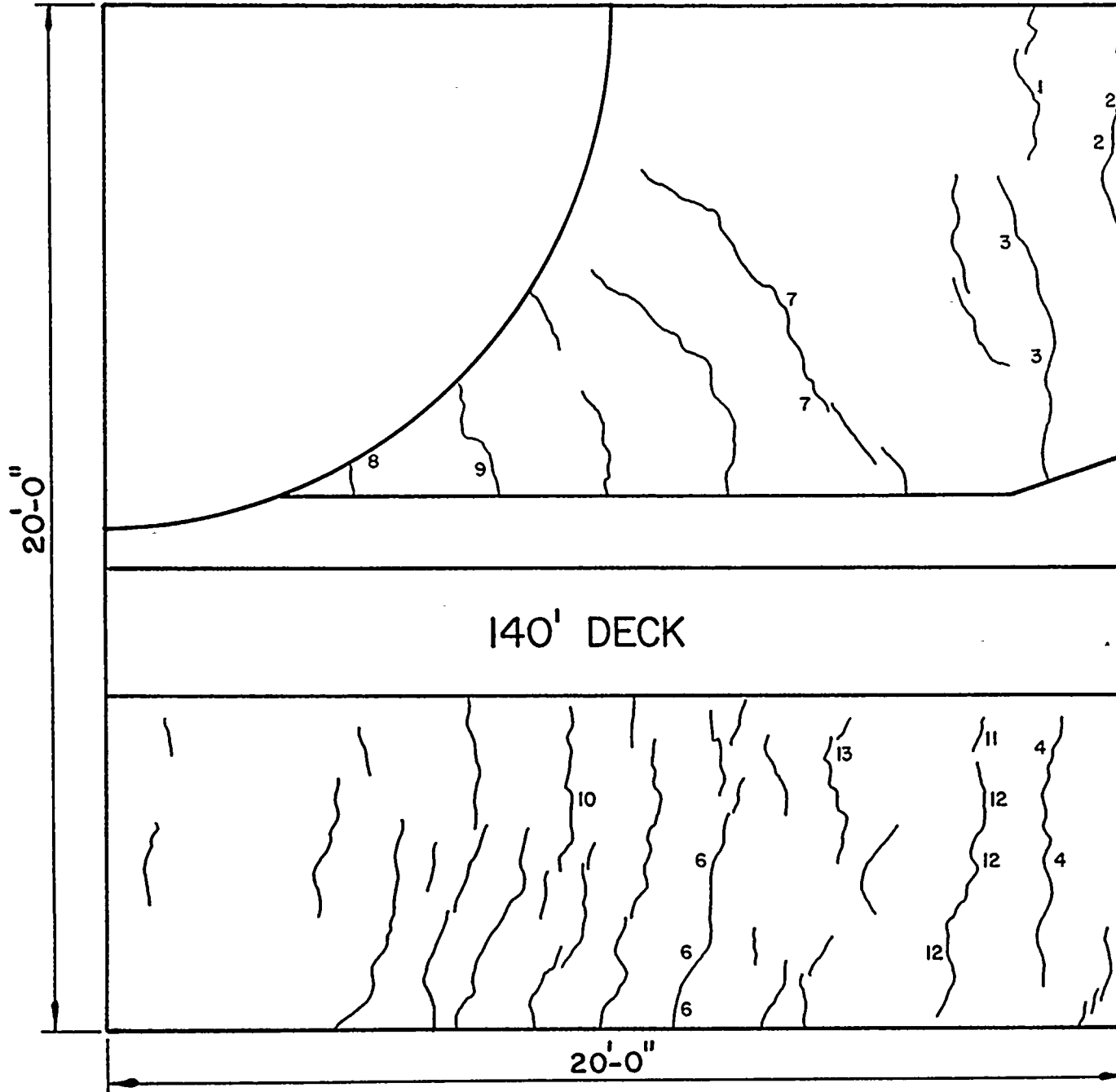


Crack No.	Max Width (Mils)
1	17
2	25
3	23
4	27
5	22
6	20
8	15
9	12
10	15
11	15
12	30
13	15

Figure 12.8 - Crack Pattern at 54 PSIG

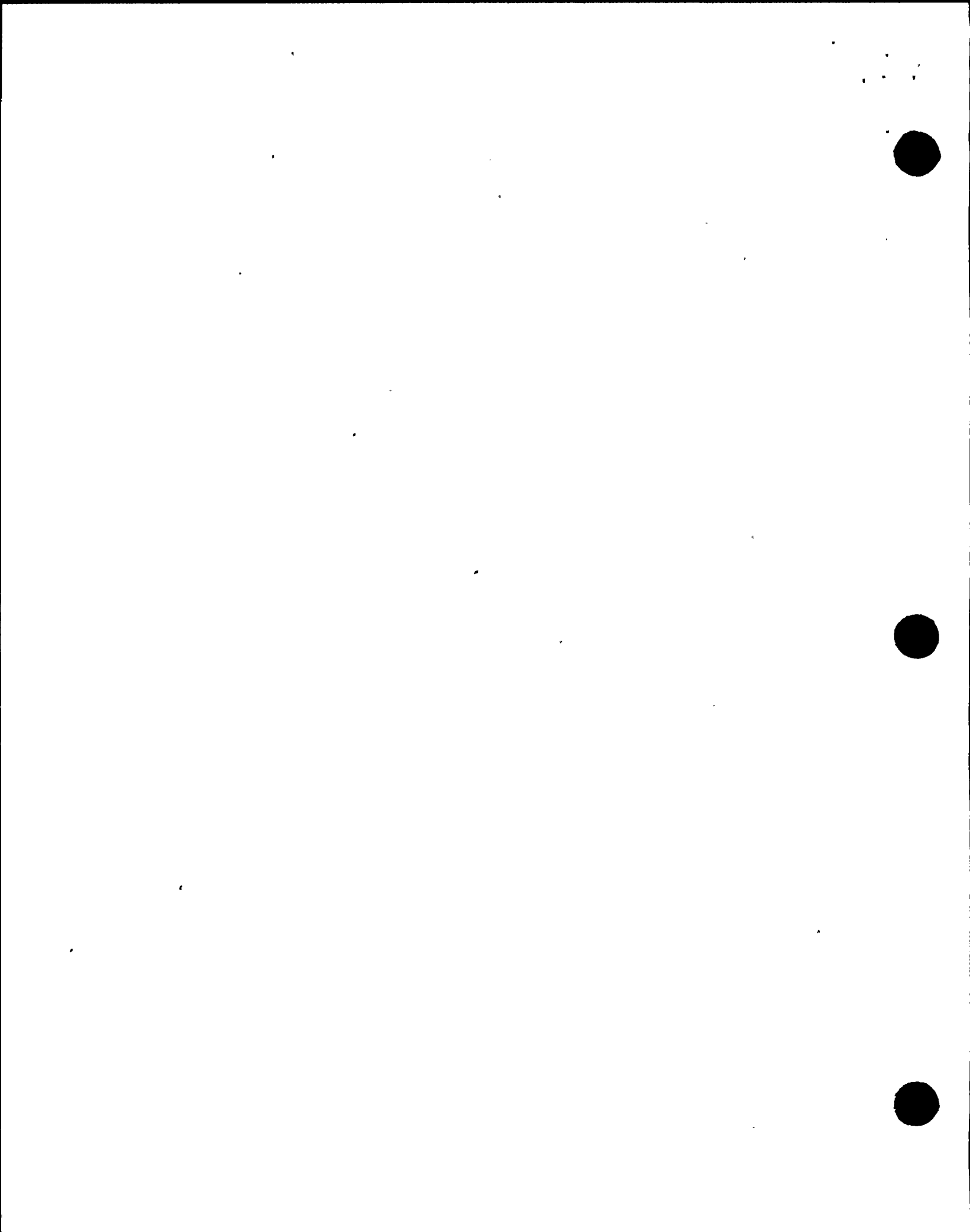


CRACK OBSERVATION AREA NO. 3-D

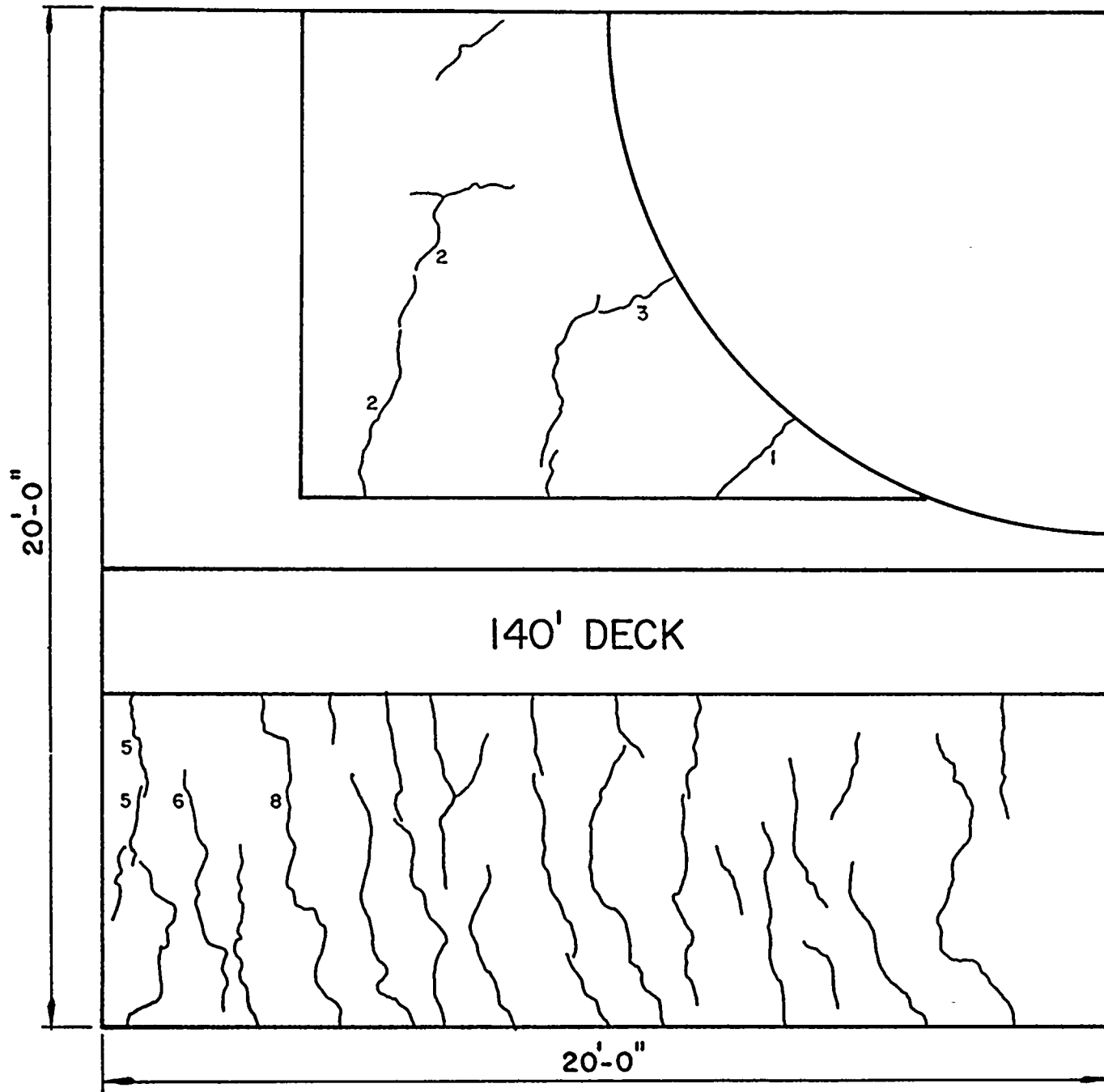


Crack No.	Max Width (Mils)
1	15
2	30
3	30
4	20
6	15
7	15
8	25
9	10
10	10
11	10
12	10
13	15

FIGURE 12.9 - Crack Pattern at 54 PSIG

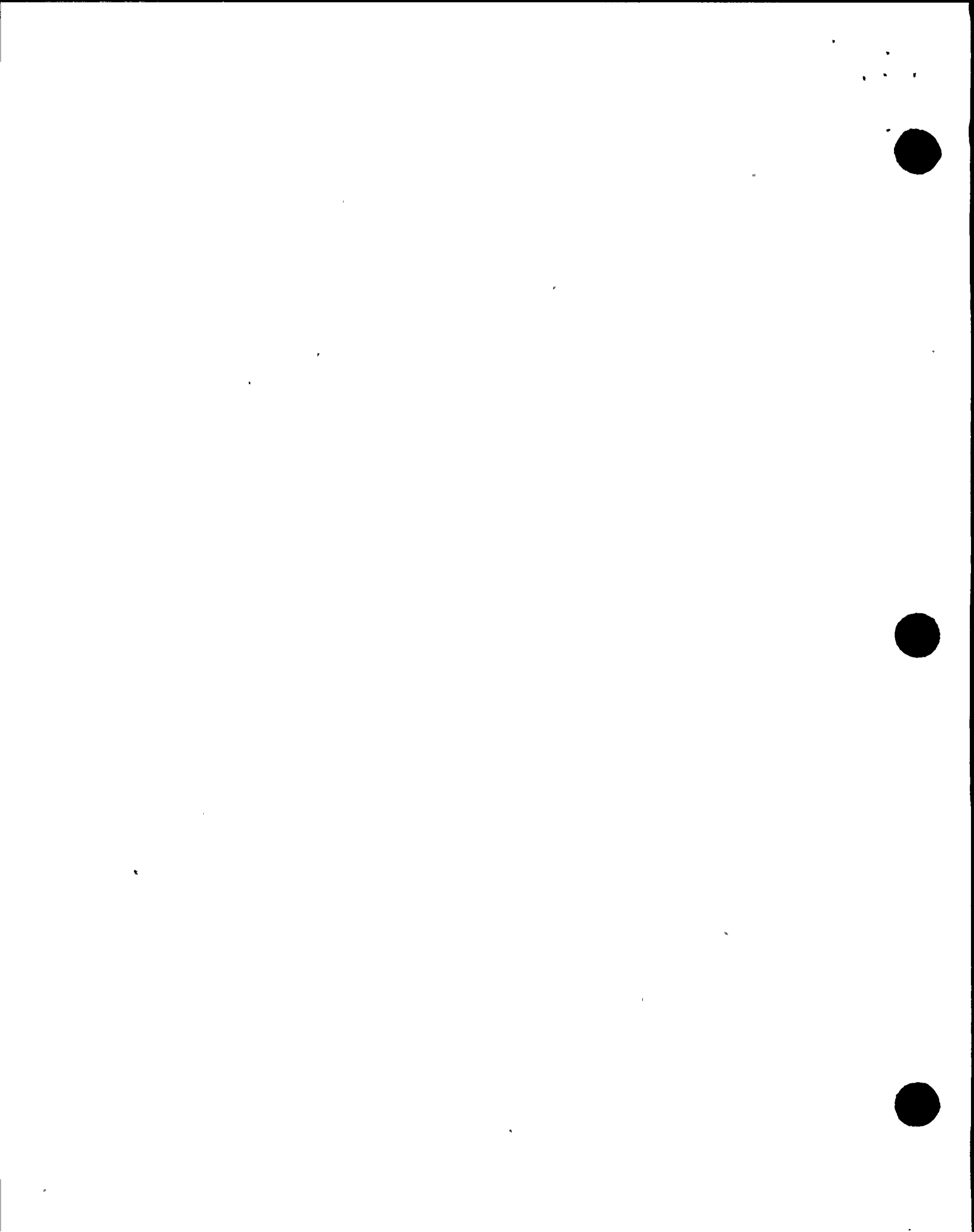


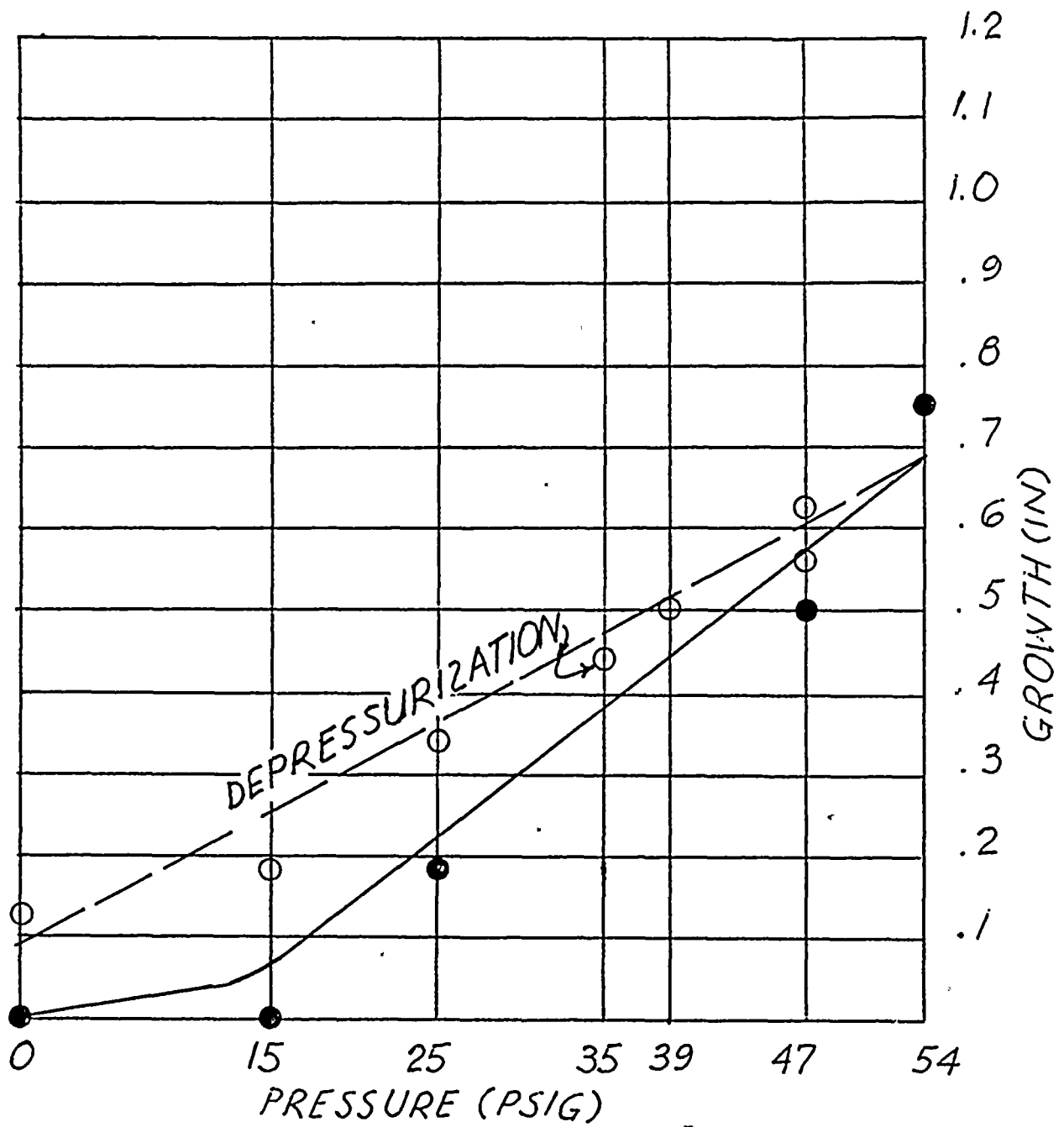
CRACK OBSERVATION AREA NO. 4-D



Crack No.	Max Width (Mils)
1	25
2	10
3	15
5	10
5	10
7	10
8	15
9	10

FIGURE 12.10 - Crack Pattern at 54 PSIG

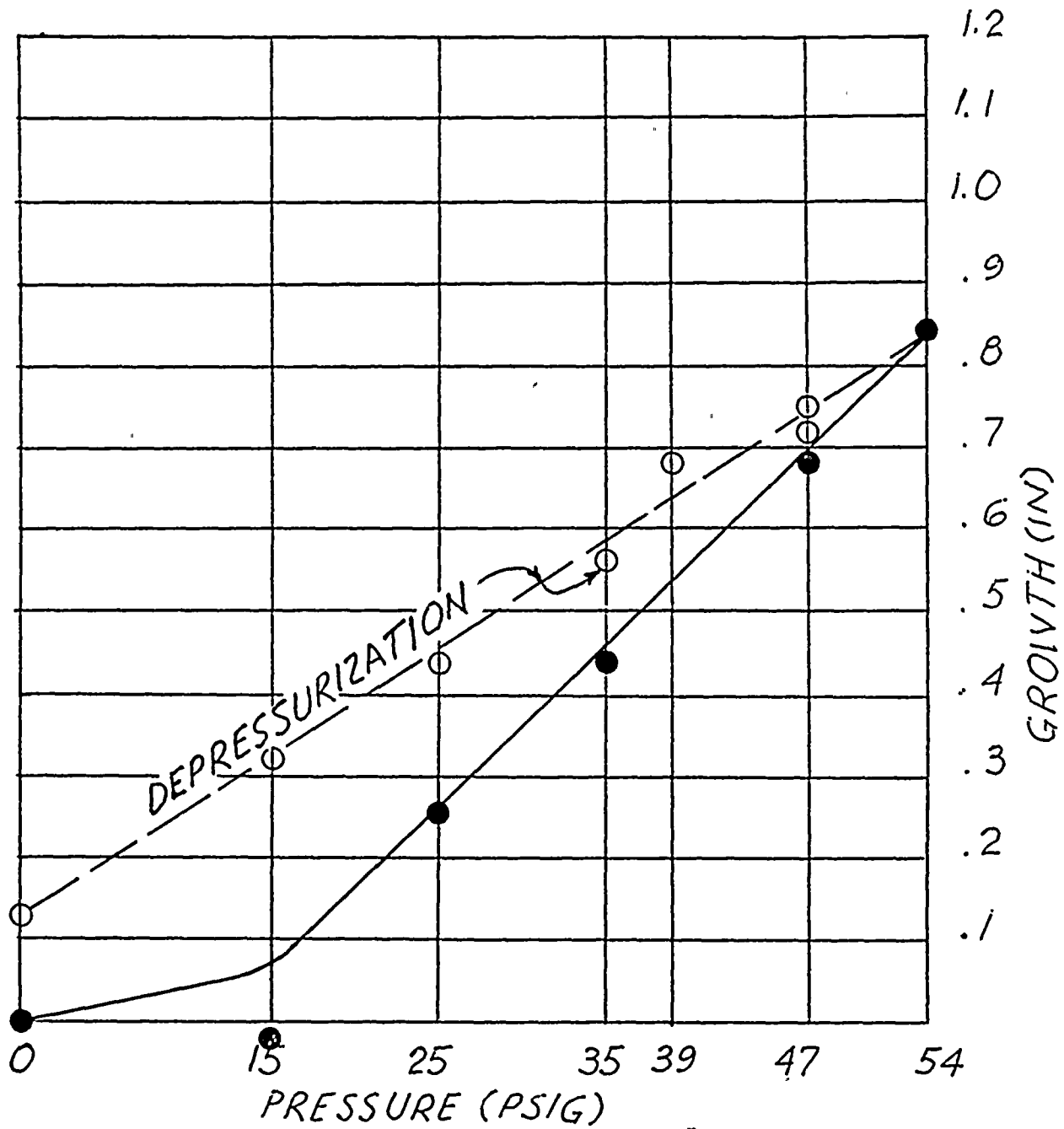




RADIAL GROWTH vs PRESSURE DIAGRAM
OBSERVATION POINT NO. 1

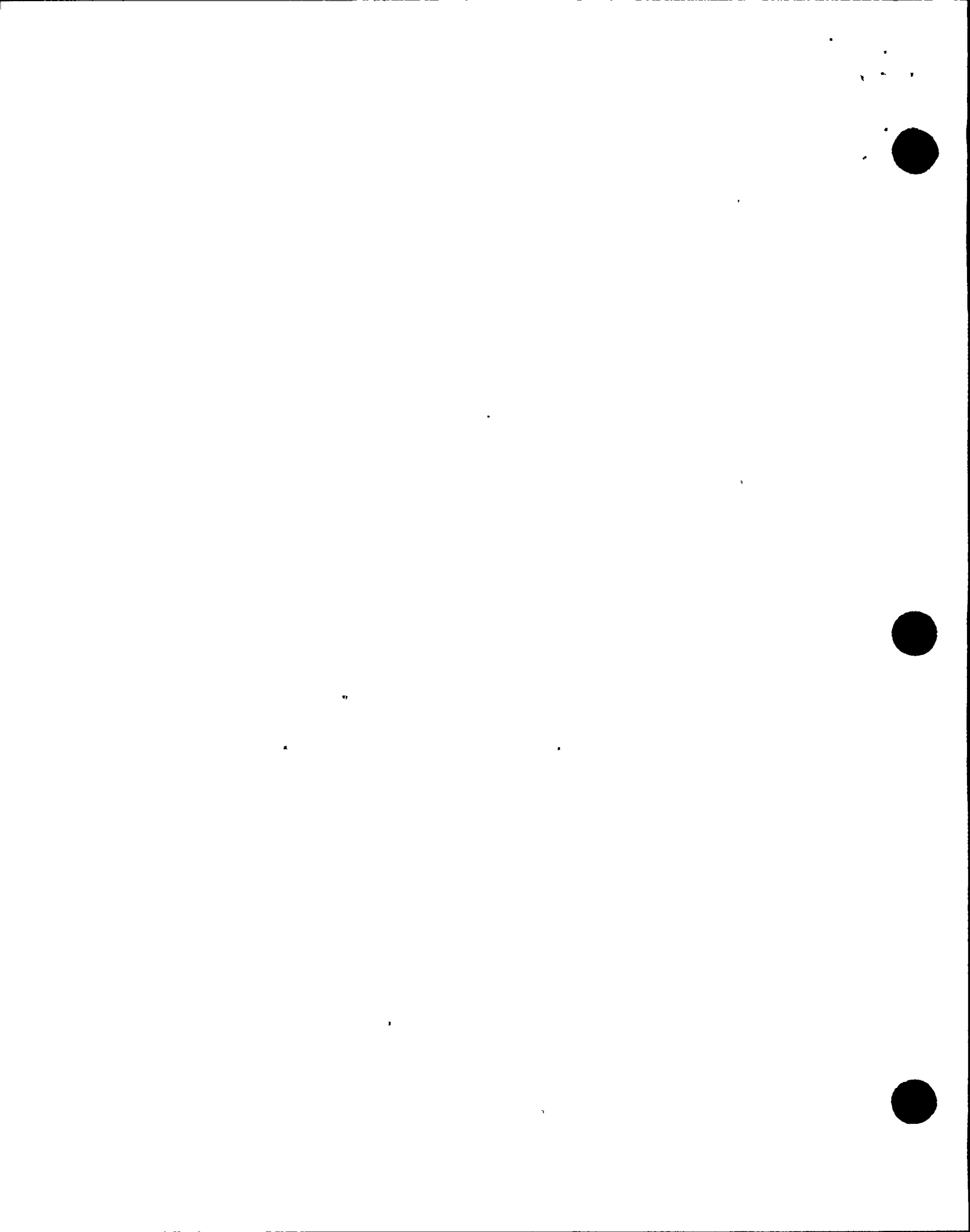
FIGURE 13.1

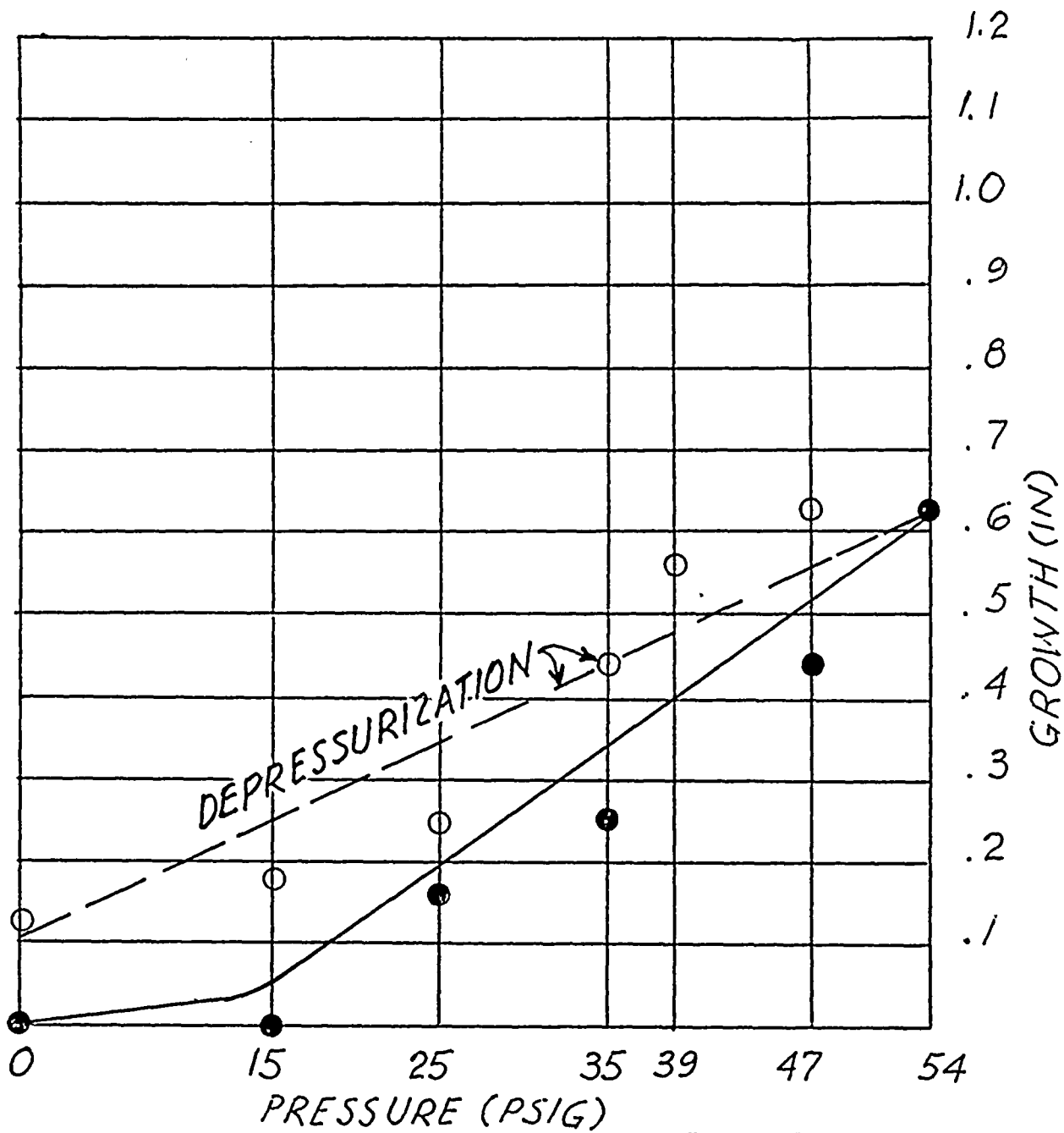




RADIAL GROWTH vs PRESSURE DIAGRAM
OBSERVATION POINT NO. 2

FIGURE 13.2

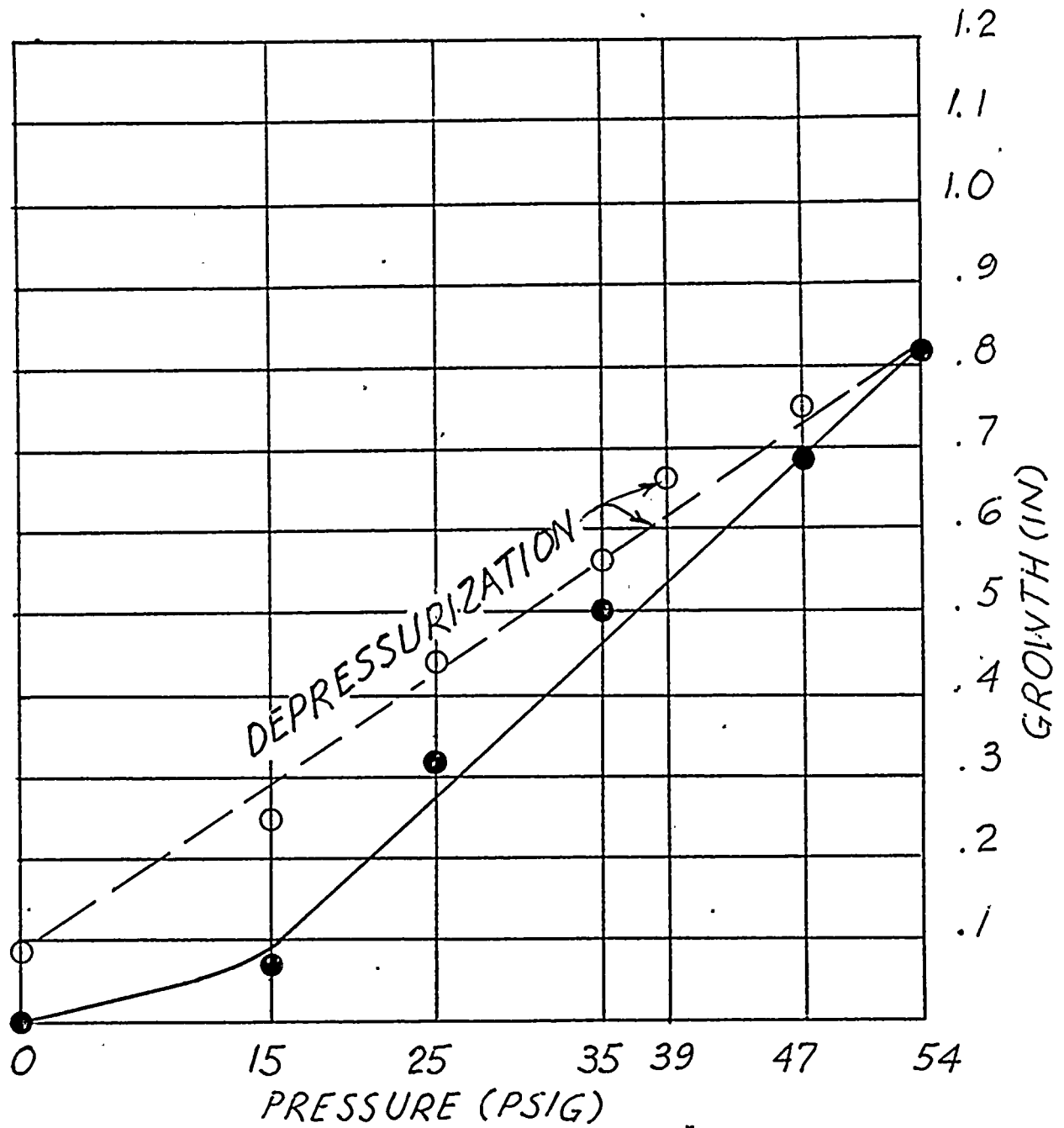




RADIAL GROWTH vs PRESSURE DIAGRAM
OBSERVATION POINT NO. 3

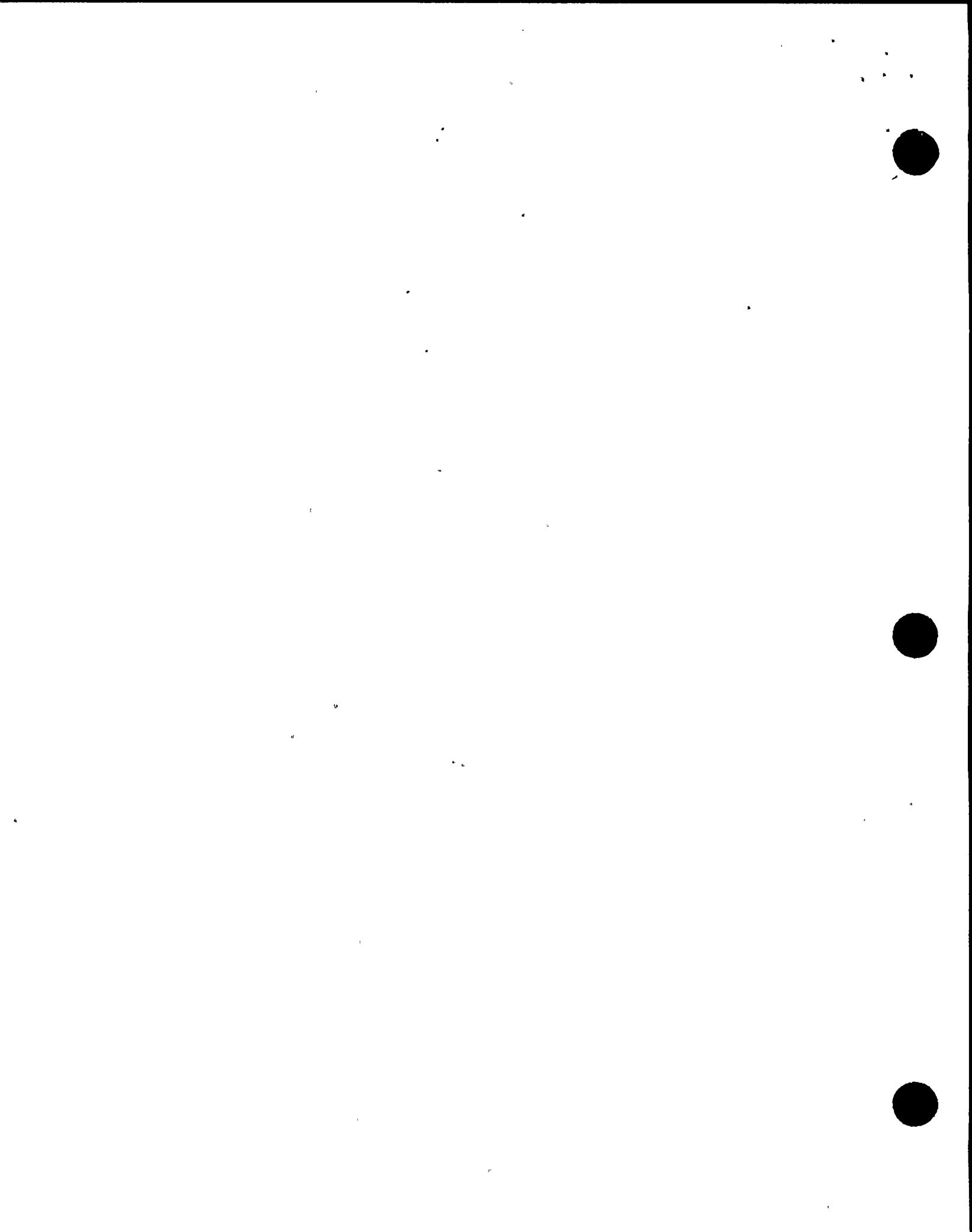
FIGURE 13.3

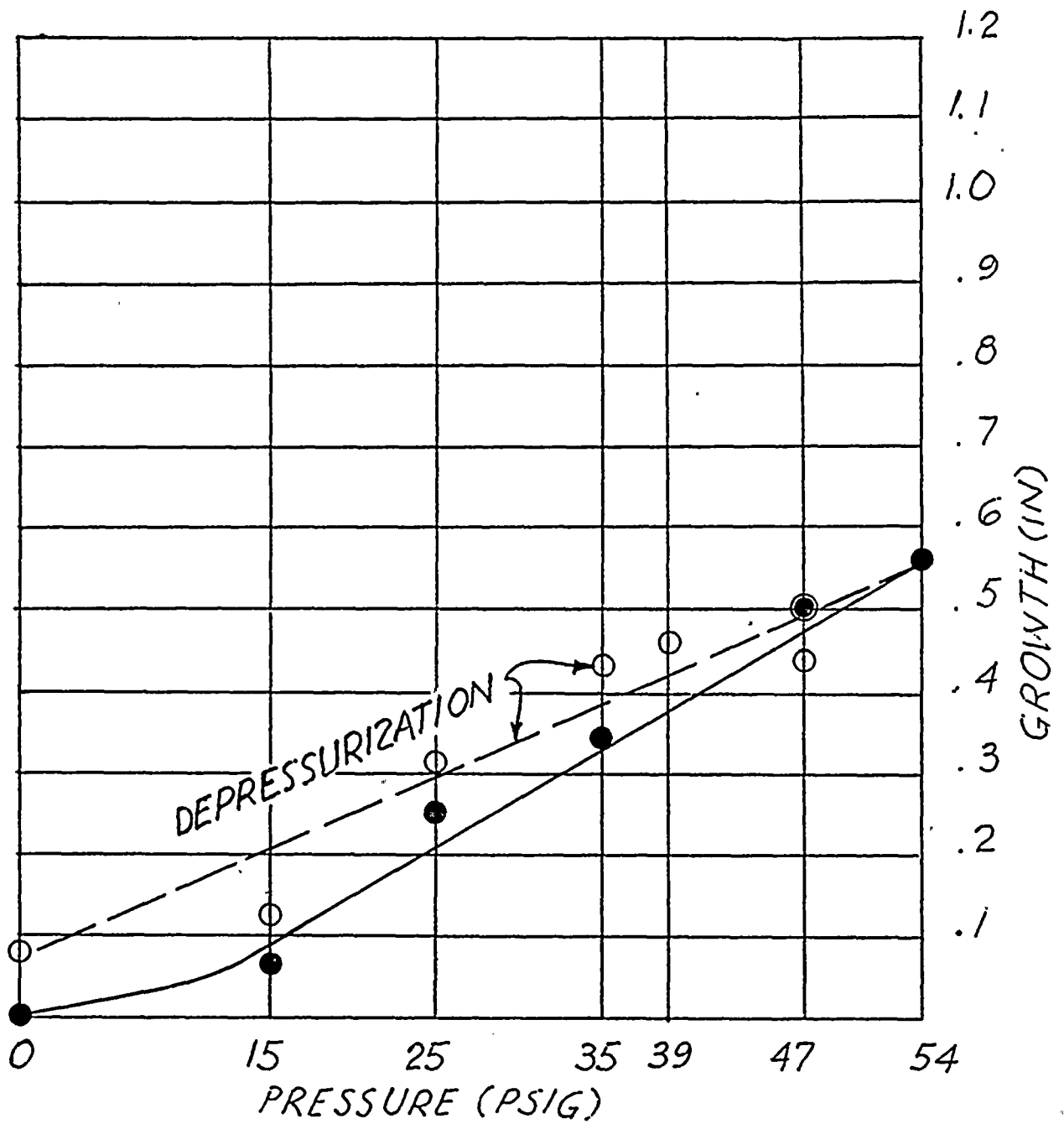




RADIAL GROWTH vs PRESSURE DIAGRAM
OBSERVATION POINT NO. 4

FIGURE 13.4

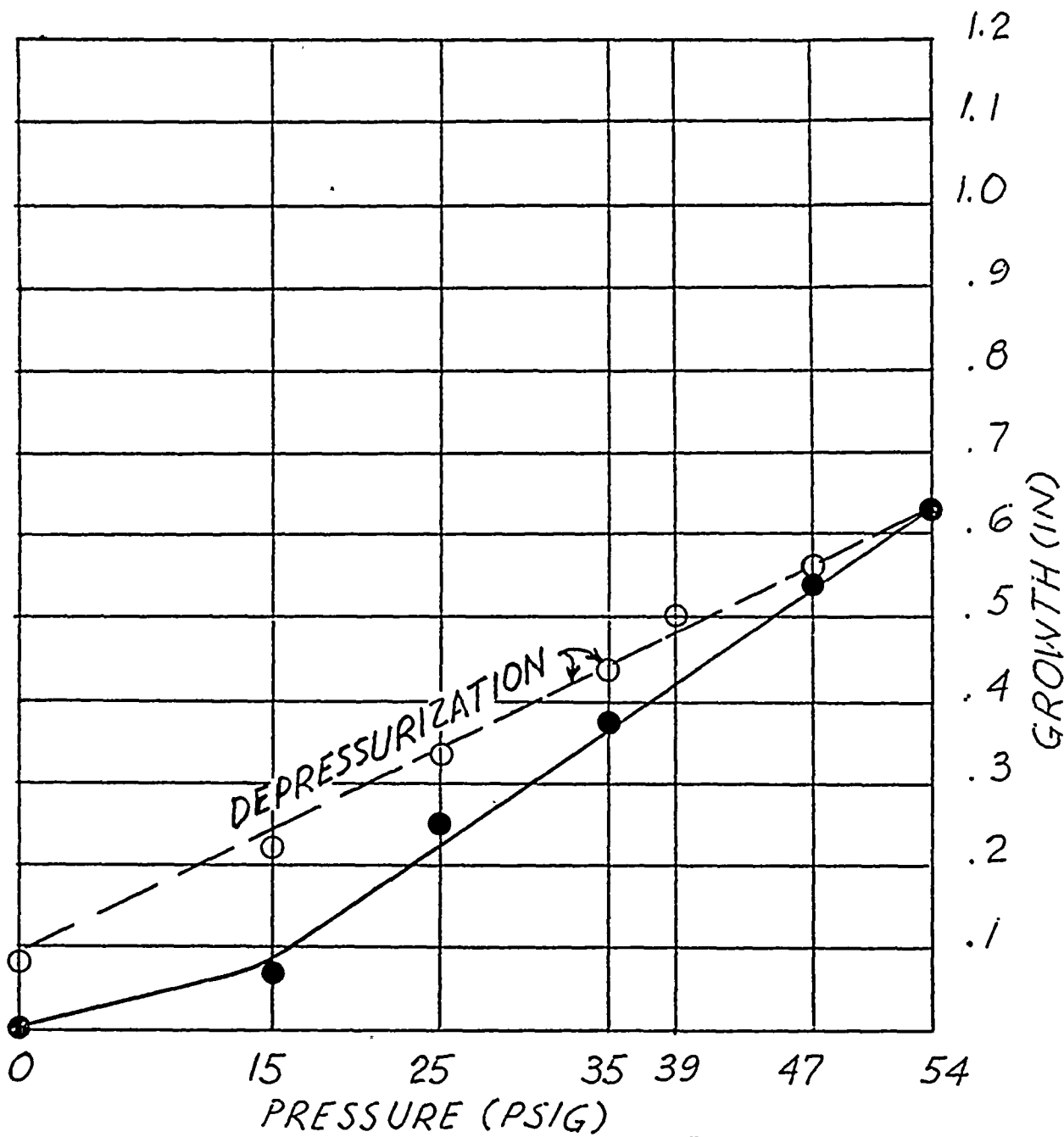




RADIAL GROWTH vs PRESSURE DIAGRAM
OBSERVATION POINT NO. 5

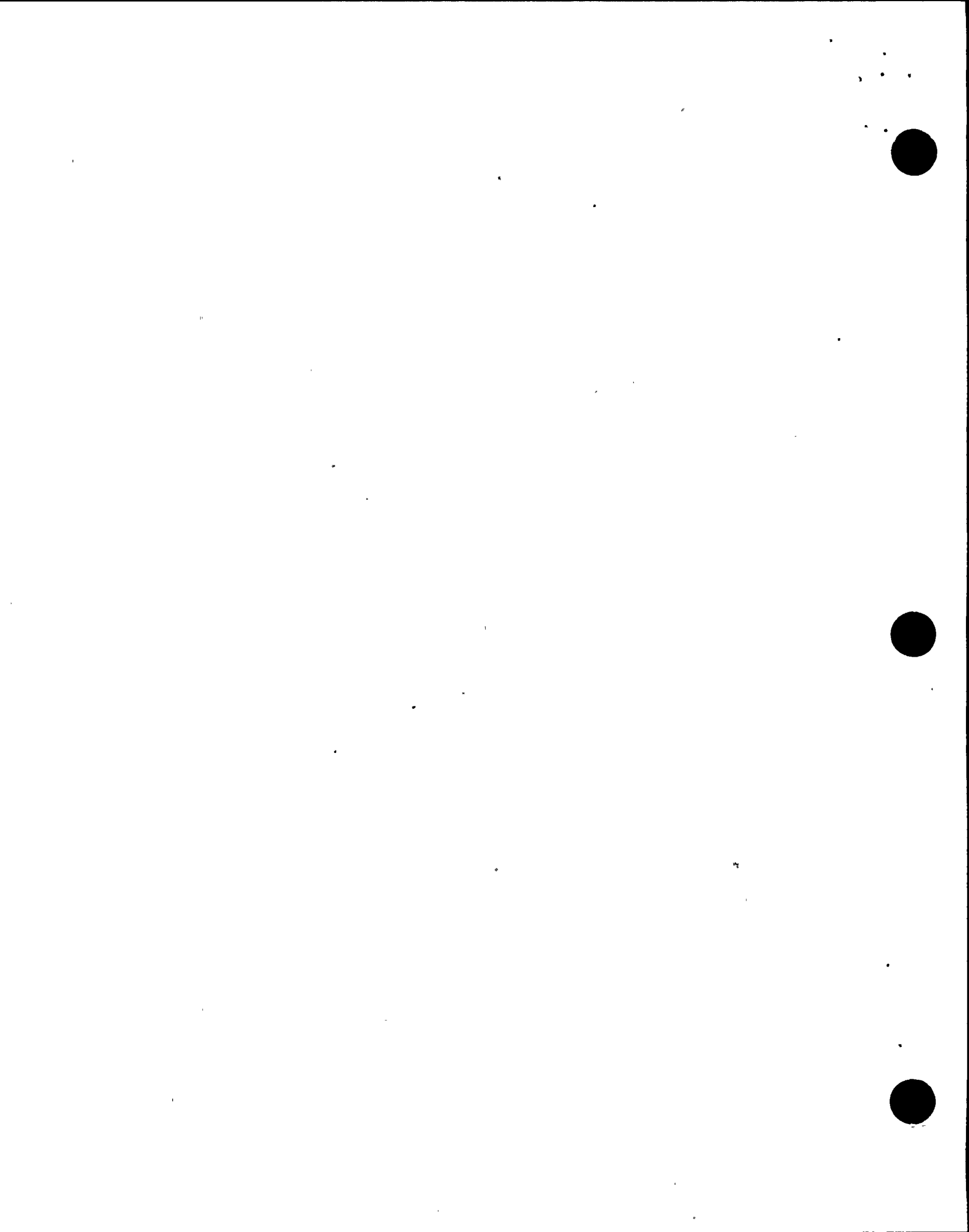
FIGURE 13.5

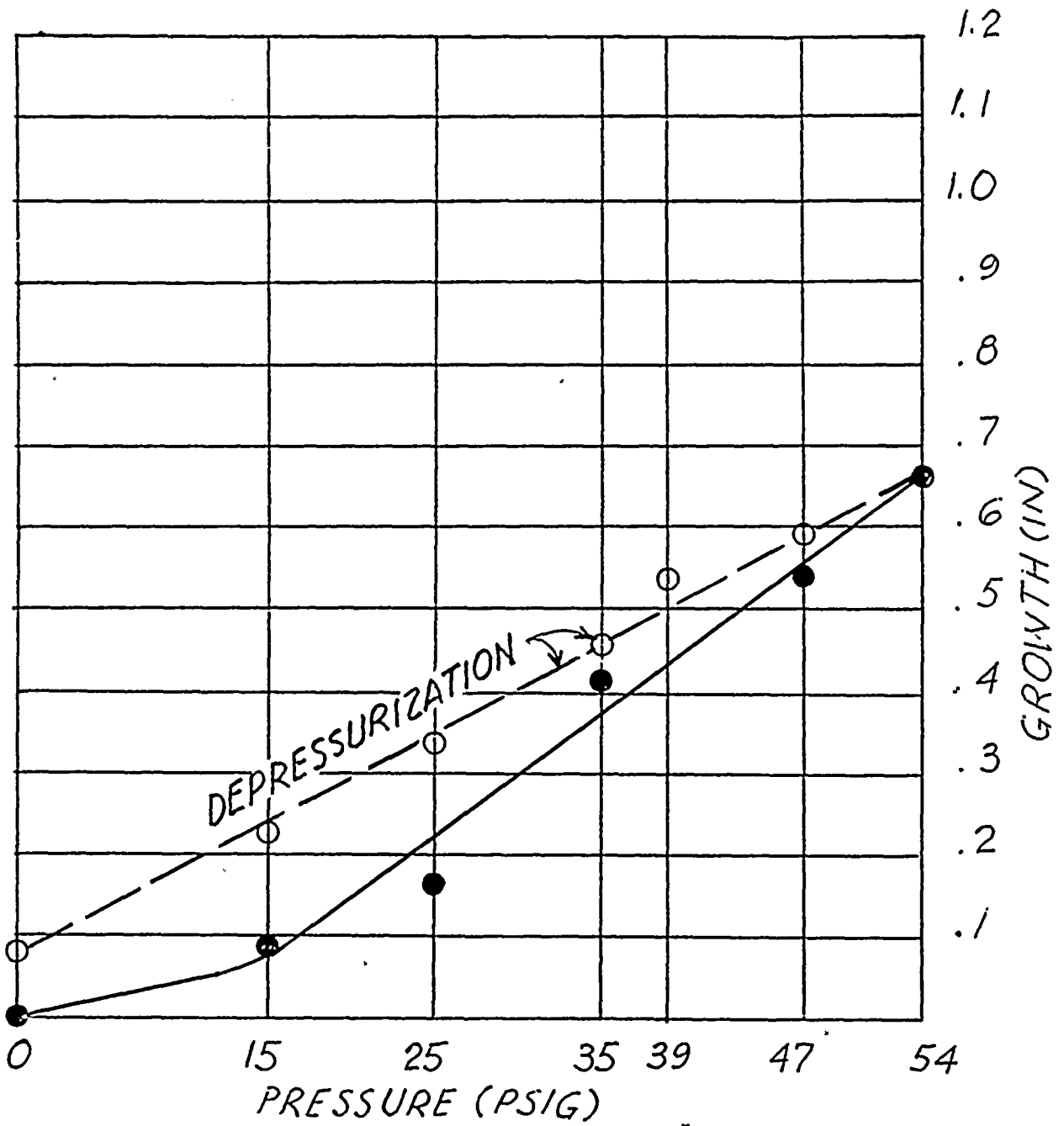




RADIAL GROWTH vs PRESSURE DIAGRAM
OBSERVATION POINT NO. 6

FIGURE 13.6

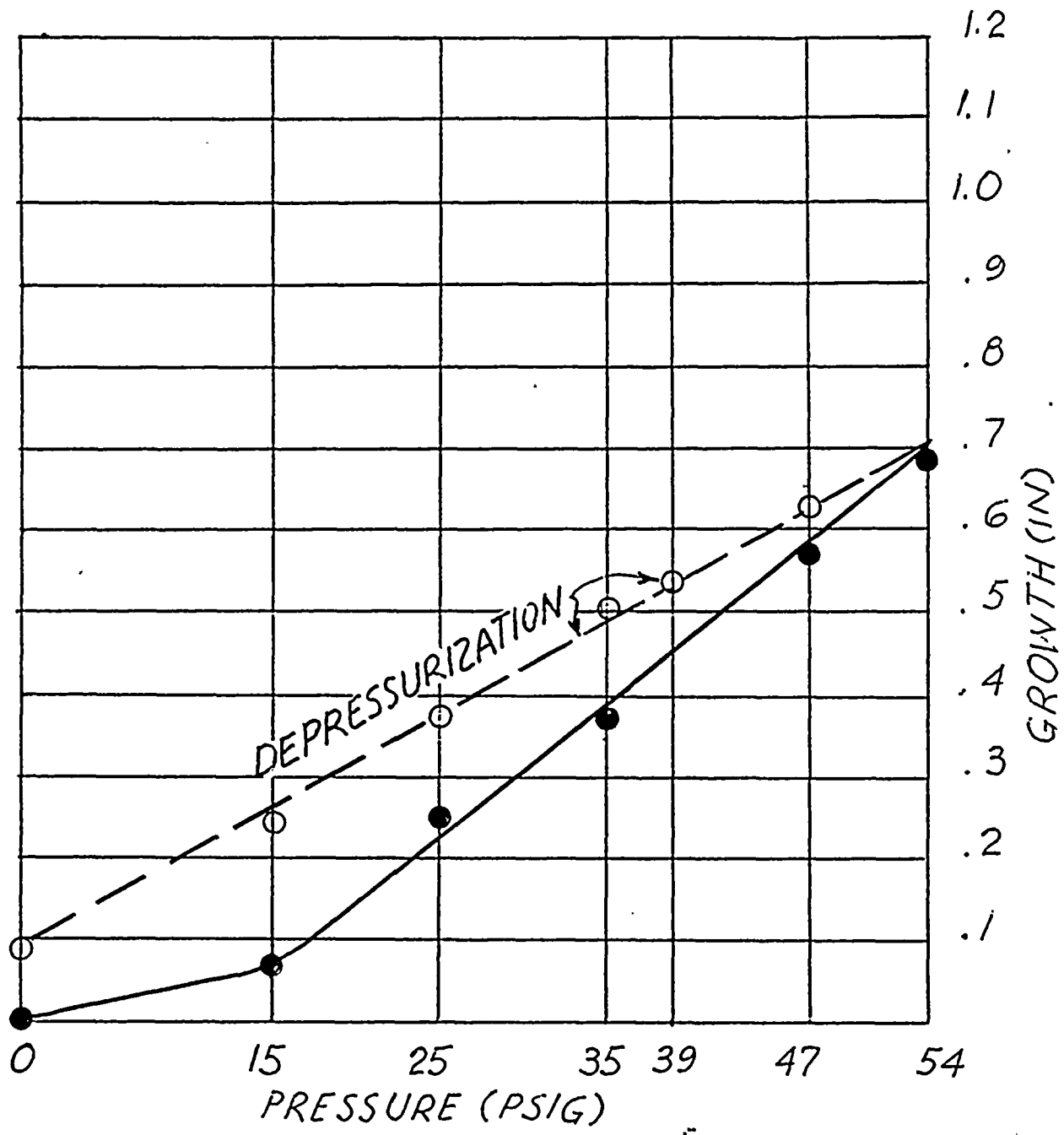




RADIAL GROWTH vs PRESSURE DIAGRAM
OBSERVATION POINT NO. 7

FIGURE 13.7

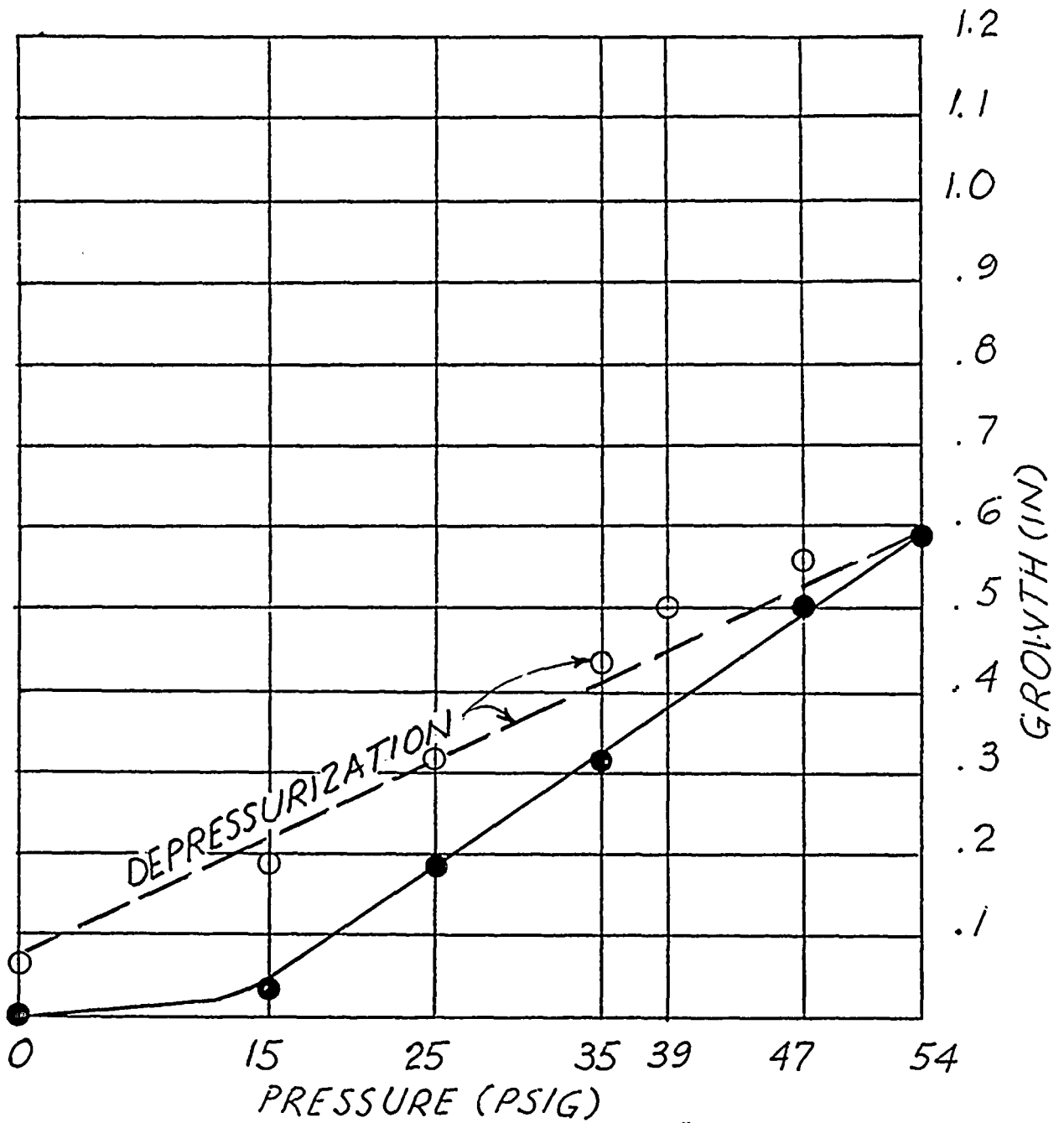




RADIAL GROWTH vs PRESSURE DIAGRAM
OBSERVATION POINT NO. 8

FIGURE 13.8

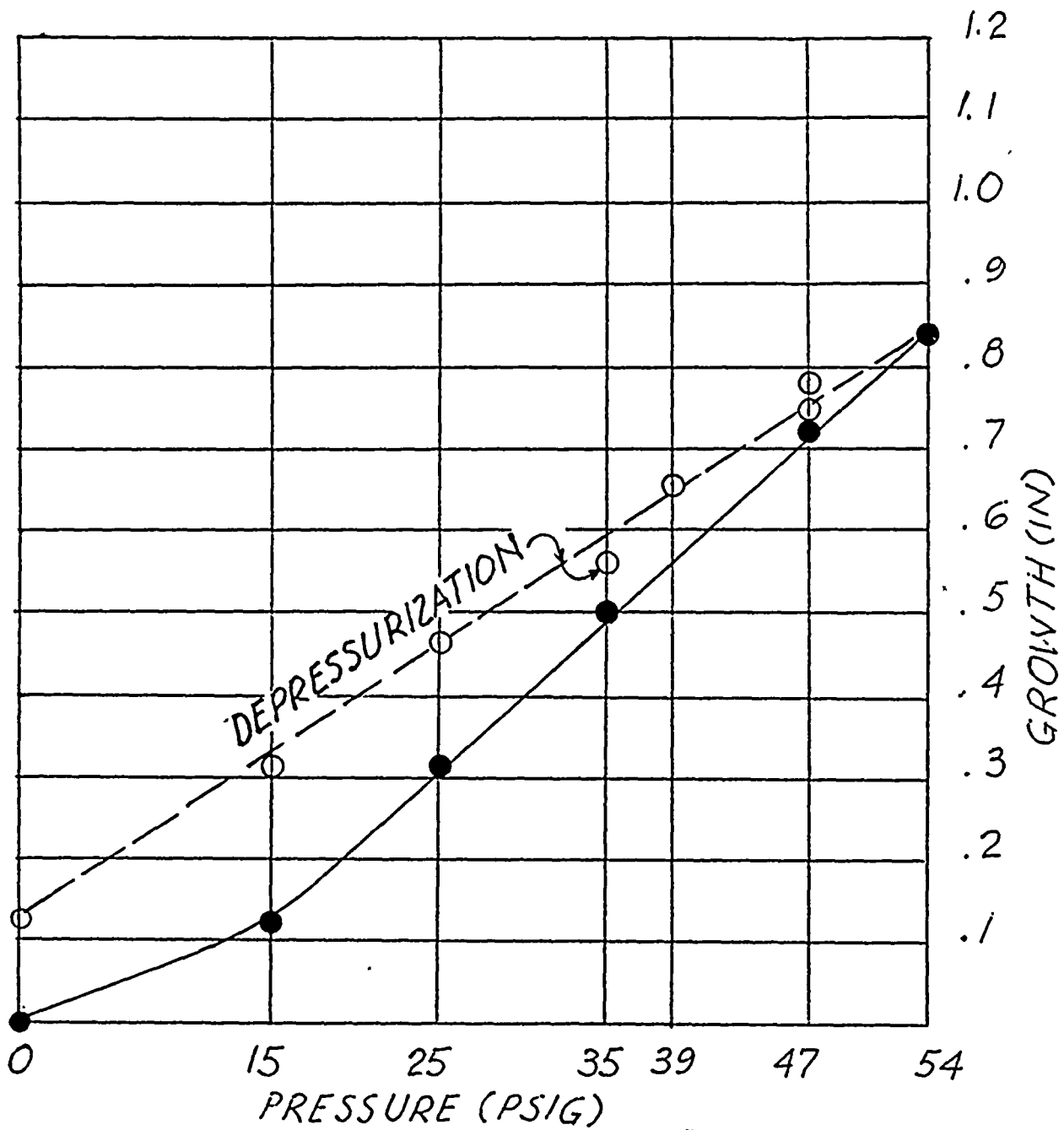




RADIAL GROWTH vs PRESSURE DIAGRAM
OBSERVATION POINT NO. 9

FIGURE 13.9

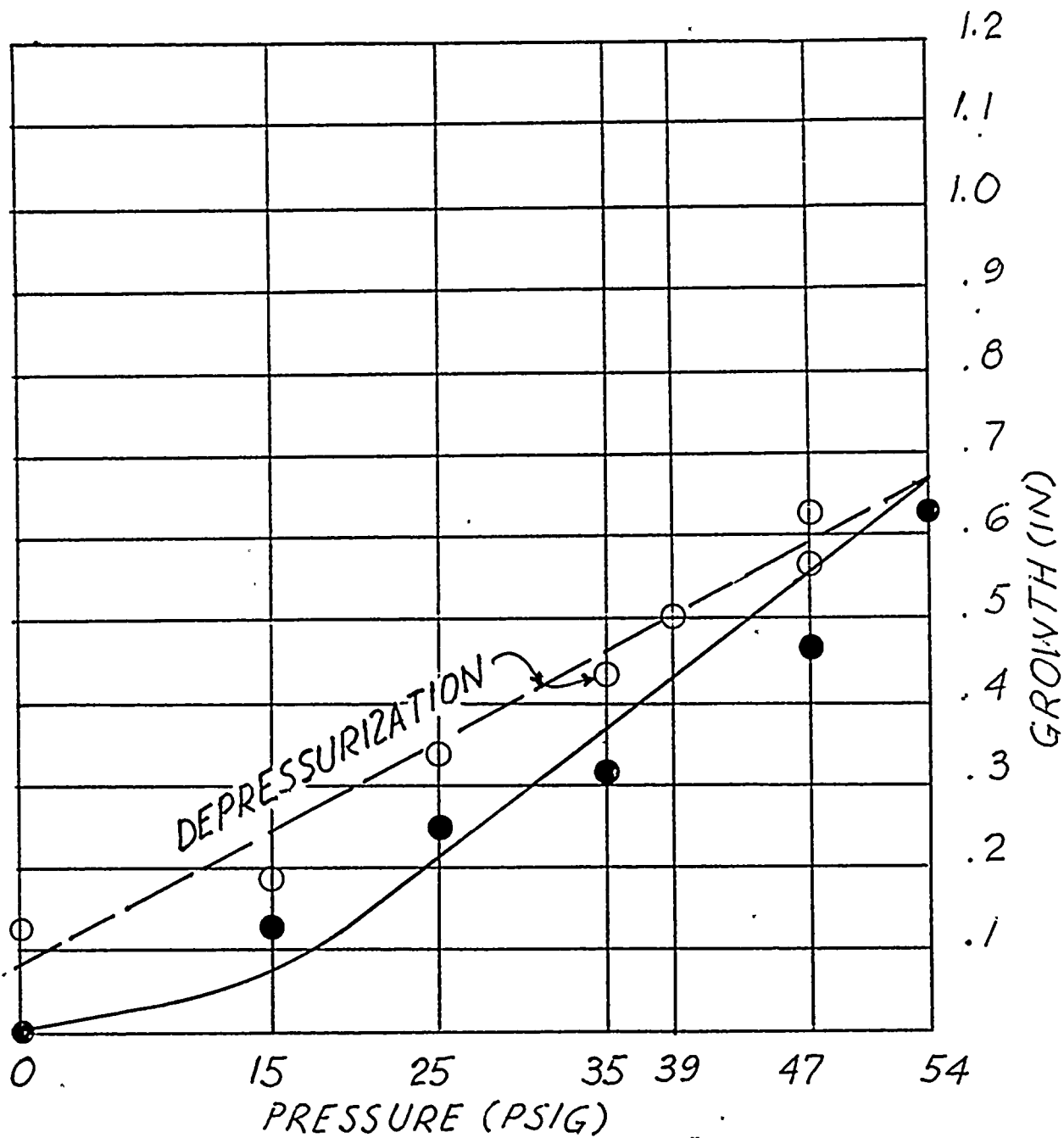




RADIAL GROWTH vs PRESSURE DIAGRAM
OBSERVATION POINT NO. 10

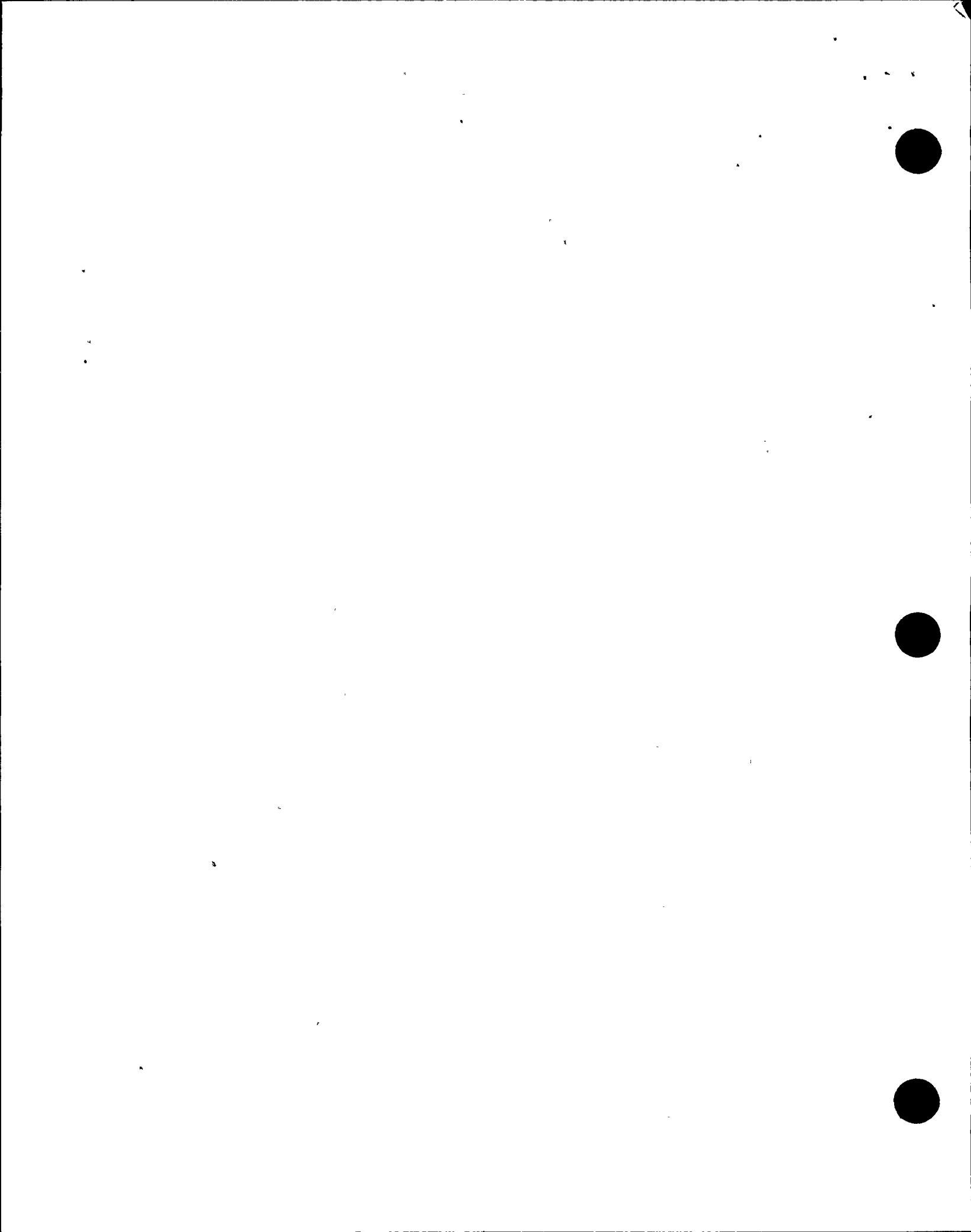
FIGURE 13.10

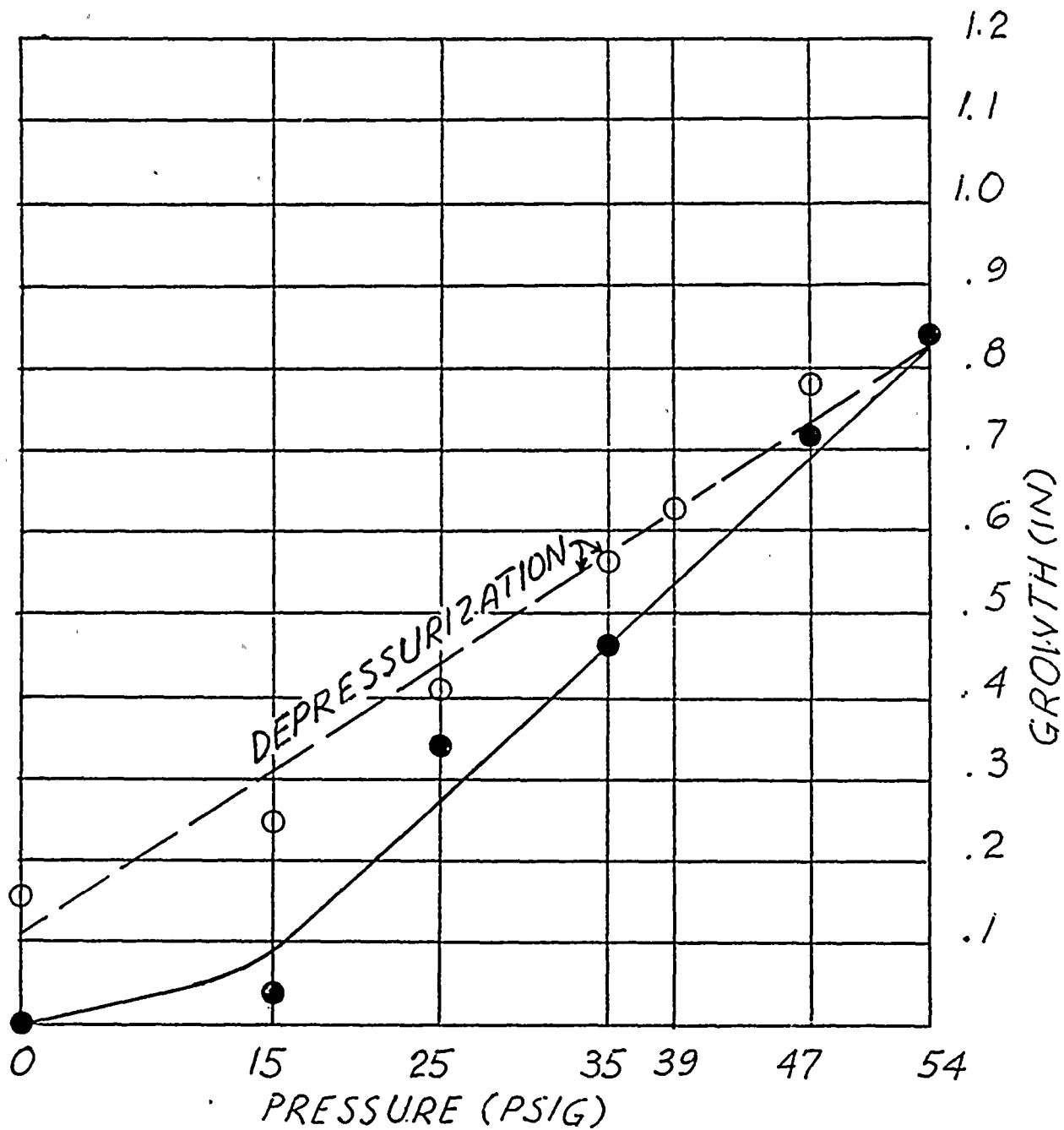




RADIAL GROWTH vs PRESSURE DIAGRAM
OBSERVATION POINT NO. 11

FIGURE 13.11

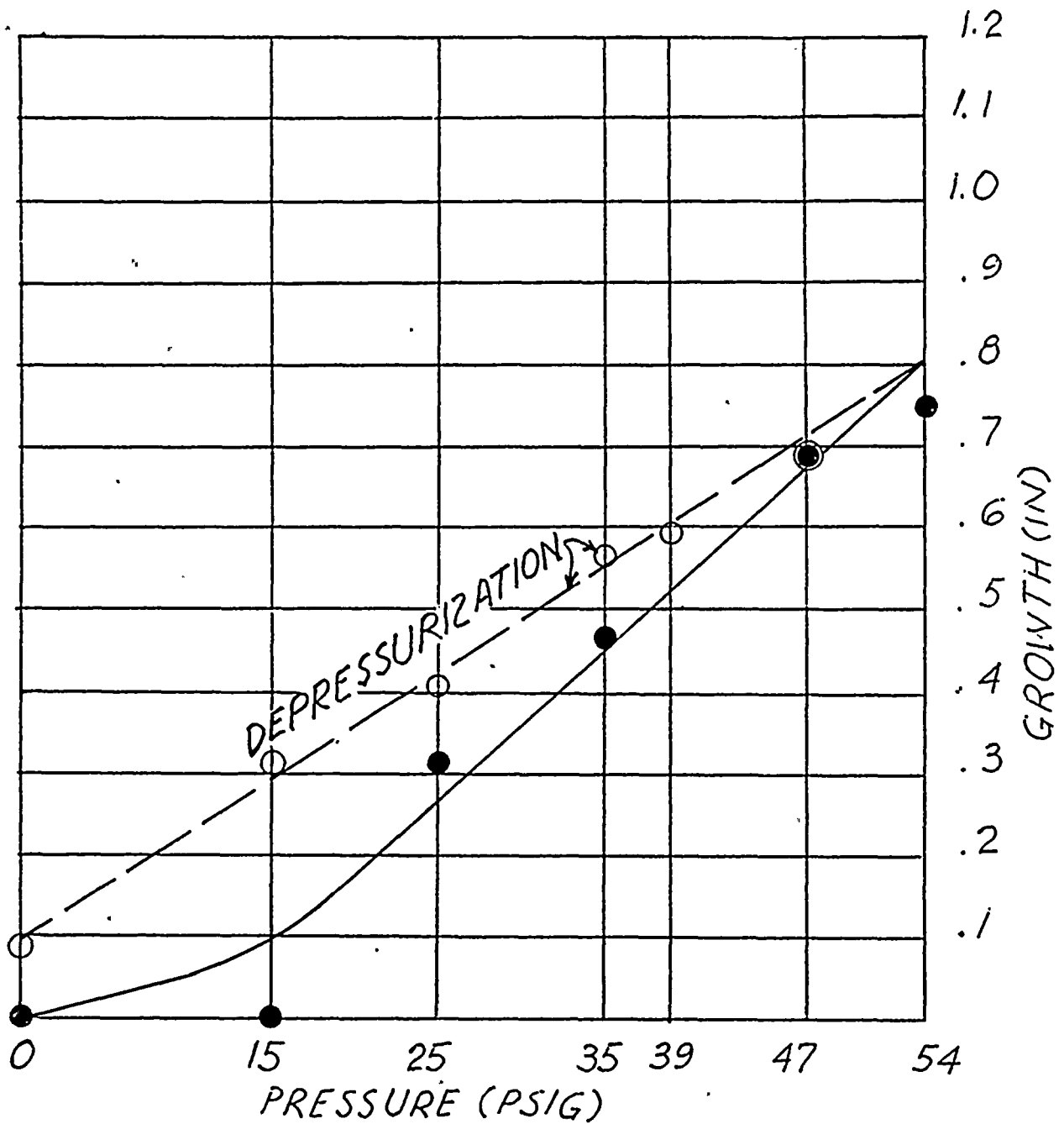




RADIAL GROWTH vs PRESSURE DIAGRAM
OBSERVATION POINT NO. 12

FIGURE 13.12

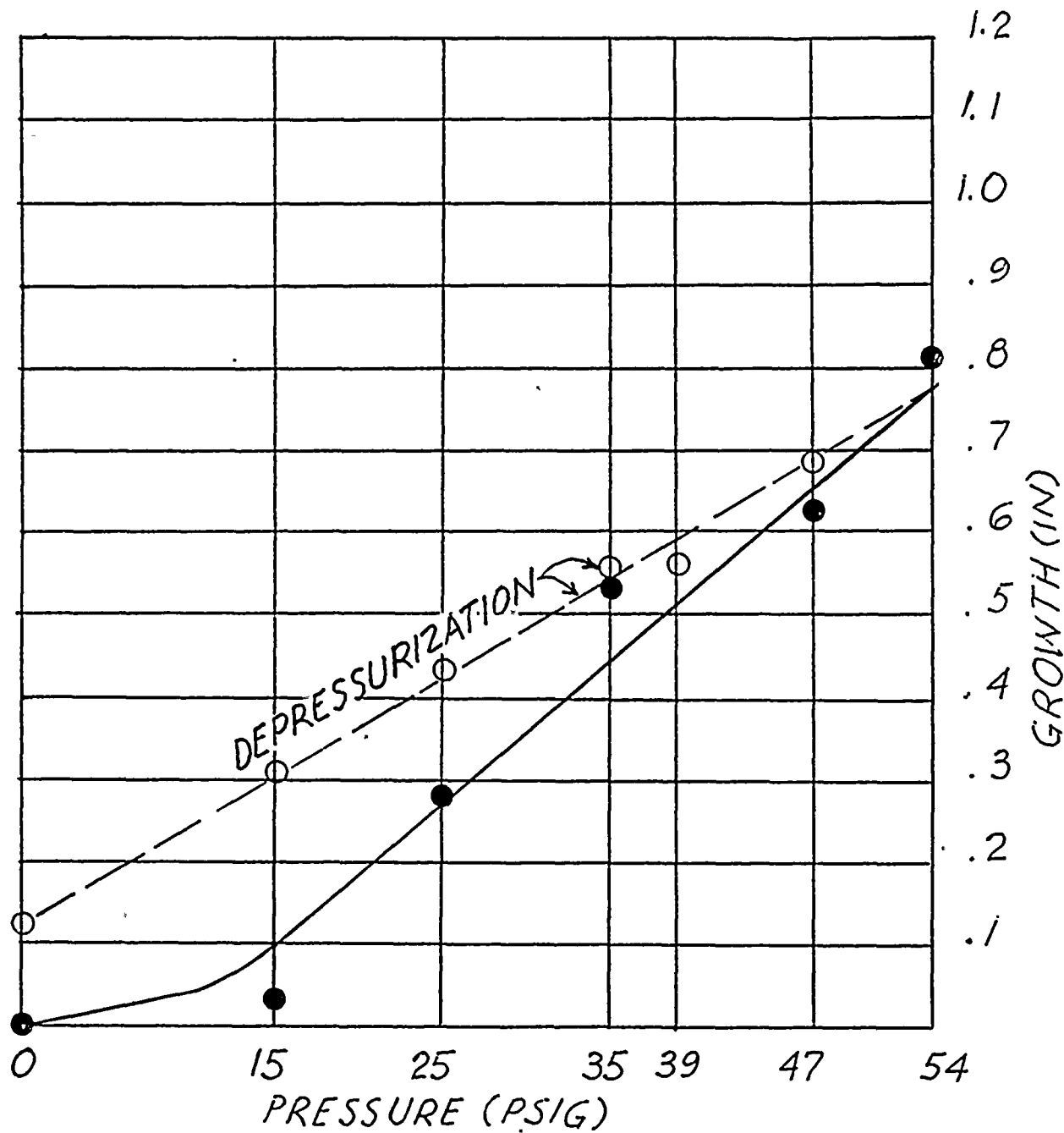




RADIAL GROWTH vs PRESSURE DIAGRAM
OBSERVATION POINT NO. 13

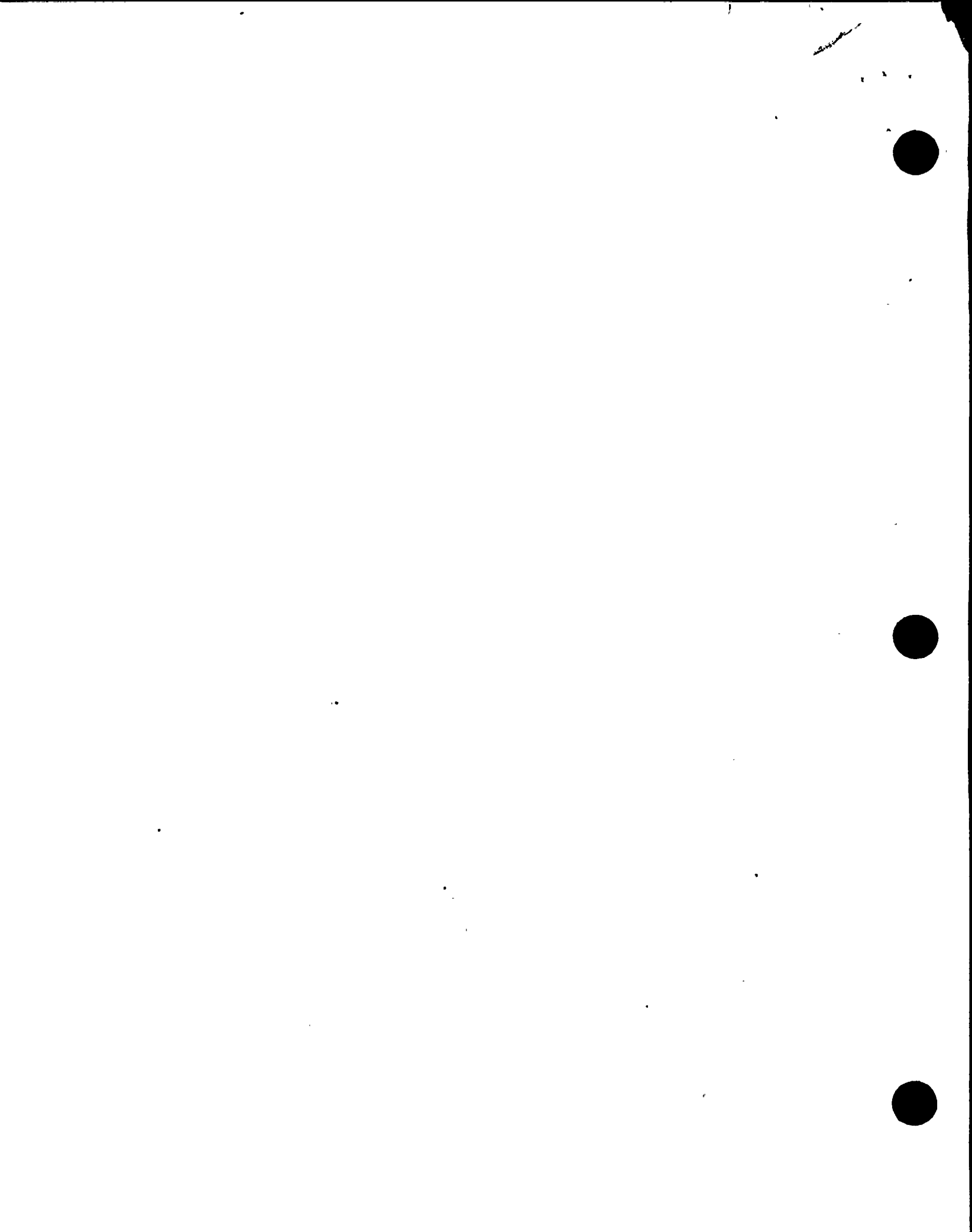
FIGURE 13.13

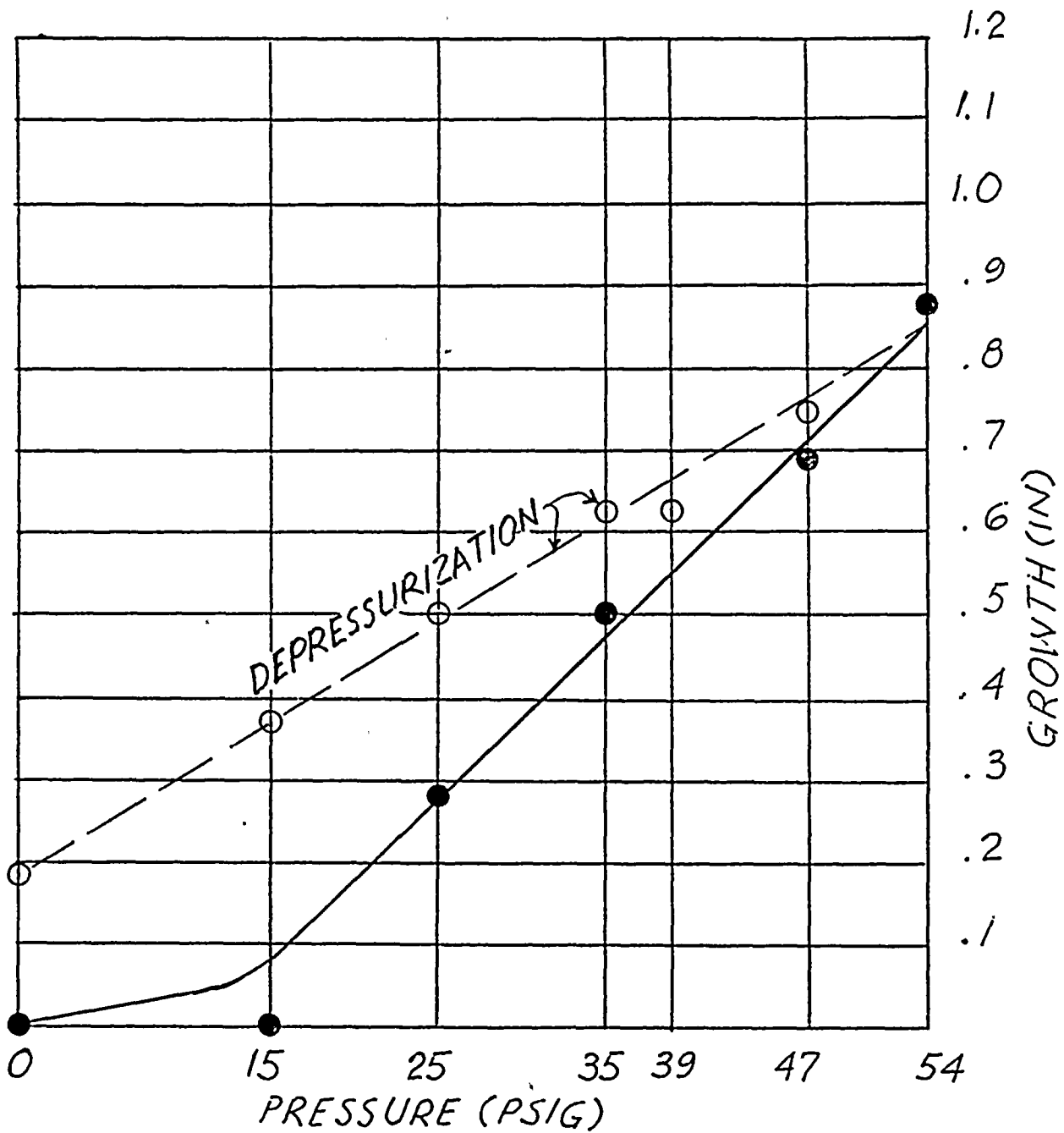




RADIAL GROWTH vs PRESSURE DIAGRAM
OBSERVATION POINT NO. 14

FIGURE 13.14

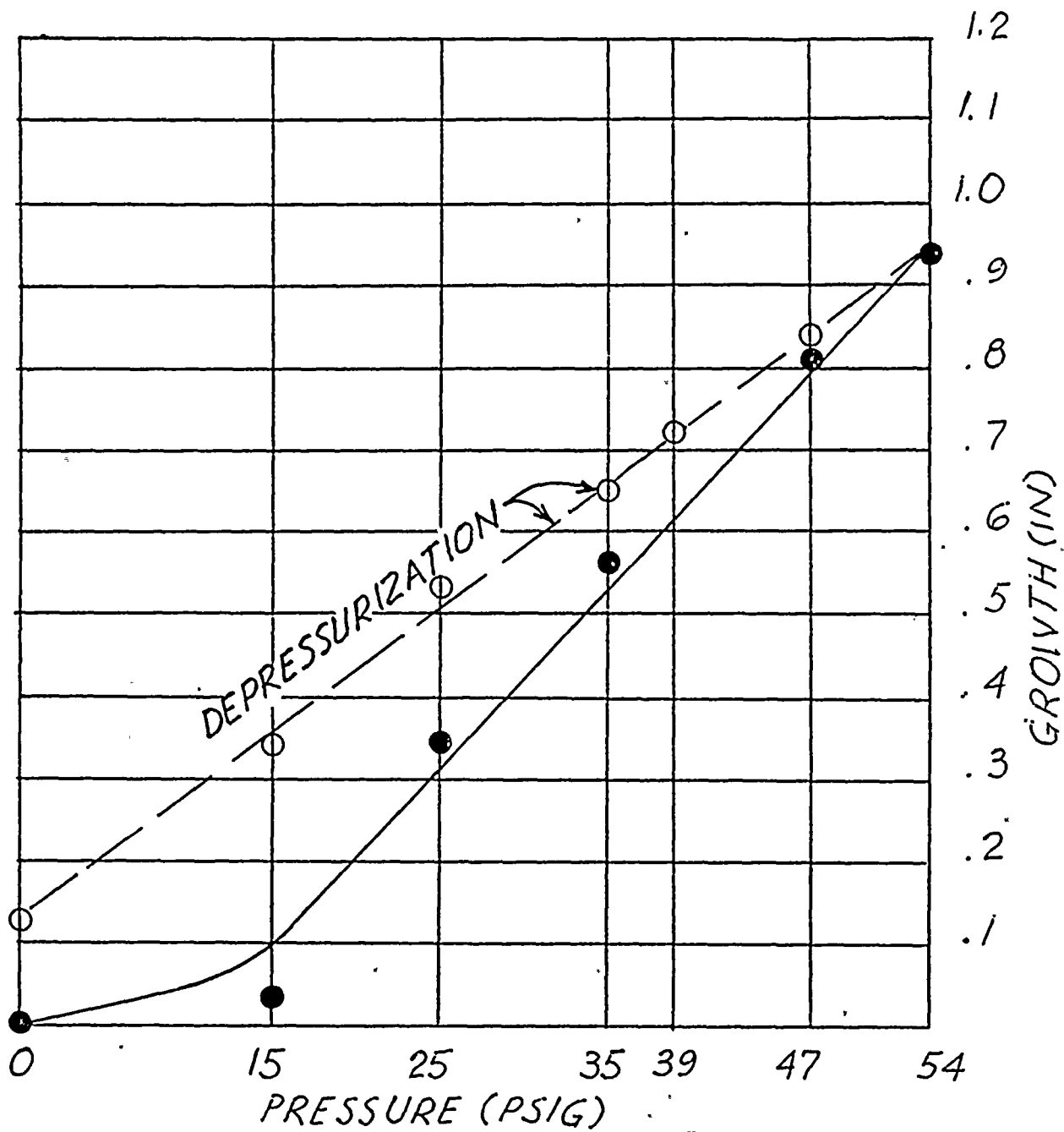




RADIAL GROWTH vs PRESSURE DIAGRAM
OBSERVATION POINT NO. 15

FIGURE 13.15

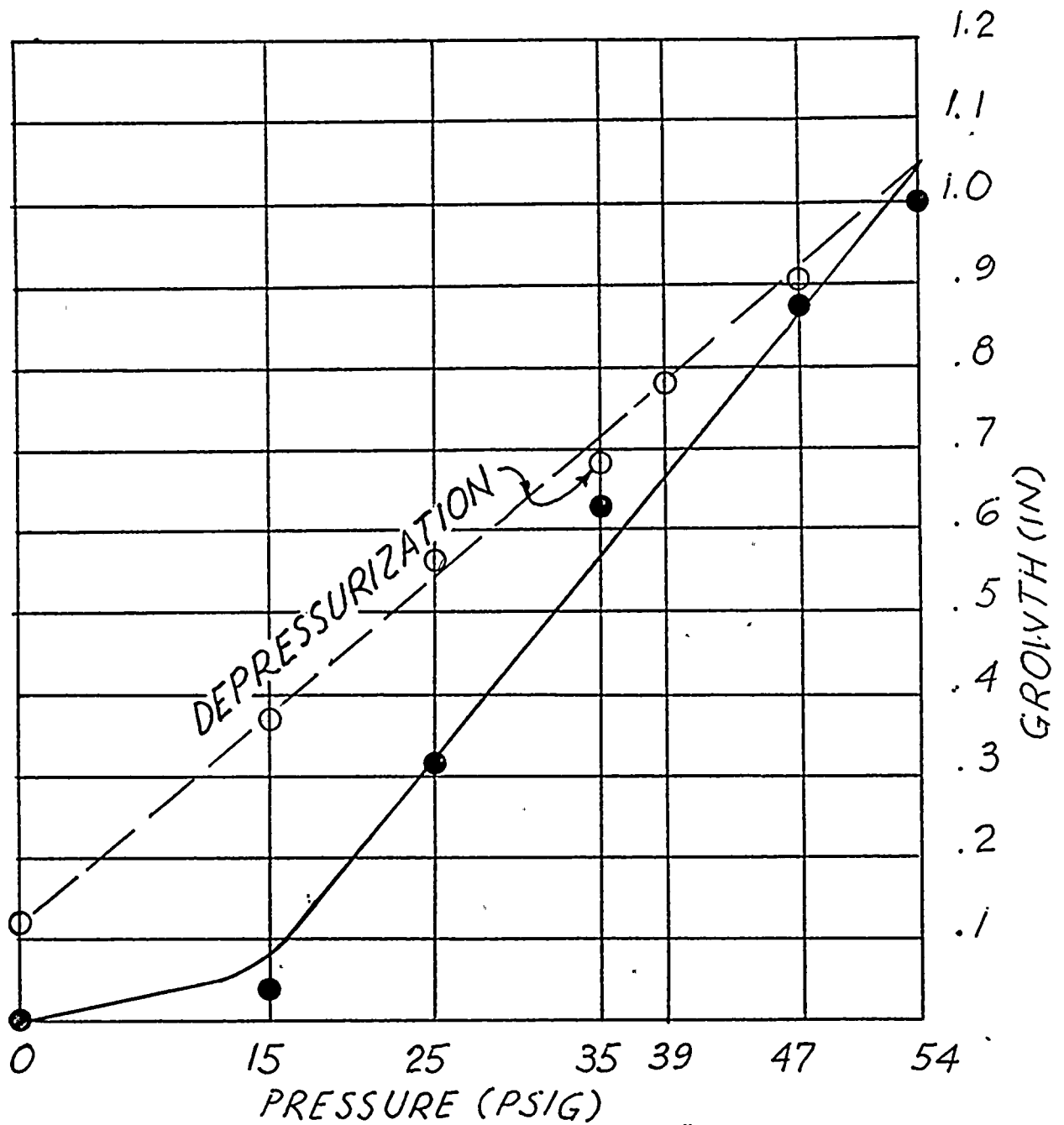




RADIAL GROWTH vs PRESSURE DIAGRAM
OBSERVATION POINT NO. 16

FIGURE 13.16

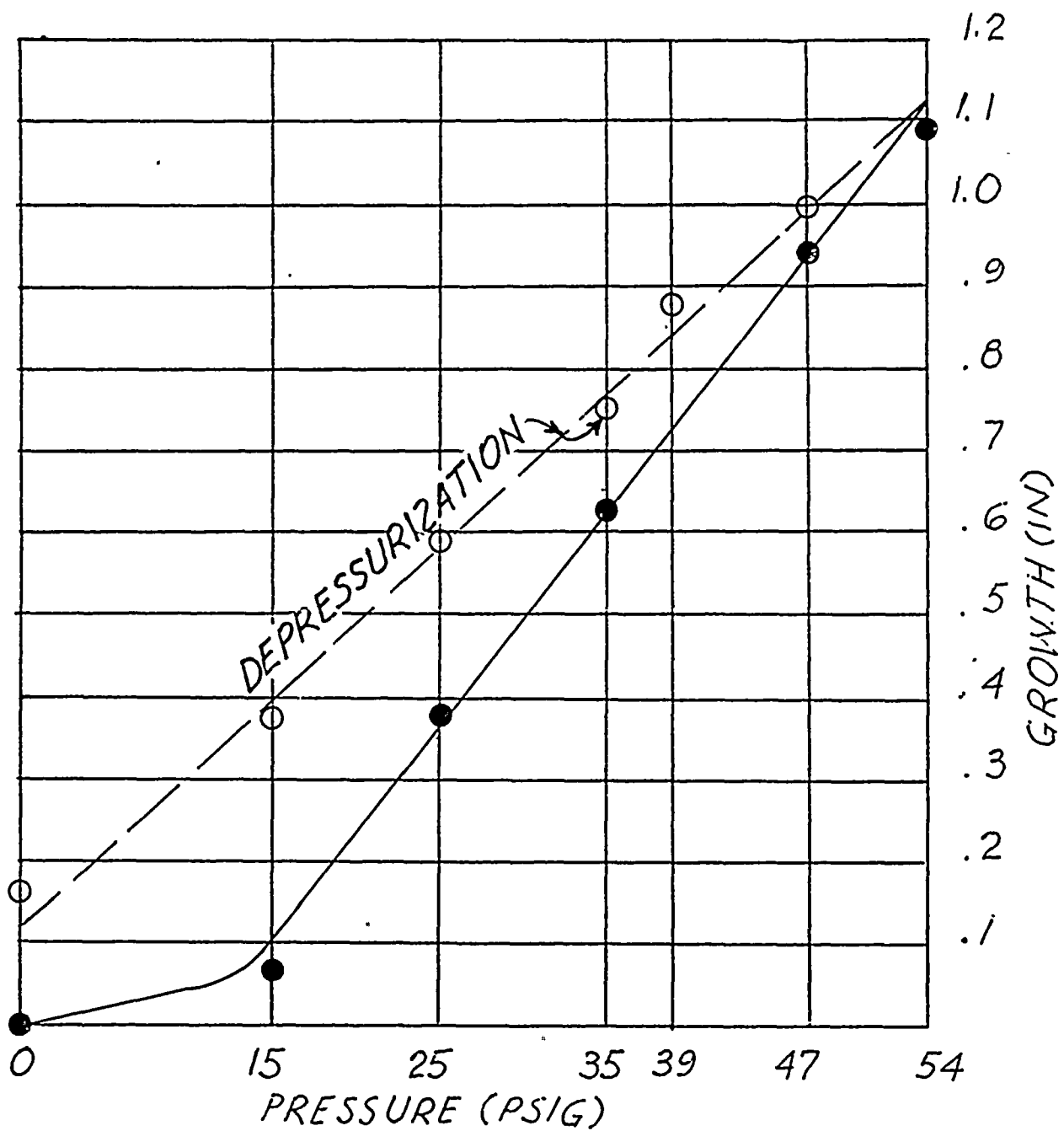




RADIAL GROWTH vs PRESSURE DIAGRAM
OBSERVATION POINT NO. 17

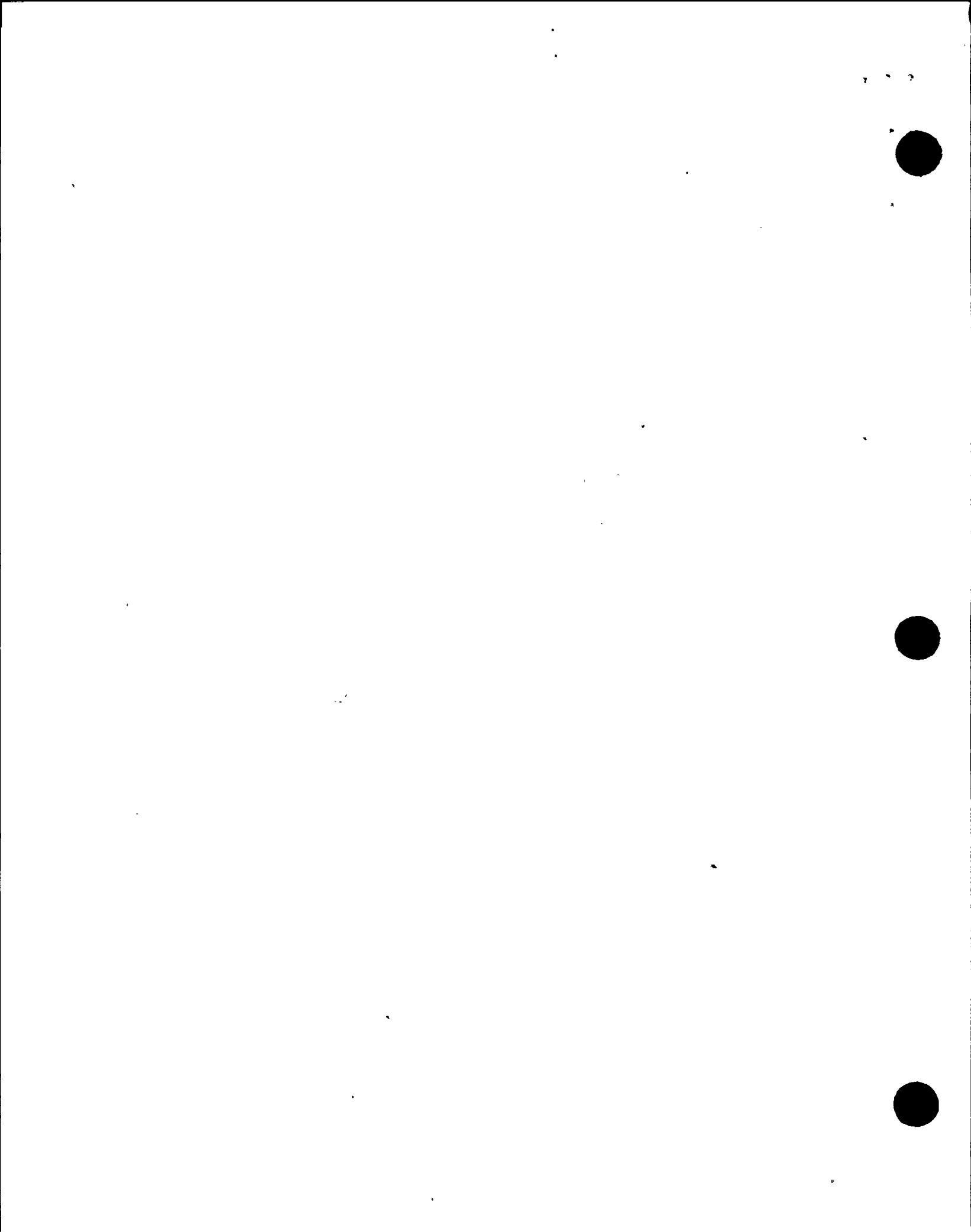
FIGURE 13.17

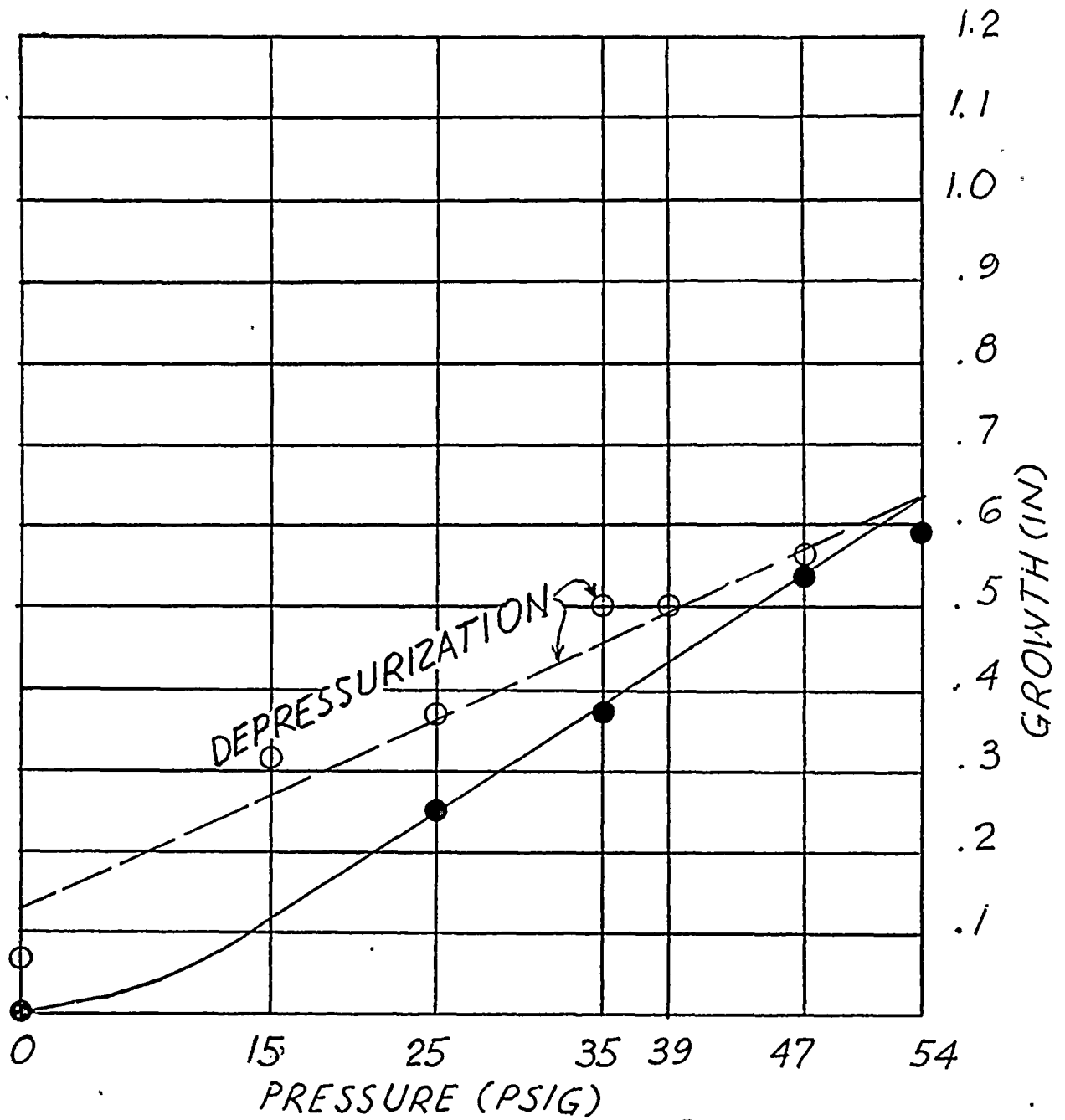




RADIAL GROWTH vs PRESSURE DIAGRAM
OBSERVATION POINT NO. 18

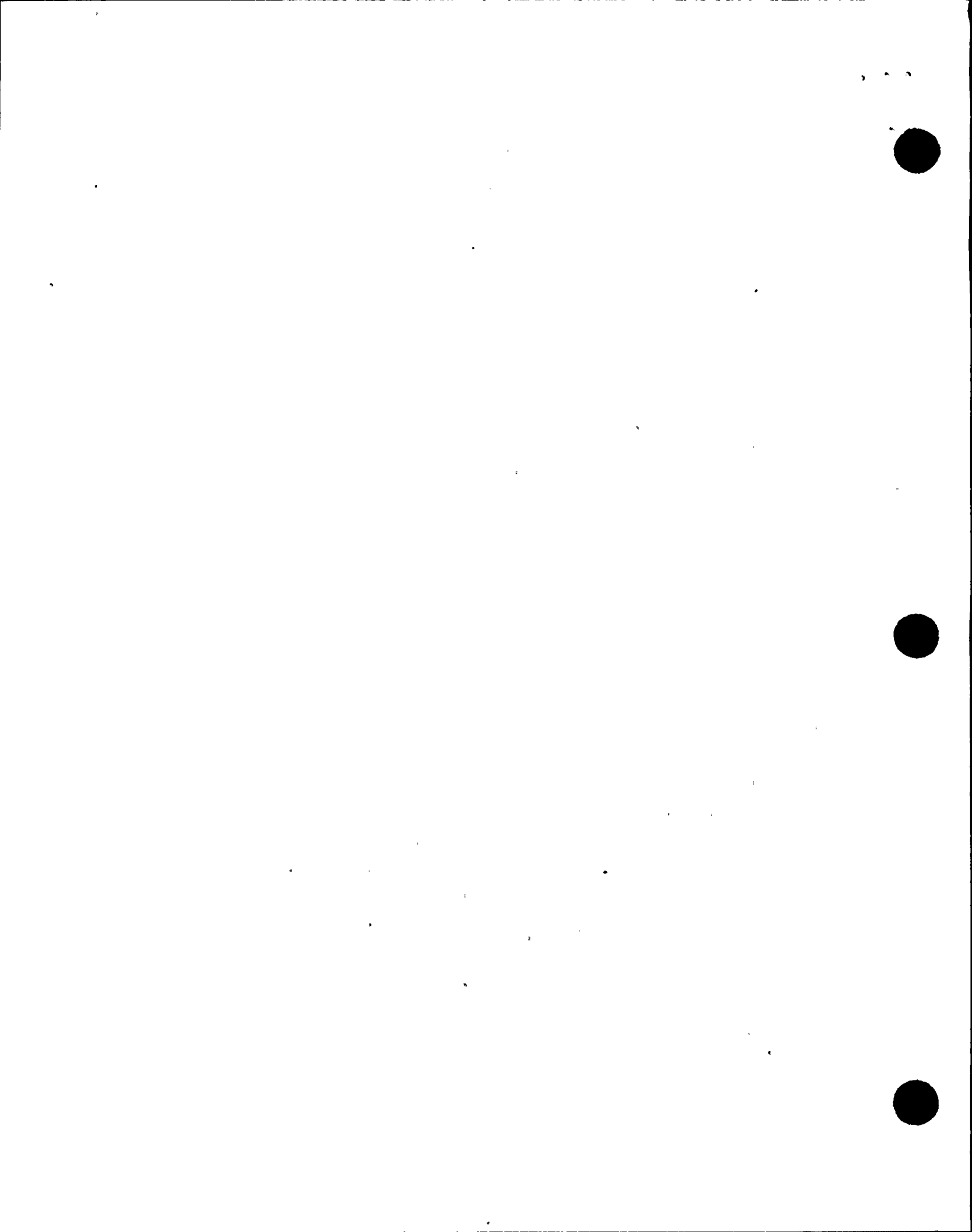
FIGURE 13.18

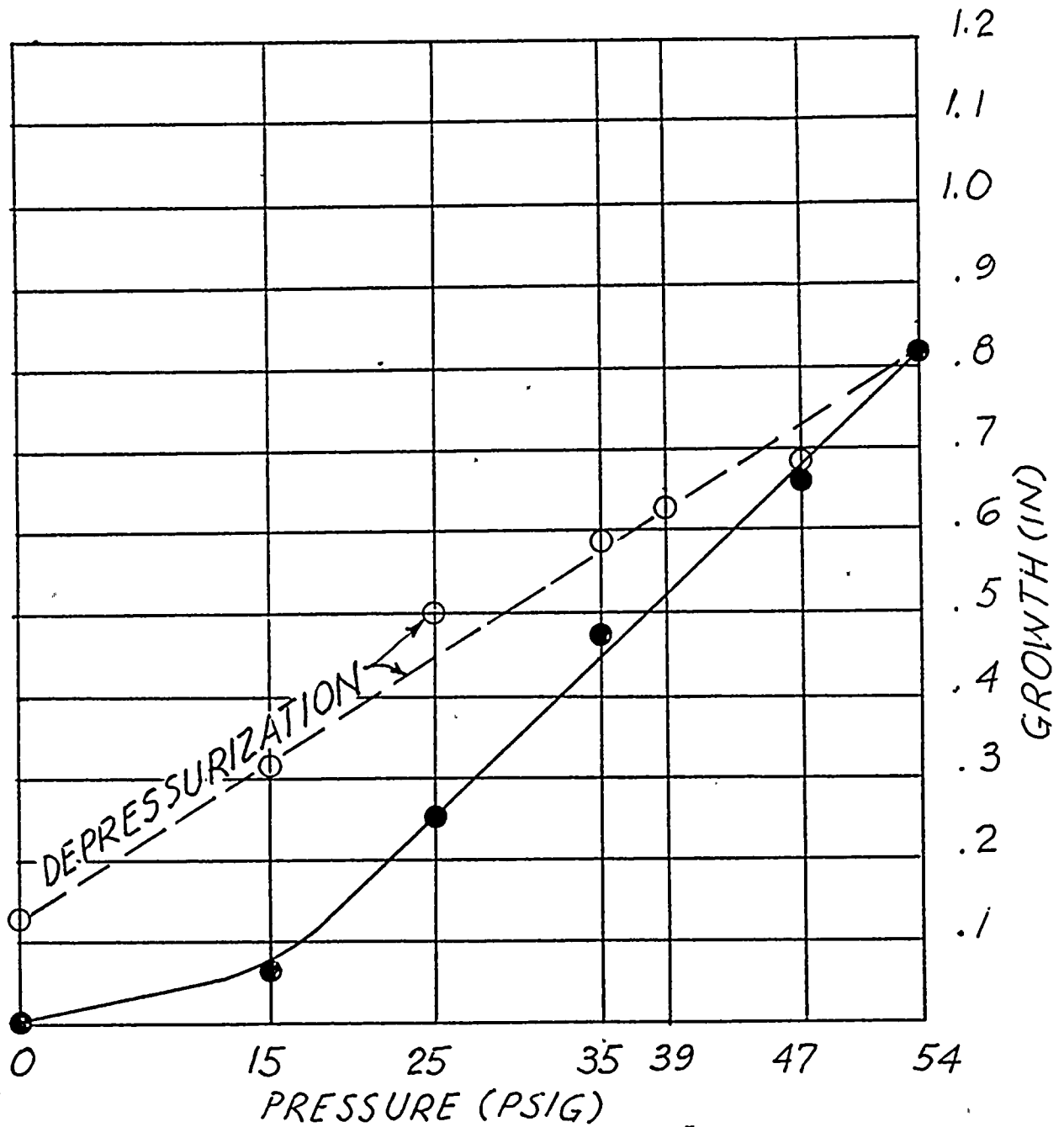




RADIAL GROWTH vs PRESSURE DIAGRAM
OBSERVATION POINT NO. 31

FIGURE 13.19

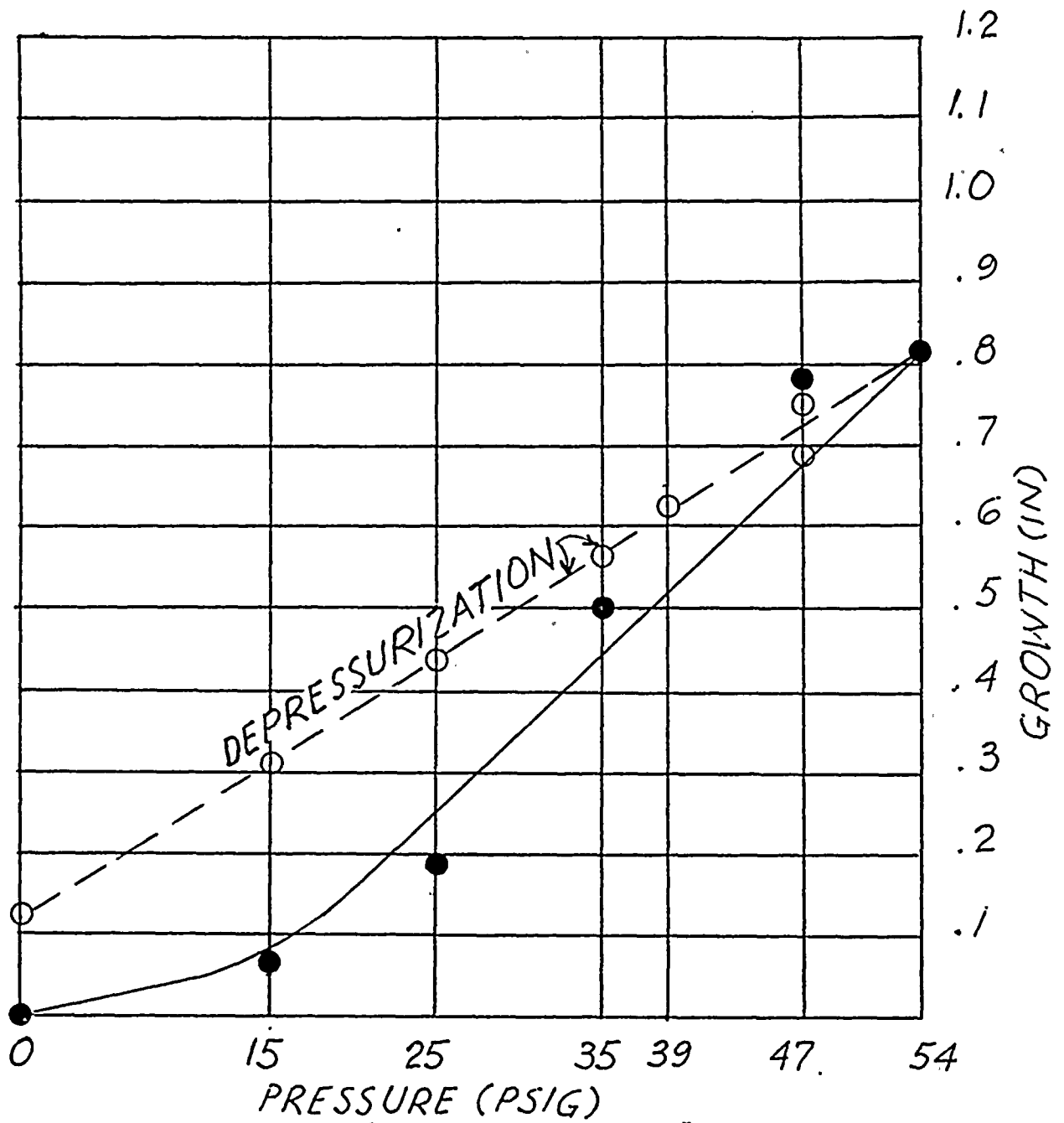




RADIAL GROWTH vs PRESSURE DIAGRAM
OBSERVATION POINT NO. 32

FIGURE 13.20

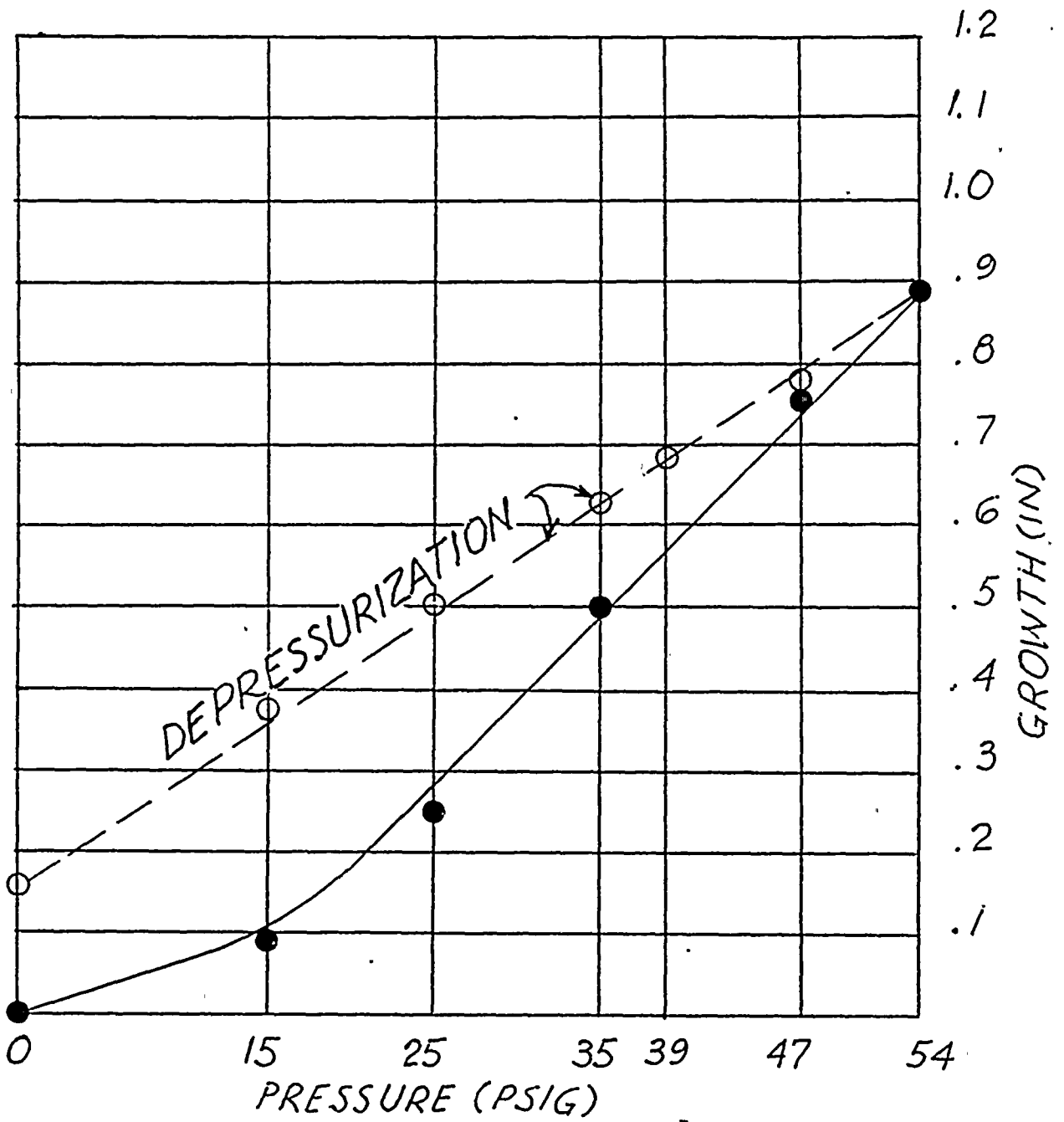




RADIAL GROWTH vs PRESSURE DIAGRAM
OBSERVATION POINT NO. 33

FIGURE 13.21

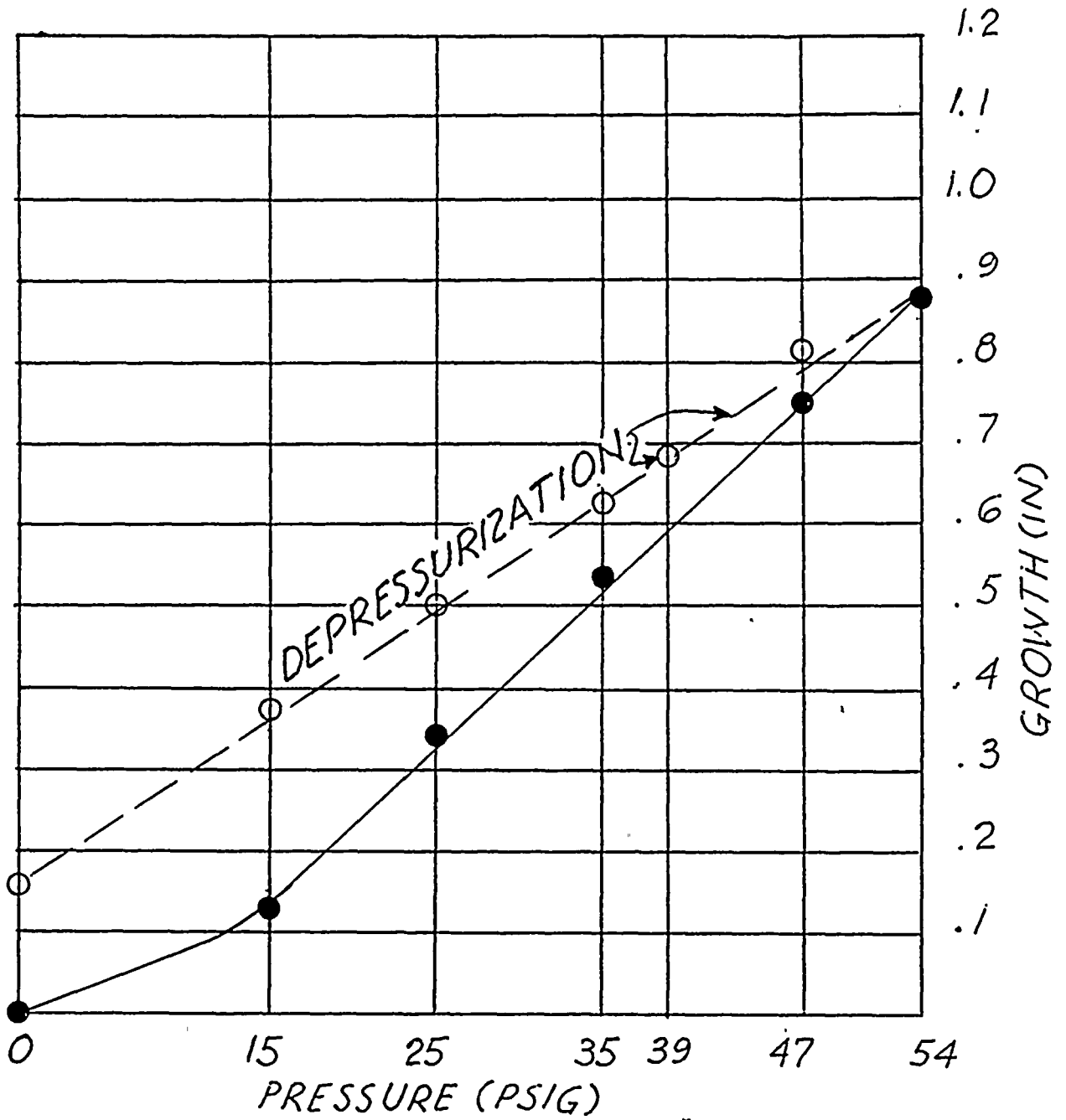




RADIAL GROWTH vs PRESSURE DIAGRAM
OBSERVATION POINT NO. 34

FIGURE 13.22

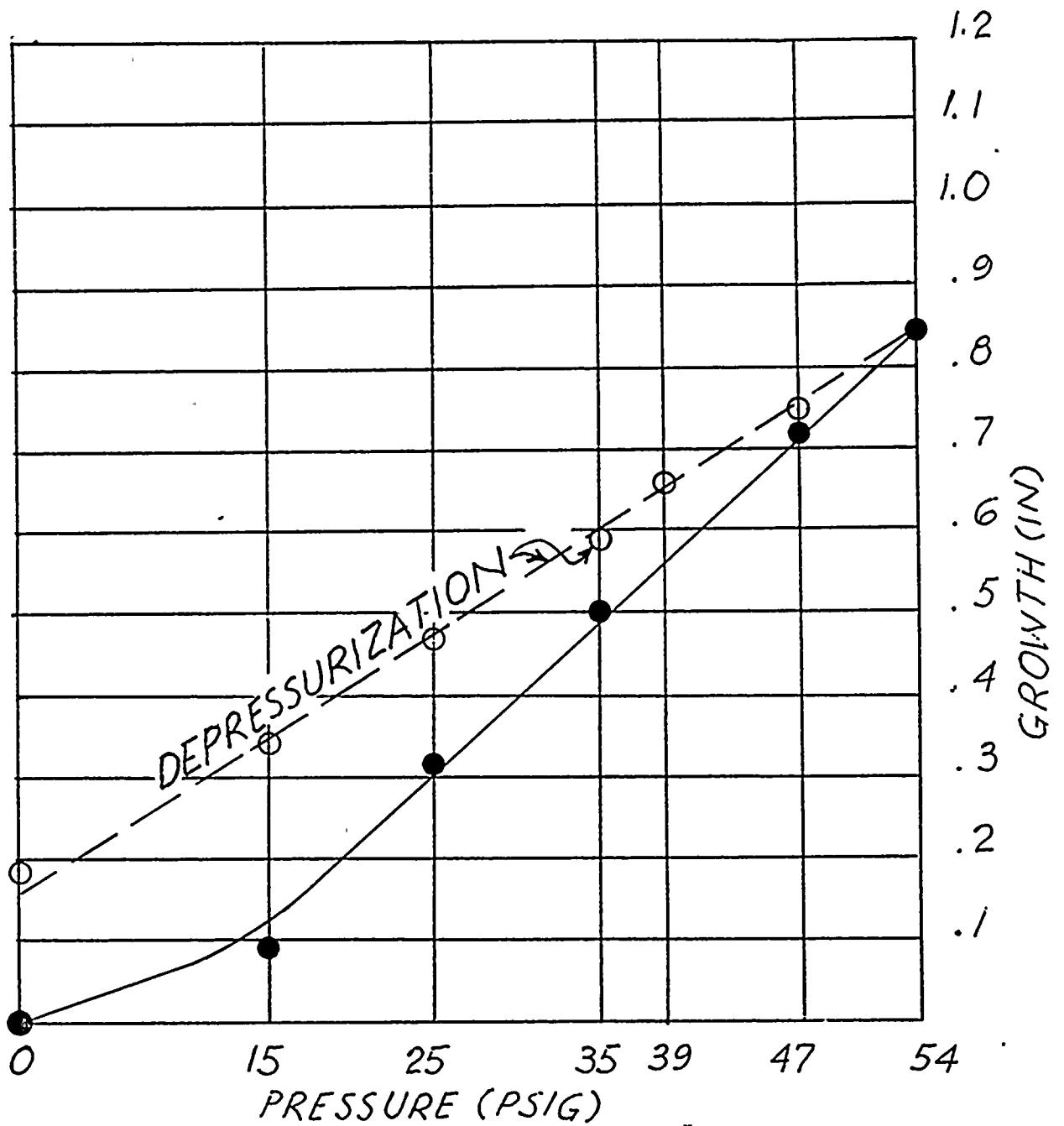




RADIAL GROWTH vs PRESSURE DIAGRAM
OBSERVATION POINT NO. 35

FIGURE 13.23





RADIAL GROWTH vs PRESSURE DIAGRAM
OBSERVATION POINT NO. 36

FIGURE 13.24

